

STATUS OF THESIS

Title of thesis Foam Modelling with Nanoparticles Effects

I SHAHRUL AIDA BINTI AB RASID

hereby allow my thesis to be placed at the Information Resource Center (IRC) of Universiti Teknologi PETRONAS (UTP) with the following conditions:

1. The thesis becomes the property of UTP
2. The IRC of UTP may make copies of the thesis for academic purposes only.
3. This thesis is classified as

Confidential

Non-confidential

If this thesis is confidential, please state the reason:

This project is a collaboration between UTP and GR&T (PETRONAS). All information here are confidential.

The contents of the thesis will remain confidential for 5 years.

Remarks on disclosure:



Signature of Author

Permanent address: A-5-8, Residensi
Hijauan Lumayan, Taman Naga
Emas, 57100 Kuala Lumpur

Date : 12 June 2022

Endorsed by
Syed M Mahmood

Signature of Supervisor

Name of Supervisor
AP Dr Syed Mohammad

Date : 12 June 2022

UNIVERSITI TEKNOLOGI PETRONAS
FOAM MODELLING WITH NANOPARTICLES EFFECTS

by

SHHRUL AIDA BINTI AB RASID

The undersigned certify that they have read, and recommend to the Postgraduate Studies Programme for acceptance this thesis for the fulfillment of the requirements for the degree stated.

Signature: Syed M Mahmood

Main Supervisor: AP Dr Syed Mohammad Mahmood

Signature: _____

Co-Supervisor: _____

Signature: 

Head of Department: Assoc. Prof. Dr. Khaled Abdalla Elraies
Chair
Petroleum Engineering Department
Dr. Khaled Abdalla Elraies

Date: 7/7/2022

FOAM MODELLING WITH NANOPARTICLES EFFECTS

by

SHAHRUL AIDA BINTI AB RASID

A Thesis

Submitted to the Postgraduate Studies Programme

as a Requirement for the Degree of

MASTER OF SCIENCE

PETROLEUM ENGINEERING

UNIVERSITI TEKNOLOGI PETRONAS

BANDAR SERI ISKANDAR,

PERAK

JUNE 2022

DECLARATION OF THESIS

Title of thesis

Foam Modelling with Nanoparticles Effects

I SHHRUL AIDA BINTI AB RASID

hereby declare that the thesis is based on my original work except for quotations and citations which have been duly acknowledged. I also declare that it has not been previously or concurrently submitted for any other degree at UTP or other institutions.



Signature of Author

Permanent address: A-5-8, Residensi
Hijauan Lumayan, Taman Naga Emas,
57100 Kuala Lumpur

Date : 12-06-2022

Witnessed by

Syed M Mahmood

Signature of Supervisor

Name of Supervisor
AP Dr Syed Mohammad

Date : 12-06-2022

DEDICATION

I dedicate this work to my loving parents, Rosnani Ismail and Ab Rasid Yaakop, which without their support and encouragement, my dreams would never come true.

ACKNOWLEDGEMENTS

Firstly, I want to thank my advisor, AP Dr Syed Mohammad Mahmood, of Petroleum Engineering at the Universiti Teknologi PETRONAS, whose expertise, understanding, guidance, and support made it possible to work on a challenging topic that was of great interest to me.

I would also like to thank Dr. Nor Idah Kechut, my industrial advisor, who steered me in the right direction whenever I needed it. Her patience and commitment helped me to make tremendous progress in my research project.

I would like to express my profound gratitude to Dr. Saeed Akbari for providing me with unconditional support and encouragement throughout this process.

Finally, I am grateful to my UTP colleagues, friends, and family who supported me during my academic life. A special thanks to the UTP-GR&T collaboration for providing financial support.

ABSTRACT

The potential use of nanoparticles as a foam stabilizer has been extensively assessed in recent studies. The nanoparticle effect in stabilizing foam has been proven in laboratory analysis but has yet to be piloted in the field. Although the conventional foam flooding process simulation is relatively established in the industry, one that incorporates nanoparticles' effect has yet to be realized. Simulating nanoparticles-stabilized foam behaviour is crucial to reduce risks and uncertainties associated with this process; nano-foam flooding can only be modelled with low accuracy as a “stabilized foam” with the current state-of-the-art. The purpose of this study was to assess the applicability of modelling nano-foam using an implicit texture model solely on the foam stability improvement in the presence of silica nanoparticles at the first level of understanding with respect to the nanoparticle stabilisation mechanism, while excluding the limiting factors that degrade foam performance (oil free and at standard conditions). Both experimental and modelling analysis were conducted to meet the research objectives. Based on established literature, silica nanoparticles were chosen in combination with MFOMAX surfactant. The nanofluid mixture compatibility were revalidated at standard condition. Then, the rheological behaviour of nano-foam regarding nanoparticle concentration, shear rate, and foam quality was assessed using a flow loop rheometer. After that, the mobility reduction factors (MRF) in surfactant foam and nano-foam flooding under the influence of nanoparticle concentration, salinity, foam quality, and total injection rate were experimentally obtained and compared. Lastly, the applicability of the existing implicit texture foam model was analysed for nano-foam.

According to the compatibility results, the optimal nanoparticle-surfactant concentration ratio varies under standard conditions. Based on laboratory analysis, the nano-foam exhibits shear-thinning behaviour as the apparent viscosity decreases with increasing shear rate up to 750 s^{-1} at varying nanoparticle concentration and foam

quality between 50% to 80%. Therefore, the current implicit texture foam model's assumption that foam is shear thinning is still valid within the studied nano-foam system. Based on the foam flooding experiments, nano-foam exhibits a significantly higher MRF at foam quality of 80% to 95% compared to surfactant foam. In addition to that, two foam decay rates were observed from the foam quality scan of the nano-foam. The established foam quality scan was used as an input to determine the critical foam model parameters ($fmmob$, F_3 , and $F_{dry-out}$) to simulate foam flow behaviour.

The existing foam model is unable to properly fit the nano-foam collapse behaviour established through the foam quality scan. Better nano-foam model parameter fit can be achieved by force-tuning the $epdry$ parameter to precisely fit one of the two decay rates separately and validated in a commercial simulator with good differential pressure matching. A modified Dry-Out function was proposed and it can represent foam collapse behaviour in the presence of nanoparticles within the current scope of the study. This research's revised Dry-Out function model provides a novel method for finding the nano-foam process's fitting parameters.

ABSTRAK

Potensi penggunaan zarah nano sebagai penstabil buih telah dinilai secara meluas dalam kajian terkini. Kesan nanopartikel dalam menstabilkan buih telah dibuktikan dalam analisis makmal tetapi masih belum diuji dalam bidang. Walaupun simulasi proses banjir buih konvensional agak mantap dalam industri, satu yang menggabungkan kesan nanopartikel masih belum direalisasikan. Mensimulasikan tingkah laku buih yang distabilkan nanopartikel adalah penting untuk mengurangkan risiko dan ketidakpastian yang berkaitan dengan proses ini; banjir nano-buih hanya boleh dimodelkan dengan ketepatan yang rendah sebagai "buih yang distabilkan" dengan terkini yang terkini. Kajian ini bertujuan untuk menilai kebolegunaan untuk memodelkan buih nano menggunakan model tekstur tersirat semata-mata pada peningkatan kestabilan buih dengan kehadiran zarah nano silika pada tahap pemahaman pertama berkenaan dengan mekanisme penstabilan zarah nano, tidak termasuk faktor pengehad yang merosotkan prestasi buih (bebas minyak dan pada keadaan standard). Analisis eksperimen dan pemodelan telah dijalankan untuk memenuhi objektif kajian. Nanopartikel silika dipilih dalam kombinasi dengan surfaktan MFOMAX berdasarkan kesusasteraan yang telah ditetapkan. Kecerassian campuran cecair nano telah disahkan semula pada keadaan standard. Kemudian, tingkah laku reologi buih nano mengenai kepekatan nanozarah, kadar ricih, dan kualiti buih dinilai menggunakan rheometer gelung aliran. Selepas itu, faktor pengurangan mobiliti (MRF) dalam buih surfaktan dan banjir nano-buih di bawah pengaruh kepekatan nanozarah, kemasinan, kualiti buih, dan jumlah kadar suntikan telah diperolehi dan dibandingkan secara eksperimen. Akhir sekali, kebolegunaan model buih tekstur tersirat sedia ada telah dianalisis untuk buih nano.

Keputusan keserasian menunjukkan nisbah kepekatan nanozarah-surfaktan optimum berbeza pada keadaan standard. Berdasarkan analisis makmal, nano-buih mempamerkan tingkah laku penipisan ricih kerana kelikatan ketara berkurangan

dengan peningkatan kadar ricih sehingga 750 s^{-1} pada kepekatan nanozarah dan kualiti buih yang berbeza-beza antara 50% hingga 80%. Oleh itu, andaian model busa tekstur tersirat semasa di mana buih adalah penipisan ricih masih sah dalam sistem buih nano yang dikaji. Berdasarkan eksperimen banjir buih, buih nano mempamerkan MRF yang jauh lebih tinggi pada kualiti buih 80% hingga 95% berbanding buih surfaktan. Di samping itu, dua kadar pereputan buih diperhatikan daripada imbasan kualiti buih buih nano. Imbasan kualiti buih yang telah ditetapkan telah digunakan sebagai input untuk menentukan parameter model buih kritikal (f_{mob} , F_3 , dan $F_{dry-out}$) untuk mensimulasikan gelagat aliran buih.

Model buih sedia ada tidak dapat menyesuaikan dengan betul kelakuan keruntuhan buih nano yang ditubuhkan melalui imbasan kualiti buih. Kesesuaian parameter model buih nano yang lebih baik boleh dicapai dengan menala paksa parameter ep_{dry} agar tepat padan salah satu daripada dua kadar pereputan secara berasingan dan disahkan dalam simulator komersil dengan padanan tekanan pembezaan yang baik. Fungsi “Dry-Out” yang diubah suai telah dicadangkan dan ia boleh mewakili gelagat keruntuhan buih dengan kehadiran zarah nano dalam skop kajian semasa. Model fungsi “Dry-Out” yang disemak semula ini menyediakan kaedah baru untuk mencari parameter kelengkapan proses buih nano.

In compliance with the terms of the Copyright Act 1987 and the IP Policy of the university, the copyright of this thesis has been reassigned by the author to the legal entity of the university,

Institute of Technology PETRONAS Sdn Bhd.

Due acknowledgement shall always be made of the use of any material contained in, or derived from, this thesis.

© Shahrul Aida binti Ab Rasid, 2022

Institute of Technology PETRONAS Sdn Bhd

All rights reserved.

TABLE OF CONTENT

ABSTRACT.....	vii
ABSTRAK.....	ix
LIST OF FIGURES	xv
LIST OF TABLES.....	xviii
CHAPTER 1 INTRODUCTION	1
1.1 Research Background	1
1.2 Problem Statement.....	2
1.3 Research Objective	4
1.4 Significant of Research.....	5
1.5 Scope of Study.....	5
1.6 Organization of the Thesis.....	7
CHAPTER 2 LITERATURE REVIEW	9
2.1 Fundamental of Foam	9
2.2 Nanoparticles in Foam Application	10
2.3 Nanoparticles Stabilization Mechanism	10
2.3.1 Particle Attachment Energy	10
2.3.2 Particle Arrangement Mechanism	11
2.3.3 Maximum Capillary Pressure to Coalesce	12
2.4 Critical Parameters Affecting Nanoparticles-surfactant Foam Performance ..	13
2.4.1 Effect of Nanoparticle and Surfactant Concentration	13
2.4.2 Effects of Nanoparticles Surface Wettability	15
2.4.3 Effect of Salinity	17
2.4.4 Effect of Flow Velocity.....	20
2.5 Foam Modelling Technique.....	22
2.5.1 Foam Propagation and Flow Characteristics.....	22
2.5.2 Empirical Foam Modelling	24
2.5.3 Foam Model Parameter Fitting Method	25
CHAPTER 3 METHODOLOGY	29

3.1 Materials	30
3.2 Experimental Equipment	32
3.2.1 Foam Tester	32
3.2.2 Foam Rheometer	33
3.2.3 Sand-pack Flooding System.....	34
3.3 Experimental Procedures	35
3.3.1 Dispersion Preparation	35
3.3.2 Nanoparticles-Surfactant Compatibility Study	36
3.3.3 Bulk Foam Stability	37
3.3.4 Nanoparticles-Stabilized Foam Rheology Study	39
3.3.5 Foam Flooding Experiments	40
3.3.5.1 Mobility reduction at varying foam quality (foam quality scan)	42
3.3.5.2 Mobility reduction at varying nanoparticles concentration	42
3.3.5.3 Mobility reduction at varying total injection rates (foam velocity scan)	42
3.3.5.4 Mobility reduction at varying salinity.....	43
3.4 Foam Simulation Model Analysis	43
3.4.1 Foam Model Parameters Estimation Method.....	44
3.4.2 Evaluation of Critical Foam Model Parameters: <i>fmmob</i> , <i>fmdry</i> , and <i>epdry</i>	45
3.4.3 Nano-Foam Model Parameters Estimation	46
3.5 Chapter Summary	47
CHAPTER 4 RESULTS AND DISCUSSION.....	49
4.1 Nanoparticles Screening and Compatibility Test	49
4.2 Dynamic Nanoparticles-Stabilized Foam Rheology	55
4.2.1 Nanoparticles-Stabilized Foam Rheology Behaviour Compared to Conventional Surfactant Foam	57
4.2.2 Nanoparticles-Stabilized Foam Rheology as a Function of Nanoparticles Concentration, Shear Rates, and Foam Quality.....	59
4.3 The Parameters Affecting the Mobility Reduction Factor of the Nano-Foam	61

4.3.1 The Effect of Foam Quality in the Absence and Presence of Nanoparticles	61
4.3.2 The Effect of Nanoparticles' Concentration at High Foam Quality ...	64
4.3.3 The Effect of Total Injection Rate at Fixed Nanoparticles Concentration.....	65
4.3.4 The Effect of Nanoparticles on Varying Salinity.....	67
4.4 Modelling of Nano-Foam Foam Transport Behaviour through Porous Media.....	68
4.4.1 The Effect of Foam Model Parameters $fmmob$ and $F_{dry-out}$	69
4.4.1.1 The Effects of $fmmob$ at Fixed F_3 and $F_{dry-out}$	69
4.4.1.2 The Effects of $F_{dry-out}$ at fixed $fmmob$ and F_3	70
4.4.2 Estimation of Nano-Foam Model Parameters.....	72
4.4.2.1 Tuning $epdry$ to Improve the Nano-Foam Model Parameters Estimation	74
4.4.2.2 Validation of Best-fit and Tuned-fit Nano-Foam Model Parameters Flow Behaviour using a Commercial Simulator...	75
4.4.2.3 Gaps Identified in the Current Foam Model Parameters Estimation Method in the Presence of Nanoparticles	77
4.4.3 Modified Foam Model Parameter Function for Nano-Foam	79
4.5 Chapter Summary	81
CHAPTER 5 CONCLUSION AND RECOMMENDATION	84
5.1 Conclusions	84
5.2 Recommendations.....	85

LIST OF FIGURES

Figure 2.1: Potential mechanisms of liquid film stabilization. (a) a monolayer of bridging particles, (b) a bilayer of close-packed particles, and (c) a network of particle aggregates (gel) inside the film. Reproduced from Horozov [30].	12
Figure 2.2: Foamability reduction noted with decreasing cationic cetyltrimethylammonium bromide (CTAB) surfactant concentration at fixed silica nanoparticles (SNPs) concentration of 0.1 wt.%. Adapted from Hu, et al. [49].	15
Figure 2.3: Hydrophilic and hydrophobic nanoparticles at their respective contact angle. Adapted from Binks, et al. [54].	16
Figure 2.4: Hydrophilic nanoparticles stabilization mechanism against film rupture as liquid continuously drained from the foam film or lamellae. Adapted from Vatanparast, et al. [56].	17
Figure 2.5: Representation of electrostatic repulsion behaviour in the absence (left) and presence of salt ions (right). Adapted from Vatanparast, et al. [56].	19
Figure 2.6: Effect of (a) monovalent salt ions (Na^+) and (b) divalent salt ions (Ca^{2+}) concentration on the foamability of the nano-ash-AOS mixture. Reproduced from Eftekhari, et al. [4].	20
Figure 2.7: Apparent foam viscosity for a single foam quality scan at constant total velocity. Adapted from Lotfollahi, et al. [17].	23
Figure 2.8: Foam behaviour scan. Reproduced from Cheng, et al. [82].	27
Figure 3.1: Research flow chart.	29
Figure 3.2: Composition of seawater.	31
Figure 3.3: Schematic diagram of Anton Paar foam tester.	33
Figure 3.4: Schematic diagram of flow loop rheometer. Reproduced from Ahmed, et al. [87].	34
Figure 3.5: Schematic diagram of the sand-pack foam flooding system. Reproduced from Hadian Nasr, et al. [89].	35

Figure 4.1: Partial hydrophobic silica nanoparticle and MFOMAX mixture at (a) 1.5:1, (b) 1:1, and (c) 1:2 concentration ratio and 1.5 wt.% NaCl shows particles precipitated at the bottom of the beaker.....	50
Figure 4.2: Hydrophilic silica nanoparticles and MFOMAX mixture at (a) 1:4, (b) 1:2, (c) 1:1, and (d) 2:1 concentration ratio and 2.0 wt.% NaCl show clear solution indicating well-dispersed nanoparticles up to 12 hours.	51
Figure 4.3: Hydrophilic silica nanoparticles and MFOMAX mixture at 1:4 (a), 1:2 (b), 1:1 (c), and 2:1 (d) concentration ratio and 3.0 wt.% NaCl. (c) shows a cloudy solution for 1:1 nanoparticles-surfactant ratio after 30 minutes, indicating the start of nanoparticle segregation.	52
Figure 4.4: Hydrophilic silica nanoparticles and MFOMAX mixture at 1:4, 1:2, 1:1, and 2:1 concentration ratio and 5.0 wt.% NaCl shows a cloudy solution. All nanoparticles-surfactant mixtures are cloudy and precipitate within the first 3 hours.	53
Figure 4.5: Foam half-life measurements at varying nanoparticles-surfactant concentration ratio at 2.0 wt.% NaCl. (x-mark represents repeated tests values)	54
Figure 4.6: Foam half-life measurement of MFOMAX foam and nano-foam at a fixed concentration ratio (0.5) and varying salinity.	55
Figure 4.7: Apparent foam viscosity trend over time in the absence and presence of nanoparticles during rheology experiment at 70% foam quality and a shear rate of 250 s ⁻¹	57
Figure 4.8: Shear rate versus shear stress in the absence and presence of nanoparticles during rheology experiment at 70% foam quality.	58
Figure 4.9: Foam viscosity curve in the absence and presence of nanoparticles during rheology experiments at 70% foam quality.	58
Figure 4.10: Foam viscosity curve with increasing nanoparticles concentration at fixed 0.3 wt.% surfactant concentration at 70% foam quality.	59
Figure 4.11: Foam viscosity curve at optimum nanoparticles-surfactant ratio and varying foam quality.	60
Figure 4.12: Mobility reduction ratio (MRF) with increasing foam quality in the absence and presence of nanoparticles. Foam collapse occurs beyond transition foam quality for surfactant-foam (in green dash line) and nano-foam (in black dash line).	

Unlike surfactant foam (in blue dash line), nano-foam (in orange dash line) does not immediately collapse after the transition foam quality.....	62
Figure 4.13: The effect of nanoparticle concentration at transition foam quality (70%) and 95% foam quality.	64
Figure 4.14: The effect of total injection rates at fixed foam quality in the absence and presence of nanoparticles.	66
Figure 4.15: Effect of salinity in the absence and presence of nanoparticles.	68
Figure 4.16: Effect of <i>fmmob</i> toward foam strength at increasing foam quality.	70
Figure 4.17: Effect of <i>fmdry</i> toward foam strength at increasing foam quality.....	71
Figure 4.18: Effect of <i>fmdry</i> toward apparent foam viscosity at varying water saturation.....	71
Figure 4.19: Effect of <i>epdry</i> toward foam strength at increasing foam quality.....	72
Figure 4.20: Nanoparticle-surfactant foam fitted behaviour.....	73
Figure 4.21: Tuned foam model parameter (<i>epdry</i>) fit for nanoparticles-surfactant foam.	74
Figure 4.22: Differential pressure trend of nanoparticles-stabilized foam modelling in CMG STARS utilizing estimated foam parameters for steady-state co-injection at 70% foam quality; best-fit nano-MFOMAX, tuned with low <i>epdry</i> as well as tuned with high <i>epdry</i>	76
Figure 4.23: Differential pressure trend of nanoparticles-stabilized foam modelling in CMG STARS utilizing estimated foam parameters for steady-state co-injection at 95% foam quality; best-fit nano-MFOMAX, tuned with low <i>epdry</i> as well as tuned with high <i>epdry</i>	76
Figure 4.24: Summary workflow or the conditions for tuning <i>epdry</i> parameters.	79
Figure 4.25: A comparison of foam model parameter fit curve for tuned-foam model fit in dotted-line (low- <i>epdry</i> and high- <i>epdry</i>) and modified <i>Fdry</i> -out function in dashed-line (at <i>epcon</i> = 1.0 and best-fit <i>epcon</i> = 0.04).....	80

LIST OF TABLES

Table 2.1: Summary of recent parameter fitting methods utilizing foam quality scan dataset.	28
Table 3.1: Properties of nanoparticles	30
Table 3.2: Properties of sodium chloride.....	31
Table 3.3: Properties of N ₂ gas at standard conditions.	31
Table 3.4: List of samples prepared for Nanoparticles-Surfactant Compatibility screening.	37
Table 3.5: List of samples prepared for bulk foam stability test.	38
Table 3.6: Range of parameters tested during foam flooding analysis.....	41
Table 4.1: Summary of flow loop rheometer experiment runs.....	56
Table 4.2: Estimated foam model parameters in the presence of nanoparticles.	73
Table 4.3: Tuned foam model parameters (low <i>epdry</i> and high <i>epdry</i> value) in the presence of nanoparticles using the current foam model function.	74

CHAPTER 1

INTRODUCTION

1.1 Research Background

Injection of Surfactant foam, which from this point onwards will be referred to as foam, was introduced to improve gas injection sweep efficiency by reducing gas mobility. Foam is generated by injecting gas into a surfactant-containing liquid phase. The injected gas is not a continuous phase in the foam. Instead, it is trapped in bubbles surrounded by a thin liquid film known as lamella. The foam can improve oil recovery by several mechanisms. Trapping gas in lamellae slows down its flow inside the reservoir, thus increasing its apparent viscosity and reducing gas channelling. In addition to that, the foam can form in a higher permeability regime, thus allowing the propagation of fluid to flow and sweep into low permeability areas [1, 2]. However, the foam has a limit in propagation due to its low stability at high temperatures and when in contact with oil [3, 4]. A stable foam allows deeper propagation into the reservoirs, thus improving the sweep efficiency further.

The nanoparticles have been proven to improve foam stability through laboratory analysis. A longer foam half-life was observed in nanoparticles' presence compared to surfactant foam [4-10]. In a laboratory study by Prigiobbe, et al. [11] observed that the maximum value of the pressure gradient of foam with nanoparticles was approximately two times larger than foam by surfactant, only indicating improved foam stability when nanoparticles are present. An increase in nanoparticles-stabilized foam (from now on referred to as nano-foam) apparent viscosity was also observed by Singh and Mohanty [12] and Li, et al. [13] during their foam flooding through porous media experiments. Extensive laboratory foam stability experiments and core flooding experiments have

been used to validate the benefits of nano-foam; therefore, more simulation studies and pilot tests are necessary [14].

Two modelling approaches have been described in the literature to simulate foam flooding processes; mechanistic and empirical models [15]. A mechanistic model simulates the full physics of foam's reaction rates as a component. Challenges associated with this modelling approach are its complexity and difficulty in identifying model parameters [16]. The empirical model, on the other hand, assumes local equilibrium. Laboratory data is used to tune the seven foam modelling parameters that describe the gas mobility reduction factor (MRF). The seven parameters are surfactant concentration, oil saturation, shear-thinning velocity, capillary pressure, oil composition effect, salinity, and water saturation or dry-out effects [17].

Previous research [18, 19] has attempted and successfully modelled nano-foam flow behaviour using mechanistic modelling. Although the mechanistic model is more robust, the local equilibrium approximation equally honours the physics of foam behaviour in porous media [20]. In addition to that, the empirical model technique has commonly been used in reservoir simulation analysis due to its simplicity as it assumes a local steady-state and quick simulation time [17, 21]. Nevertheless, there is still limited research reported that could be found on nano-foam empirical modelling [22]. This study attempts to evaluate the applicability to model nano-foam using an implicit texture model solely on the foam stability improvement in the presence of nanoparticles, excluding the limiting factors that deteriorate the foam performance, to increase the magnitude of nano-foam performance for evaluation. Since the empirical model uses laboratory data to determine the foam model parameters [17, 20, 23, 24], it is crucial to confirm that the fitting parameters can represent the nano-foam behaviour.

1.2 Problem Statement

This study attempts to evaluate the applicability to model nano-foam using an implicit texture model as a function of foam stability and performance improvement in the presence of nanoparticles and in the absence of oil. The knowledge gaps identified

through the literature related to nano-foam flow behaviour are described in the following paragraphs.

Creating a homogeneous and stable nanofluid mixture is a challenge due to nanoparticle agglomeration [14]. An optimum concentration exists, and different surfactant types, combined with different nanoparticle types, may affect stability due to their synergic interaction [25]. Silica nanoparticles were chosen based on an extensive nanoparticle screening evaluation at high temperature and in the presence of light oil by Razali, et al. [26] with the same surfactant. Therefore, the compatibility test between silica and MFOMAX will be re-established to determine the optimum surfactant and nanoparticle concentration ratio under the standard conditions and in the absence of oil.

Surfactant foam generally exhibits shear-thinning behaviour, and it is one of the implicit texture foam model parameters [3, 17, 27]. However, recent studies reported contradicting nano-foam rheology behaviour with increasing shear rate, salinity, and foam quality [28, 29]. It is crucial to identify and understand the nano-foam rheological behaviour since the shear-thinning velocity effect is one of the essential foam model parameters required in the empirical model.

Several parameters affect the nano-foam stability, which is related to the nanoparticle-stabilized foam mechanism. One of those is particle arrangement at the lamellae during film drainage, which in turn depends on nanoparticle concentration [30]. However, contradictory findings were highlighted in the literature where the optimum nanoparticles-surfactant ratio was higher in Yekeen, et al. [31] and Li, et al. [32], and a lower ratio was observed by Razali, et al. [7]. Similarly, contradicting findings were observed with nanoparticle surface wettability. Based on the nanoparticles' stabilization mechanism, partially hydrophobic nanoparticles effectively enhance foam stability by adhering to the gas-liquid interface [30]. However, Singh and Mohanty [33] visually observed the retarding process of liquid draining from lamellae consisting of hydrophilic nanoparticles, thus improving the foam stability. With these conflicting reports, it is crucial to identify the critical parameters affecting nano-foam stability and their relative effects to enhance the understanding of their associated stabilization mechanism and behaviour.

As briefly discussed earlier, the foam flow can be modelled using a mechanistic population balance or empirical modelling techniques [17]. Researchers [18, 34] have conducted nano-foam modelling analysis using mechanistic population balance modelling techniques. However, such techniques are associated with complexity and difficulty in determining the foam model parameters [17]. The empirical model incorporates the foam effect by modifying gas mobility based on the fractional flow theory. The gas mobility is modified based on foam model parameters fitted to experimental data. However, the nano-foam collapse behaviour may be different from surfactant foam behaviour due to the nanoparticles' stabilization mechanism [30, 35, 36]. Therefore, identifying and validating foam models' parameters to represent nano-foam behaviour is a crucial step in empirical model.

1.3 Research Objective

The research's general objective was to assess the applicability and establish an effective approach to estimate the model's parameters for implicit texture modelling for foam flooding with nanoparticles as a stabilizer. The specific objectives were as follows:

1. To re-established silica nanofluid mixture compatibility tests with the surfactant at standard conditions in the absence of oil.
2. To assess the rheological behaviour of nano-foam as a function of nanoparticle concentration, shear rate, and foam quality.
3. To compare the mobility reduction factor obtained in surfactant foam and nano-foam flooding under the influence of nanoparticles concentration, salinity, foam quality, and total injection rate.
4. To assess the applicability of the existing foam model to the Dry-Out function used in the implicit texture modelling technique to incorporate nanoparticle effects.

1.4 Significant of Research

The rheology of nano-foam and surfactant-foam as a function of nanoparticle concentration, shear rate, and foam quality is established using a flow loop rheometer. The study provides an understanding of the conditions when nano-foam will exhibit shear-thinning behaviour and validates the conflicting results observed in the literature. The current implicit texture foam model assumes that foam is shear-thinning. The study will determine if enhancing the shear-thinning function in the model is necessary for nano-foam modelling.

Critical parameters affecting the mobility reduction factor of nano-foam and surfactant foam have been identified as a function of nanoparticle-surfactant concentration, foam quality, salinity, and total injection rates. Sensitivity analysis of these parameters provides crucial inputs on the factor that significantly affects the nano-foam mobility reduction factor. In addition to that, a comparison with surfactant foam performance provides insight into the nanoparticle stabilization mechanism during nano-foam flow and serves as an input into the modelling analysis.

The nanoparticle stabilization mechanisms described in the literature mainly hamper foam from collapsing at very high foam quality conditions. However, the implicit texture model foam dry-out function assumes that foam will immediately collapse upon reaching its critical capillary pressure to coalesce. The modelling analysis will verify whether the current foam model can simulate the nano-foam flow behaviour in porous media. A modified Dry-Out function applicable in implicit texture modelling for nano-foam is proposed to increase the accuracy of the prediction behaviour.

1.5 Scope of Study

The scope of this study consists of experimental and modelling analysis, as described in the following paragraphs. Silica nanoparticles were utilized for this study based on the extensive research by Razali, et al. [26] on nanoparticle screening evaluation and findings, as the same surfactant was used. Based on the research, additional enhancement is needed to further improve the nanofluid stability at high

temperatures and in the presence of oil. The current study attempts to evaluate the applicability to model nano-foam using an implicit texture model solely on the foam stability improvement in the presence of nanoparticles. The experimental activities were conducted at the standard condition and oil-free conditions to increase the magnitude of nano-foam performance with respect to the foam stabilization mechanism for evaluation. Therefore, the effect of the limitations in this study can be extended in future research.

A preliminary nanoparticle screening through a nanofluid mixture compatibility test with the MFOMAX surfactant was repeated at standard conditions without oil. Silica nanoparticles were chosen for this study based on a previous research [26] due to their low cost and good compatibility with the formation. Two types of nanoparticles were screened: hydrophilic and slightly hydrophobic silica nanoparticles. Nanoparticles that can remain dispersed in the surfactant solution for a minimum of 6 hours or more at 30,000 ppm salinity were chosen for this study.

The rheological behaviour study for surfactant foam and nano-foam was conducted using a foam rheometer at room temperature. The nitrogen gas was employed to generate the foam in the flow loop as it generates a more durable foam. The flow loop pressure was fixed at 500 psi due to the limitation of the nitrogen gas pressure supply. A flow curve or a viscosity curve was established by shearing the generated foam at five (5) different shear rates for each parameter tested. A total of 22 flow curves were established at varying nanoparticle concentrations, foam quality, and salinity for rheological behaviour comparison.

The foam flooding experiments were conducted using a sand pack flooding system. The experiments were performed at room temperature and standard conditions using a tightly packed sand pack of a mixture of quartz river sand grains of various sizes (between 212 and 425 microns) and cemented with silica flour. High porosity and permeability were desirable in the sand pack to mitigate the capillary end effect. Nitrogen gas was co-injected into the system to generate foam. The experimental analysis was designed to study the nano-foam behaviour by testing one factor at a time (OFAT) at varying nanoparticle concentrations, salinities, foam qualities, and total injection rates. A total of 33 foam flooding experiments have been performed. For easy

performance comparison, the surfactant concentration was fixed throughout the experiments.

The foam modelling analysis was conducted using the implicit texture model method. The analysis focused on estimating the critical foam model parameters: the reference mobility reduction factor, shear-thinning velocity effect, and the foam dry out effect. Fitting to experimental data established for foam quality scan and foam velocity scan determines foam model parameters. The foam dry-out function in the implicit texture model was revised based on the nano-foam behaviour observed in the foam quality scan. The revised foam dry-out function was established through curve fitting with the experimental data.

1.6 Organization of the Thesis

This thesis comprises five chapters, the details of which are briefly described below:

- Chapter 1 describes the background of the nano-foam EOR application and the existing gaps in the area. The chapter also includes an overview of the research, a brief description of the issues, the research objectives, and the significance of the study to the field of interest.
- Chapter 2 presents a literature review survey and critically evaluates the solution methods available in the area of the study available in the literature. The comprehensive review includes the nanoparticle stabilization mechanisms, parameters affecting nano-foam performance, experimental methods of foam stability measurements and foam flow experiments, as well as the current modelling method to date.
- Chapter 3 discusses the methodology used in this study. All the material and equipment utilized in this study are explained in detail along with all related experimental procedures. The enhancement and details of the foam model used in this study are also presented.

- Chapter 4 demonstrates the results and discussion of this study. This chapter elaborates on the critical findings observed for nano-foam rheology behaviour, the critical parameters affecting nano-foam stability, and different nano-foam collapse behaviour observed as opposed to conventional foam. The observed behaviour was used to identify foam model parameters and optimize foam model function.
- Chapter 5 summarizes the results and concludes the study along with future recommendations.

CHAPTER 2

LITERATURE REVIEW

The current chapter presents a comprehensive literature review about foam flooding considering the mentioned objectives of this study. Firstly, the fundamentals of foam application are discussed, followed by the use of nanoparticles in foam application. Secondly, the nanoparticle stabilization mechanism in foam is explained. Thirdly, an overview of critical parameters affecting nano-foam flow performance is discussed. In the last section, the current foam modelling techniques are discussed, emphasising empirical foam modelling and the methods available to determine foam model parameters in the literature.

2.1 Fundamental of Foam

The foam was introduced to improve the sweep efficiency during the gas injection process—the foam consists of gas and water with surfactants acting as the foaming agents. Foam is a gas phase dispersed in a liquid phase known as lamellae. The gas phase trapped between lamellae aims to increase gas relative viscosity and decrease gas mobility in porous media [37, 38]. The number of separated bubbles per unit volume is known as foam texture. Finely textured foam has lots of lamellae; thus, the bubble size is smaller. Finely textured foam leads to significant mobility reduction and is hence referred to as a “strong” foam, while coarser foam with a larger bubble size is referred to as “weak” foam [39]. In some cases, the surfactant may be designed to have dual functions, as a foamer and as an agent to reduce interfacial tension, contributing to the enhancement of oil recovery.

2.2 Nanoparticles in Foam Application

Although surfactants have been commonly used as foaming agents to improve gas flood sweep efficiency, they suffer from low stability in reservoir conditions. Nanoparticles-stabilized foam has been observed to have the ability to withstand harsh environments and high-temperature conditions [14]. It has also been proven to have a higher apparent viscosity than surfactant foam in previous laboratory research [4, 18, 40]. Nanoparticles, often ranging from 1 to 100 nanometres in diameter, have low retention in geological formations [41]. In addition to that, nanoparticles can be manufactured with specific characteristics to meet certain emulsion quality, texture, and stability [42].

2.3 Nanoparticles Stabilization Mechanism

The nanoparticle stabilization mechanism has been extensively described in previous research [30, 36, 43, 44]. Three mechanisms are described: the particle attachment energy, the particle arrangement mechanism, and the enhancement of maximum capillary pressure to coalescence. Details of these mechanisms are provided in the following subsections.

2.3.1 Particle Attachment Energy

Nanoparticles have been described as having the ability to position themselves at the film surface of the lamellae. Nanoparticles can either locate themselves inside the film or at the gas-liquid interface, where some nanoparticles are firmly attached to the film's surface [30]. A particle can attach itself to the film's surface when the particle attachment energy required is achieved [44]. The attachment energy (E) of a single, spherical nanoparticle to air-water surfaces is given by Equation (1):

$$E = \pi R^2 \gamma (1 - \cos \theta)^2 \quad (1)$$

where R is the particle radius, θ is the contact angle, and σ is the air-water surface tension. The equation suggests that extremely hydrophilic particles ($\theta < 90^\circ$) and hydrophobic particles ($\theta > 90^\circ$) do not stabilize foam. An increase in attachment energy is equivalent to an increase in foam stability, as an equivalent amount of energy is required to separate a particle from the air-water surface. Maximum possible attachment energy can be achieved at the condition where a particle is neither hydrophilic nor hydrophobic at $\theta = 90^\circ$ [36, 44].

2.3.2 Particle Arrangement Mechanism

Horozov [30] observed that nano-foam stability is a function of the particle's ability to form a barrier around gas bubbles, stabilize the lamellae in between the bubbles, and form a three-dimensional network in the bulk-aqueous phase. The barrier is critical during the thinning of lamellae or liquid films separating the gas bubbles. At this condition, the foam lamellae are bound to collapse as the capillary pressure exerted on them is higher than their critical capillary pressure to coalesce.

The nanoparticle re-arrangement was observed as the water drained out of the lamellae [30]. As the thick film is forced to thin, the particles inside the film exist in a loosely packed monolayer arrangement. Particles in this arrangement cannot resist the hydrodynamic flow and are drawn away from the centre, thus leaving the thinnest part of the film vulnerable to rupture. A continuously thinning film then causes the nanoparticles to form a packed bilayer arrangement with the nanoparticles attached on the opposite film surface—further lamellae thinning causes re-arrangement of the nanoparticles to form a closed-pack monolayer. In contrast to particles in a dilute monolayer, a closed-pack monolayer can oppose the hydrodynamic flow, thus slowing down the film thinning and rupture.

The nanoparticle concentration is a crucial parameter in the particle arrangement mechanism. A closed-pack nanoparticle arrangement can easily be achieved in the lamellae at a high nanoparticle concentration. In addition to that, the excess nanoparticle can form a three-dimensional network particle in the foam film, as shown

in Figure 2.1 (c). The nanoparticle network will keep the bubble well separated and prevent the lamellae from rupturing in this condition.

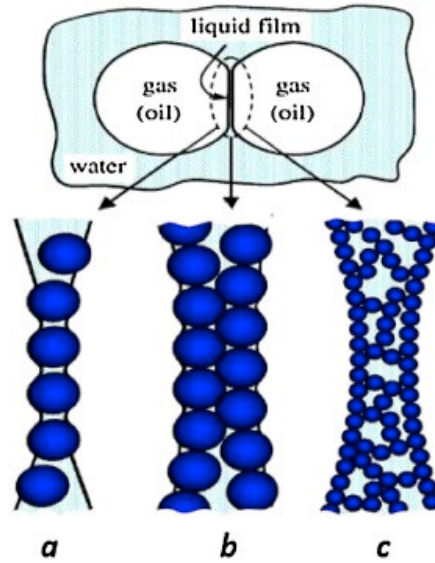


Figure 2.1: Potential mechanisms of liquid film stabilization. (a) a monolayer of bridging particles, (b) a bilayer of close-packed particles, and (c) a network of particle aggregates (gel) inside the film. Reproduced from Horozov [30].

2.3.3 Maximum Capillary Pressure to Coalesce

To stabilise the foam, the nanoparticle must exist either at the gas-liquid interface or inside the liquid film [36]. Two conditions describe the nanoparticle stabilization mechanism through maximum capillary pressure to coalesce. The first condition, where the nanoparticles exist at the gas-liquid interface, is described by particle attachment or detachment energy. The second condition was described by ENREF 14 Denkov, et al. [43], where maximum capillary pressure (P_c^{max}) was introduced to define a thin liquid film's stability in between bubbles, represented by Equation (2).

$$P_c^{max} = p^* \frac{2\sigma}{R} \quad (2)$$

where p^* is a parameter that describes the interface coverage by particles and particle arrangement in the liquid film, R is the spherical solid particle's radius, and σ is the

interfacial tension between gas and liquid. The higher the value of P_c^{max} , the higher pressing forces a thin liquid film can withstand between two bubbles.

An equation for maximum capillary pressure, which includes particle stability at the interface, is described in Equation (3). The corresponding p and z are parameters for different particle arrangements and contact angles, respectively [36]. Based on Equation (3), it is observed that capillary pressure to coalescence in the presence of nanoparticles in the liquid film is higher compared to conventional foam liquid film. This allows the thin film between bubbles to withstand higher forces before rupture.

$$P_c^{max} = p \frac{2\sigma}{R} (\cos \theta + z) \quad (3)$$

2.4 Critical Parameters Affecting Nanoparticles-surfactant Foam Performance

Surfactant foam performance is mainly affected by surfactant concentration, gas type, oil saturation, salinity, temperature, and pressure. Additional parameters were identified to affect foam stability in the presence of nanoparticles, such as nanoparticle types, size, shape, wettability, and concentration. Nanoparticles and surfactant concentrations, injection rate, foam quality, and salinity are among the parameters that critically affect nano-particle-surfactant foam performance reported in the literature [45].

2.4.1 Effect of Nanoparticle and Surfactant Concentration

The effect of nanoparticle concentration on foam stability has been revealed experimentally by previous research. The enhancement of foam stability was observed with bulk foam stability and the improvement of average pressure drop, apparent viscosity, and additional oil recovery in flooding experiments [10, 13, 28, 31, 46-50].

The foam half-life was reported to increase with increasing nanoparticle concentration, even in the presence of decane [28, 47]. An increase in differential pressure and apparent foam viscosity was observed in high temperatures and pressure

conditions using a capillary tube [13]. The nanoparticles improve the apparent foam viscosity and enhance sweep efficiency, increasing oil recovery at a core-scale investigation at reservoir conditions [48].

Although enhancement of foam stability at increasing nanoparticle concentration has been proven in laboratory analysis, some findings conclude the detrimental impact of nanoparticle concentration on foam stability and foamability. AlYousef, et al. [51] observed that increasing nanoparticle concentration does not necessarily enhance foam stability and significantly reduces foamability. This behaviour occurs when the nanoparticles and surfactants used in a system have charge interaction.

In addition to that, an earlier study by Hu, et al. [49] has also reported a reduction in foamability, mainly when nanoparticles and the surfactant utilized are opposite-charged, as presented in Figure 2.2. As nanoparticle concentration rises, more surfactant molecules are adsorbed on nanoparticle surfaces. Subsequently, zeta potential reduction was observed experimentally [50]. Zeta potential is an exponential variance between the outer boundary, an immobile stern layer of the nanoparticle, and the bulk solution. Reduction in zeta potential or zero zeta potential is achieved when the concentration of ions attached to the surface and the nanoparticles' surface charge attain equilibrium [52]. Since surfactant molecules are attached to the nanoparticle's surface charge, fewer surfactant molecules are available in the mixture, thus decreasing the nanoparticle-stabilized foam's foamability [31, 50]. Parallel findings were observed by AlYousef, et al. [51] using hydrophilic silica in three non-ionic surfactants.

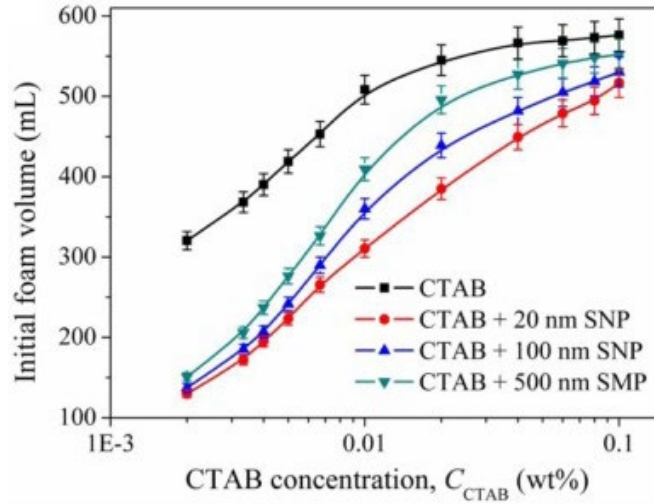


Figure 2.2: Foamability reduction is noted with decreasing cationic cetyltrimethylammonium bromide (CTAB) surfactant concentration at a fixed silica nanoparticles (SNPs) concentration of 0.1 wt.%. Adapted from Hu, et al. [49].

In summary, it has been observed that rising nanoparticle concentration may possibly enhance foam stability. However, it may also decrease its foamability subject to the nanoparticles and surfactant type used. Hence, it is essential to identify the optimum nanoparticle concentration to obtain optimum foamability and foam stability with the selected surfactant prior to any NP-surfactant foam actual application due to their synergistic interaction [14, 25, 53].

2.4.2 Effects of Nanoparticles Surface Wettability

Nanoparticle surface wettability has been reported as a dominant parameter in the nanoparticle foam stabilization mechanism [44]. The nanoparticle surface wettability is the contact angle between the particles and the gas-liquid surface. Hydrophilic particles have a contact angle of less than 90° , and a considerable fraction is in the liquid phase. A particle with these contrasting characteristics is a hydrophobic nanoparticle, as shown in Figure 2.3 [54].

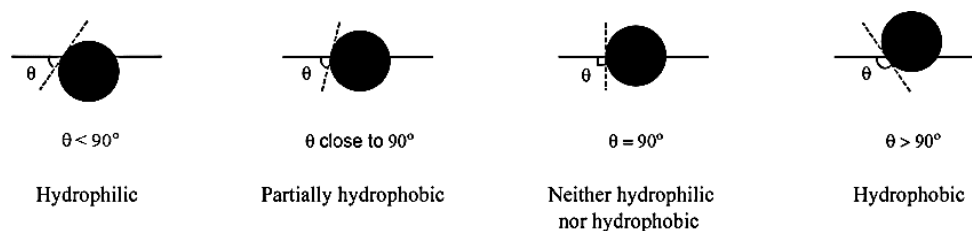


Figure 2.3: Hydrophilic and hydrophobic nanoparticles at their respective contact angles. Adapted from Binks, et al. [54].

Hydrophilic nanoparticles were found to enhance foam stability, although the particles do not firmly attach to the gas-liquid interface [30, 55]. Singh and Mohanty [33] visually witnessed the retarding process of liquid draining from foam lamellae comprising hydrophilic nanoparticles in anionic surfactant utilizing a confocal microscopy image. Their results revealed that the lamellae thickness was thicker in nanoparticles' presence, suggesting slow liquid drainage. The foam film became planar once the critical film thickness was achieved, and additional draining of liquid in the lamellae caused the liquid to be drawn toward the particles. The nanoparticle packing and re-arrangement in the lamellae stabilized the foam film. As shown in Figure 2.4, nanoparticles may be rearranged from a bi-layer to a monolayer arrangement. Most notably, hydrophilic nanoparticles in a similar charge surfactant environment do not decrease foamability. By contrast, it elevates the surfactant adsorption onto the gas-liquid interface via electrostatic repulsion, thus effectively lowering the solution's interfacial tension [56].

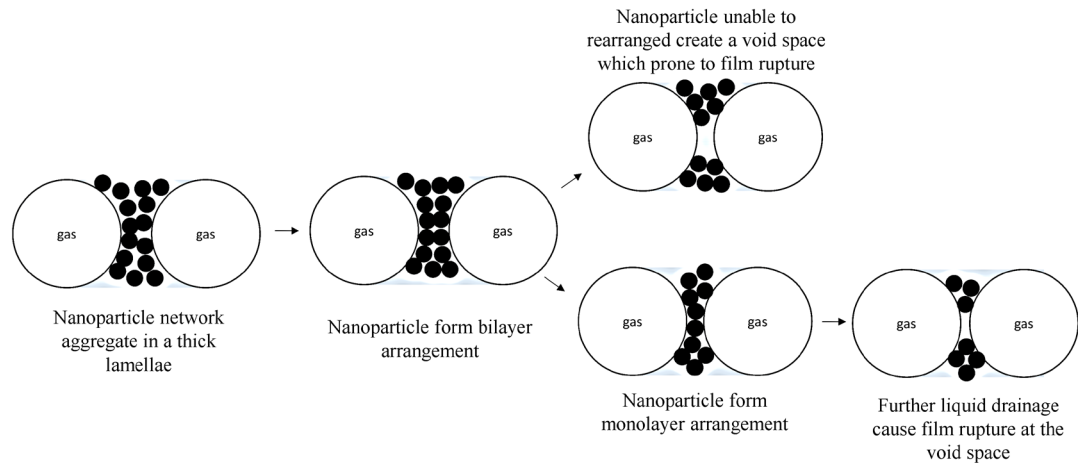


Figure 2.4: Hydrophilic nanoparticle stabilization mechanism against film rupture as liquid continuously drains from the foam film or lamellae. Adapted from Vatanparast, et al. [56].

Partially hydrophobic nanoparticles were found to enhance foam stability by binding to the gas-liquid interface. These nanoparticles can achieve the maximum attachment energy with a contact angle close to 90° , thus improving foam stability [30, 36, 43, 44]. In the presence of negatively charged silica nanoparticles with a cationic surfactant, Arriaga, et al. [57] reported an improvement in the bulk foam stability of nano-foam at a partially hydrophobic state. As the nanoparticles become partially hydrophobic, the contact angle improves along with the foam stability. However, an increase in contact angles beyond 90° could create big aggregates. Thus, it reduces the foam stability as nanoparticles cannot “be attached” at the gas-liquid interface due to gravitational force [55]. Nevertheless, the improvement of foam stability was more significant for partially hydrophobic nanoparticles [46]. Therefore, characterization of the contact angle of nanoparticles used to maximize foam stability is essential as it correlates to different nanoparticle stabilization mechanisms of foam.

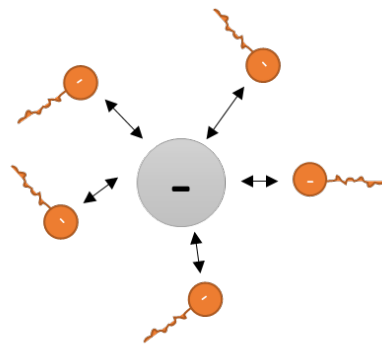
2.4.3 Effect of Salinity

To date, several researchers have observed an unfavourable effect of salinity on nanoparticle-stabilized foam performance. Noor, et al. [8] explored foam stability at different Alpha Olefin Sulfonate (AOS) surfactant, silica nanoparticle, and brine

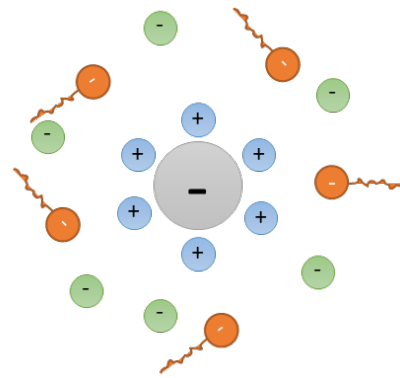
concentrations using foam half-life and bubble size analysis under standard conditions. Their findings show that adding 1.0 wt.% of sodium chloride (NaCl) decreased the nanoparticles-stabilized foam stability as larger foam bubbles were formed, causing rapid foam collapse. A similar conclusion was observed by Xiao, et al. [29] via dynamic foam stability measurement. They discovered that the maximum foam apparent viscosity was achieved at a lower foam quality, indicating that the solution's salt ions lessened the nanoparticle-stabilized foam's stability as the foam collapse was initiated earlier.

On the contrary, Li, et al. [13] reported that foam half-life was significantly improved with increasing salinity between 2 wt.% and 10 wt.%, although the foamability was slightly decreased. Similar results were also observed by Xu, et al. [58] and Qian, et al. [59] up to 5 wt.% salinity.

Different results may be due to numerous ionic interactions between salt, nanoparticles, and surfactants being used. Several researchers saw that increasing the salinity caused aggregation due to the reduction in surface tension and zeta potential as shown in **Figure 2.5**, thus reducing foam stability [56, 60]. As exhibited in **Figure 2.6**, monovalent salt ions have been reported to have a minor impact on foam stability in contrast to divalent salt ions [61]. This is due to better divalent cation screening of nanoparticle charges compared to monovalent cations [4, 50, 60-62] as the presence of electrolytes alters the free energy of the double-layer formation at the particle surface, thus reflected in the value of contact angle and the ability of the particle to absorb at the gas-liquid interface [63]. Such observation was demonstrated based on changes in nanoparticle surface contact angle [63] and via generated nano-foam with similar mobility, consistency, and stability in 10.0 wt.% NaCl in comparison with 1.0% CaCl₂ [64]. Though the nanoparticles' interaction with salt ions was limited, laboratory analysis had successfully crafted a highly stabilized foam using nanoparticles at high salinity conditions [65]. Therefore, additional research may be performed to understand the actual mechanism between nanoparticles and salt ions in the presence of surfactant molecules and their effect on nanoparticle fluid mixture stability and the stabilized foam performance.



Repulsion of similar charges nanoparticles and surfactant molecules in the absence of salt ions



Positive charged salt ions attracted onto the nanoparticles surface reducing the electrostatic repulsion

Figure 2.5: Representation of electrostatic repulsion behaviour in the absence (left) and presence of salt ions (right). Adapted from Vatanparast, et al. [56].

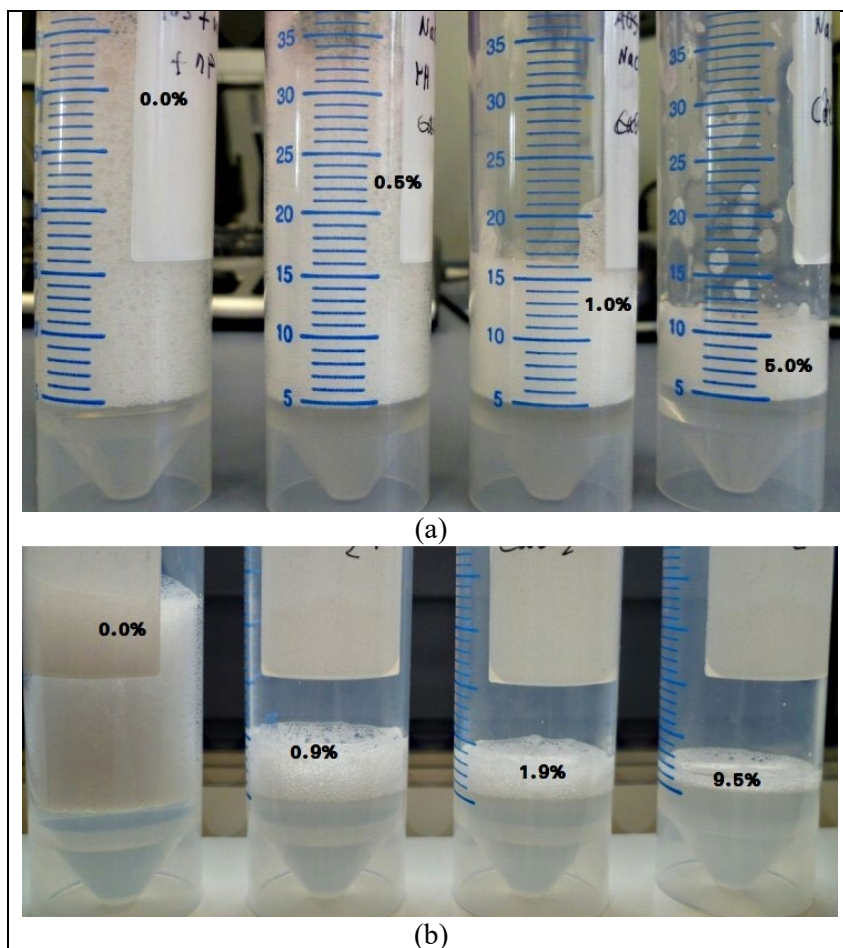


Figure 2.6: Effect of (a) monovalent salt ions (Na^+) and (b) divalent salt ions (Ca^{2+}) concentration on the foamability of the nano-ash-AOS mixture. Reproduced from Eftekhari, et al. [4].

2.4.4 Effect of Flow Velocity

The effect of flow velocity or injection velocity on foam stability is commonly determined during foam flow experiments using a capillary tube [28, 66] or flow experiments in a porous medium [31, 67]. The foam stability is represented by the apparent foam viscosity in this condition. The flow velocity describes the effects of nanoparticle-stabilized foam stability and the foam flow rheological behaviour. A condition in which apparent foam viscosity decreases with increasing velocity describes the shear-thinning flow behaviour [67]. Whereas a condition at which apparent foam

viscosities increase with increasing flow velocity is known as shear-thickening flow behaviour.

Several studies have experimentally reported a reduction in apparent foam viscosity with an increase in flow velocity during foam flow experiments. Yekeen, et al. [61] reported that the apparent foam viscosity reduces with increasing injection flow rates through co-injection flow experiments. The results obtained correspond to shear-thinning behaviour consistent with conventional surfactant foam.

However, Maurya and Mandal [28] reported both shear-thinning and shear-thickening behaviour as the shear rate increased from 1 to 1000 (1/s). It appears that the nanoparticles' surfactant foam exhibits shear thickening behaviour beyond the shear rate of 100 s^{-1} . The behaviour observed occurs at fixed nanoparticles with varying surfactant concentrations and vice versa. The rheology converted from shear-thinning to shear thickening may occur due to the shift in the emulsion's microstructure [68].

Xiao, et al. [29] studied the effect of shear rates on foam rheology at different foam qualities and salinities in the presence of silica nanoparticles using the flow loop apparatus at 1140 psi and a temperature of 40°C . They reported indicating that the foam exhibited shear thinning behaviour at all foam qualities. However, different rheological behaviour was observed at high salinity conditions (5 wt.%), at which foam exhibits pure shear thickening behaviour at all-foam qualities in the absence of oil. In addition to that, they also discovered a critical shear rate upon which nanoparticle surfactant stabilized foam was stable in high salinity conditions.

Based on the discussed findings, it can be concluded that the shear rate is not the only factor affecting the degree of the apparent viscosity. The foam rheology behaviour may vary at different nanoparticles or surfactant concentrations [28] and salinity [29]. It is commonly understood that foam exhibits shear thinning behaviour; however, there is still a lack of understanding of the extent of shear thickening behaviour in nanoparticles-stabilized foam, which called for an in-depth investigation.

2.5 Foam Modelling Technique

The foam implicit texture model will be used in this research to model nano-foam flow behaviour. The foam flow characteristics, the governing equations, and modelling methods are explained in this section.

2.5.1 Foam Propagation and Flow Characteristics

The term “mobility reduction factor” (MRF), unitless, is the ratio of foam mobility to gas. A higher value of MRF describes significant gas mobility reduction, foam stability, and foam strength. Therefore, mobility is considered a critical characteristic of foam flow behaviour. The mobility reduction ratio is measured through pressure drop across the core during foam injection, and it is described in Equation (4).

$$MRF = \frac{\mu_f}{\mu_g} = \frac{\left[\frac{kA\Delta p}{QL}\right]_f}{\left[\frac{kA\Delta p}{QL}\right]_g} = \frac{\Delta p_f}{\Delta p_g} \quad (4)$$

where Q , k , A , L , μ , and Δp are flow rate, absolute permeability, the cross-section area of the core plug, core length, viscosity, and pressure drop across the core, respectively. The subscript “ f ” stands for the foam experiment, and “ g ” represents the gas experiment.

Foam propagation is described by the time required for foam to reach a given depth in the reservoir [69]. Multiple pressure ports along a core can monitor the foam propagation [70]. Several studies have reported that the propagation rate is similar to the injection rate in the absence of oil during core flooding experiments [71-73]. However, a strong dependence of foam propagation on oil saturation was observed by Mannhardt and Svorstøl [73]. Whereby, higher oil saturation decreases foam propagation.

Foam flow characteristics are described by foam quality scans, as shown in Figure 2.7. The consequent foam apparent viscosity at variable foam quality was determined through foam flooding experiments at a fixed total injection velocity. The foam quality

is the ratio of gas to total fluid injected at a specified pressure and temperature, as shown in Equation (5), and the apparent foam viscosity is calculated using Darcy's Equation. It is a function of the pressure gradient concerning foam relative permeability and the total fluid rates injected as described in Equation (6).

$$f_g = \frac{u_g}{u_g + u_l} \quad (5)$$

$$\mu_{app} = \frac{-k_{rg}^f \nabla p}{u_g + u_l} \quad (6)$$

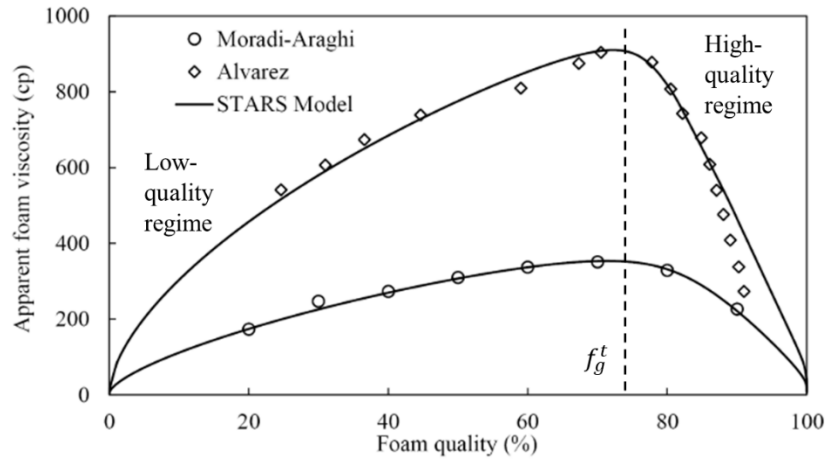


Figure 2.7: Apparent foam viscosity for a single foam quality scan at constant total velocity. Adapted from Lotfollahi, et al. [20].

The foam quality scan consists of a low-quality regime and a high-quality regime, as shown in Figure 2.7. As foam flows through porous media, gas mobility decreases, and the apparent foam viscosity increases with increasing foam quality. The apparent foam viscosity increases until it reaches the maximum achievable value at the transition foam quality, f_g^* . Beyond the transition foam quality, the apparent foam viscosity decreases with increasing foam quality, which describes the foam collapse behaviour. The foam quality scan is a critical input required to simulate the foam flow in porous media.

2.5.2 Empirical Foam Modelling

There are two groups of foam modelling techniques. A mechanistic model is based on the population balance theory, which aims to describe the physics of foam generation and decay [74]. It simulates the effect of bubble size or foam texture on gas mobility through the process of lamellae creation and destruction [20]. A mechanistic model is essential to represent the foam created at the entrance region, the foam propagation at the edge of the foam bank, and conditions in which the foam generation is uncertain [75]. Although the mechanistic model is more robust as it expresses the full physics of foam, it is associated with complexity in determining the foam model parameters [76], thus increasing the computational cost of the simulated runs [77]. In addition to that, there is a limit to measuring the critical mechanistic model inputs, such as the bubble size of foam texture and quantifying the trapped gas fraction in the core's pore throat during laboratory analysis [78]. Previous researches measure the bubble size of foam texture either using view cells at the core outlet, CT scanner, or via micro models [77-79].

Rather than looking at the physics of foam generation and foam decay, empirical models are based on fractional flow in gas mobility reduction, where foam is expressed by modifying gas relative permeability. During foam generation and destruction, the local equilibrium condition is assumed, allowing an abrupt foam collapse at limiting capillary pressure or limiting water saturation [16, 17, 76]. Unlike mechanistic modelling, local equilibrium approximation can be useful for large scale calculation as its solution can be obtained without complex calculation [77]. A recent study has demonstrated nanoparticle stabilized foam modelling using CMG for nanoparticle-stabilized CO₂ foams without surfactant and oil-free conditions [22]. The simulation results were in good agreement with experimental data, and the foam model parameters, reference mobility reduction ($fmmob$), critical water saturation ($fmdry$), and dry-out slope ($epdry$), were affected by water saturation, differential pressure, and apparent viscosity.

In CMG STARS modelling, mobility reduction is described as FM, and it is used to modify gas relative permeability as described in Equation (7).

$$k_{rg\ foam} = FM \times k_{rg} \quad (7)$$

Where mobility reduction occurs, FM is multiplied by gas relative permeability k_{rg} to obtain modified gas relative permeability at the condition in which foam exists. FM is a function of several parameters that affect gas mobility reduction, and it is described as per Equation (8):

$$FM = \frac{1}{1 + fmmob \times F_1 \times F_2 \times F_3 \times F_4 \times F_5 \times F_6 \times F_{dry}} \quad (8)$$

$fmmob$ is the maximum mobility reduction of gas and is also known as a reference mobility reduction factor. All foam model parameters except $fmmob$ are constrained to a maximum value of 1, as they will only reduce the effect of the gas mobility reduction factor. The parameters affecting gas mobility reduction in foam modelling are surfactant concentration (F_1), oil saturation (F_2), shear-thinning velocity (F_3), foam generation (F_4), oil composition (F_5), salinity (F_6), and foam dry-out (F_{dry}).

2.5.3 Foam Model Parameter Fitting Method

The determination of foam model parameters is the first step in the foam modelling process. Foam model parameters are computed based on foam behaviour, mainly the changes between low-quality regimes and high-quality regimes. There are two types of laboratory data utilized to identify model parameters; pressure-drop contours as a function of the superficial velocity of gas and water [80, 81] or foam quality scan, which is used in CMG empirical foam modelling as in **Figure 2.7**.

To date, the foam model parameter fitting method has commonly focused on fitting the reference foam mobility factor ($fmmob$), the shear-thinning velocity effect (F_3) in the low-quality regime, and foam collapse due to critical capillary pressure ($F_{dry-out}$) for the high-quality regime [3, 17, 76, 82]. The functions of F_{dry} and F_3 are given in Equations (9) and (10), respectively.

$$F_{dry} = 0.5 + \frac{\arctan(epdry \times (S_w - fmdry))}{\pi} \quad (9)$$

$$\text{If } N_{ca} > f_{mcap}, F_3 = \left(\frac{f_{mcap}}{N_{ca}} \right)^{epcap}; \quad (10)$$

else, $F_3 = 1$,

with,

$$N_{ca} = \frac{k \nabla p}{\sigma_{wg}} \quad (11)$$

where S_w , N_{ca} , k , ∇p , σ_{wg} are the water saturation, capillary number, permeability, pressure gradient, and gas-water surface tension, respectively. In total, there are five (5) parameters required to successfully simulate foam behaviour, which are f_{mmob} , f_{mdry} , $epdry$, f_{mcap} , and $epcap$, with the following assumptions:

- f_{mdry} is equal to critical water saturation, S_w^* at which the foam will collapse if the transition between the low and high-quality regimes is abrupt.
- $epdry$ controls the rapidity of the foam collapse.
- f_{mcap} is the smallest possible capillary number expected in foam simulation. However, it affects other parameters' values, although it is not considered a foam parameter per se [76].
- $epcap$ designates the shear-thinning behaviour in the low-quality regime.

The method used to fit foam model parameters to foam quality scans has been extensively studied in previous research. The initial foam model parameter fitting method attempted to capture the foam coalescence in the high-quality regime, where the gas mobility increases as the S_w approaches S_w^* . Although the model is derived to represent the foam coalescence, it represents the low-quality regime reasonably well [82]. Another method that focuses on capturing high-quality regime behaviour was later proposed using the contour hybrid plot method to fit the foam quality scan [83].

Cheng, et al. [82] introduced a method that can represent both foam flow regimes. Instead of assuming Newtonian fluid behaviour in the low-quality regime, it is modified to allow for shear-thinning behaviour, as observed in the reported experimental study [3]. This method fitted the foam model parameters to pressure-drop contours as a function of the superficial gas and water velocity as per **Figure 2.8**. The maximum ∇p

corresponds to f_g^* , which lies between low-quality and high-quality regimes. In this method, S_w^* is equivalent to $fmdry$ and is calculated using Equation 12 based on the ∇p response in the high-quality regime. $fmmob$ is estimated utilizing the fractional flow equation describe in Equation 13 using the value of f_g^* . A log-log plot ∇p vs. u_g is constructed to fit for shear-thinning behaviour to solve for $epcap$. Here, the $epdry$ is assumed to be the most substantial value where the foam will immediately collapse. This method was later extended to fit the foam quality scan in **Figure 2.8** [76].

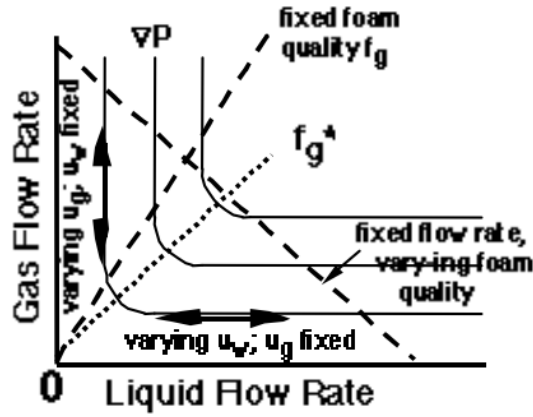


Figure 2.8: Foam behaviour scan. Reproduced from Cheng, et al. [82].

$$\nabla p = u_w \frac{\mu_w}{Kk_{rw}(S_w^*)} \quad (12)$$

$$f_g^* = 1 - \left(1 + \frac{k_{rg}^o(S_w^*)}{fmmob k_{rw}(S_w^*)} \right)^{-1} \quad (13)$$

The most recent method reviewed utilizes the MATLAB algorithm to fit the foam model parameters using a constrained non-linear least-square minimization approach [3]. All five (5) foam parameters were fitted concurrently, and equal weight was assigned to all parameters. This method improved the estimation of $epdry$ instead of assuming the largest possible value. Table 2.1 summarizes the available methods utilizing the foam quality scan dataset.

Table 2.1: Summary of recent parameter fitting methods utilizing foam quality scan dataset.

Method	Description	$fmmob$	$fmdry$	$epdry$	$fmcap$	$epcap$
Ma et al., 2012	<p>It was a fitting foam quality scan to transition apparent foam viscosity using the contour hybrid plot method. The superposition of both contours is used to determine the corresponding $fmmob$ and $fmdry$ at measured fg^* and μ_{app}^*.</p> <p>Contour plot 1: $fg^*(Sw^*, fmmob, fmdry)$</p> <p>Contour plot 2: $\mu_{app}^*(Sw, fmmob, fmdry)$</p>	✓	✓		-	-
Boije 2016	<p>Foam quality scan is fitted to a concave curve in the low-quality regime and a straight line to (1,0) for the high-quality regime.</p> <p>The intersection of both fitted curves is solved for fg^*.</p> <p>$fmdry$ is calculated using the Darcy equation by solving $krw(Sw^*)$</p> <p>$epcap$ is determined through a datum point in the low-quality regime</p>	✓	✓	Assume largest possible <i>(immediate foam collapse)</i>	Assume smallest possible <i>(shear thinning of foam)</i>	✓
Kapetas et al., 2016	<p>Fitting foam quality scan in MATLAB using a constrained non-linear least-square minimization approach to compute all parameters concurrently</p> <p>Equal weight was assigned to all the experimental data during fitting.</p>	✓	✓	✓	✓	✓

CHAPTER 3
METHODOLOGY

This chapter comprises the materials, laboratory equipment, and experiments conducted for this research. In addition to that, experimental conditions, setup, and procedures are described in detail for bulk foam stability experiments, foam rheology assessments, and foam flooding experiments. The objective of this study is to model the transport behaviour of nanoparticle-stabilized foam in porous media. However, before modelling assessments, it is crucial to understand the critical parameters that affect the rheology of stabilized foam with nanoparticles and their impact on gas mobility reduction. Therefore, this study will cover both experimental analysis and simulation modelling, as shown in Figure 3.1.

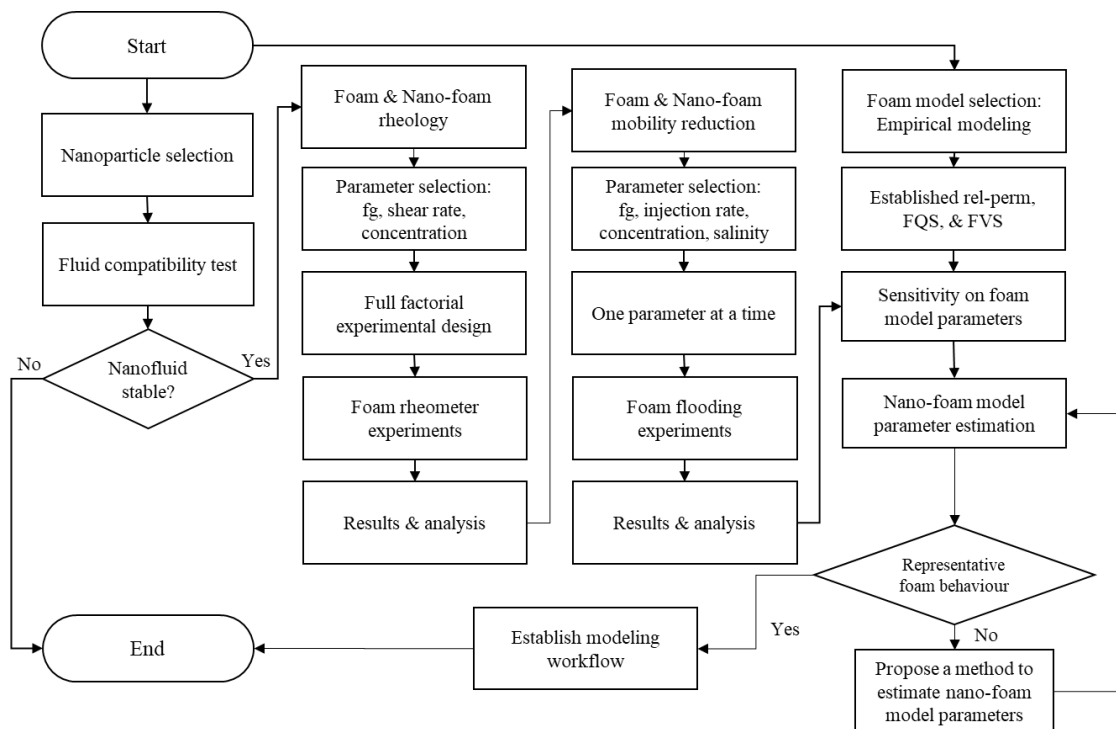


Figure 3.1: Research flow chart.

3.1 Materials

This research focused on fundamental phenomena. Therefore, part of the materials' selection is based on general conditions, and any unique conditions were avoided.

PETRONAS Research Sdn. Bhd. (PRSB) provided surfactant chemicals. The surfactant is a mixture of anionic and amphoteric surfactants called MFOMAX. For confidentiality purposes, the properties of the surfactant were not made available.

Two (2) nanoparticles were screened in this study provided by PRSB in reference to a preliminary nanoparticle screening in seawater, at a high temperature (110°C), and in the presence of light oil as observed by Razali, et al. [26] because the same surfactant was used in this study. The two (2) utilized nanoparticles are hydrophobic nanoparticles and aqueous nanoparticles. The nanoparticles' properties are shown in Table 3.1.

Table 3.1: Properties of nanoparticles

Nanoparticles	Particle size, nm
SiO ₂ (hydrophobic)	12 nm (average)
SiO ₂ (hydrophilic)	10 – 20 nm

This study's selected range of salinity was based on the salinity of the actual field application's injected seawater. The actual properties of injected seawater comprise several types of salt. This study utilized synthetic brine using sodium chloride (properties are provided in Table 3.2). As shown in Figure 3.2, the injected seawater mainly consists of sodium chloride ions. Although seawater majorly consists of sodium chloride, the presence of divalent salt ions may deteriorate the performance of the nanoparticles in the salt ions [26, 65]. This is the limitation of the current study and may be addressed in future research. Table 3.2 illustrates the properties of sodium chloride utilized in this study.

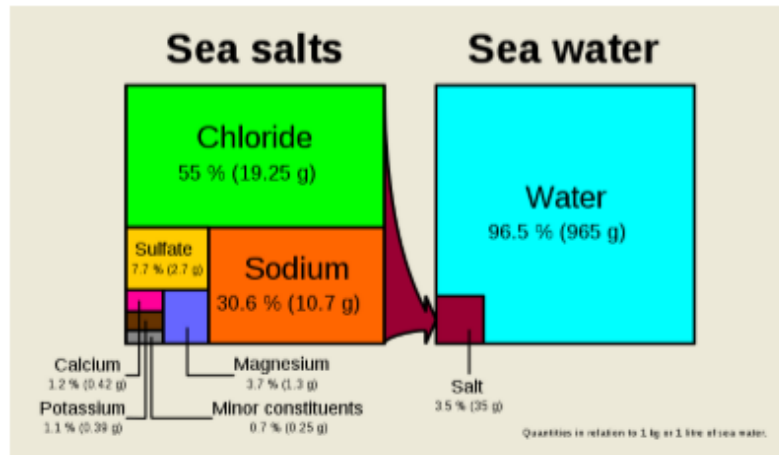


Figure 3.2: Composition of seawater.

Table 3.2: Properties of sodium chloride.

Description	Formula	Molar mass (g/mol)	Melting point (°C)	Density (g/cm ³)
Sodium chloride	NaCl	58.44	801	2.17

In this study, pure Nitrogen (N₂) gas was used to generate foam. For four main reasons, nitrogen gas was selected instead of Carbon Dioxide (CO₂) and Methane (CH₄) gas. Firstly, CO₂ is corrosive when mixed with water. Secondly, N₂ is abundantly available and generates more durable foam compared to CO₂ and CH₄ [84]. Thus, more significant results can be observed for analysis [85, 86]. Thirdly, CO₂ is soluble in water. Therefore, it is not suitable for immiscible flooding activities. Finally, CH₄ is not preferred as it is highly flammable, although it is more representative of the actual injection strategy. The properties of N₂ gas at standard conditions are shown in Table 3.3.

Table 3.3: Properties of N₂ gas at standard conditions.

Density (g/mol)	Viscosity (cp)	Critical pressure (psi)	Critical temperature (°C)
0.001251	0.0177	492.3	-146.9

3.2 Experimental Equipment

Various numbers of experiments were conducted to achieve the objectives of this research at the first stage of nano-foam performance evaluation under standard conditions in the absence of oil. The experiments conducted are to re-establish the nano-fluid mixture stability, investigate bulk foam stability using a foam tester, investigate nano-foam rheology using a foam rheometer, and establish the mobility reduction factor and foam quality scan using a sand pack flooding system. This section provides a general description of the types of equipment used in this study.

3.2.1 Foam Tester

An Anton Paar foam tester was used to conduct a bulk foam stability test. This instrument is used to measure foam characteristics such as foamability and foam half-life in a closed system at a specific temperature. It consists of a water-bath arrangement equipped with digitally indicating circulation thermostats with a cooling coil, temperature probe, and self-optimizing electronic heating control with temperatures ranging between 24 °C and 95 °C. A cylindrical gas diffuser is used to generate foam in the testing cylinder. A schematic diagram of the foam tester is illustrated in Figure 3.3.

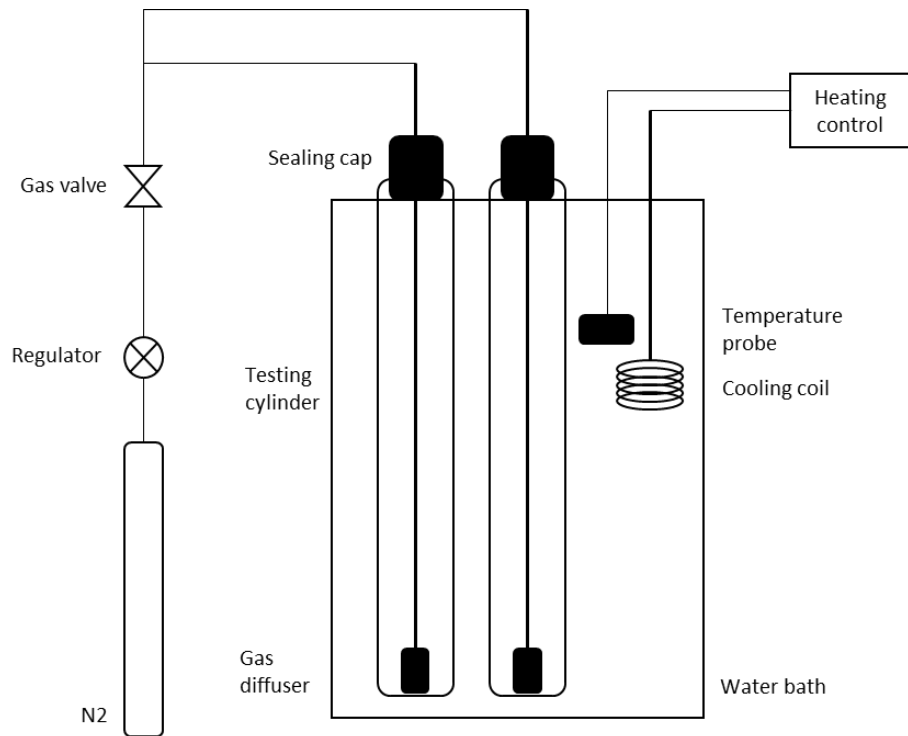


Figure 3.3: Schematic diagram of Anton Paar foam tester.

3.2.2 Foam Rheometer

A pressurized foam rheometer model 8500 by Ametek Chandler Engineering was utilized to study foam rheology. The equipment can measure foam rheology at standard conditions and under high temperature and pressure conditions. The system comprises a Coriolis mass flow meter, a view cell with a camera system, a positive displacement (PD) pump, a high-pressure syringe pump, gas and liquid control valves, and a back-pressure regulator as shown in Figure 3.4. The corresponding foam rheology behaviour as a function of shear rate and apparent viscosity will be measured across a flow loop.

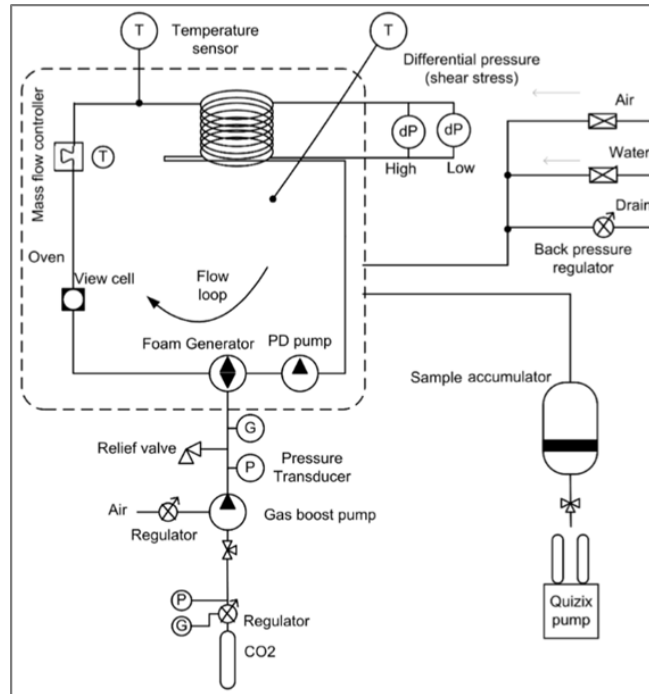


Figure 3.4: Schematic diagram of flow loop rheometer. Reproduced from Ahmed, et al. [87].

3.2.3 Sand-pack Flooding System

An existing sand-pack flooding system that was utilized in UTP and its configuration is shown in Figure 3.5. The sand-pack system can perform several types of foam flooding, such as co-injection foam flooding, surfactant alternating gas injection, and pre-generated foam flooding. A mixture of quartz river and silica flour is packed in the sand-pack holder with a length of 60 cm and a diameter of 3.9 cm. Sand-pack was used in this study and typically has higher permeability compared to typical cores. The different grain sizes of quartz rivers between 212-425 μm were packed into the system. Silica flour of approximately 10% of the total weight was added to reduce the sand pack's permeability. A sieving machine was utilized to shake the sand in its holder for better packing as the sand was gradually added into the holder. A total of 1297 g of sand was packed into the sand-pack holder.

A long sand-pack system is utilized to mitigate the capillary end effect during flooding [88]. The system comprises a dual HPLF piston pump for continuous injections, an accumulator for gas, water, and sample solutions, a digital weighing scale

at the inlet and outlet of the liquid accumulator, a mass flow controller at the gas cylinder, and back-pressure control valves. There are six pairs of differential pressure transmitters installed across the sand pack. Each pair of differential pressure transmitters consists of a low pressure transmitter (0-5 psi) and a high differential pressure transmitter (0-30 psi) to increase the accuracy of measurements.

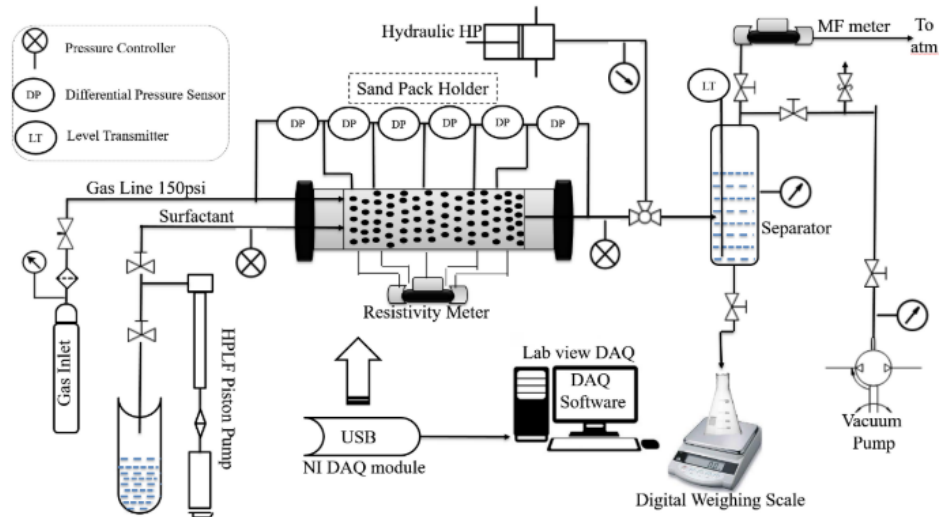


Figure 3.5: Schematic diagram of the sand-pack foam flooding system. Reproduced from Hadian Nasr, et al. [89].

3.3 Experimental Procedures

The experimental procedures to achieve the objectives of this study are discussed in this section. It includes the technique applied to prepare the nanoparticles-surfactant mixtures, foam stability measurements, nanoparticles-stabilized foam rheology study, and steady-state co-injection nano-foam flooding.

3.3.1 Dispersion Preparation

A diluted solution for SiO₂ nanoparticles and MFOMAX was prepared at 1.0 wt.% from their mother solution, respectively. A surfactant solution without the presence of

nanoparticles was prepared as a base case for the study. The brine solution was mixed accordingly to achieve a concentration of 0.3 wt.% MFOMAX in 2.0 wt.% of NaCl. In the presence of nanoparticles, surfactant in brine solution was prepared first at either 1.0 wt.%, 2.0 wt.%, 3.0 wt.%, or 5.0 wt.%. Then, the nanoparticle solutions are added according to their proper ratio. The mixture was stirred for approximately 15 minutes, followed by sonicating at 15% amplitude for at least 15 minutes or until the solution became clear. The surfactant and nanoparticles mixture samples used for each experiment are listed in each section, respectively.

3.3.2 Nanoparticles-Surfactant Compatibility Study

It is crucial to study the fluid-fluid stability between nanoparticles, surfactants, and brine solution before conducting any stability measurements or foam flooding experiments. This study aimed to identify and revalidate the suitable silica nanoparticles to be used with MFOMAX at standard conditions in the absence of oil through nanoparticle-surfactant mixture stability. Silica nanoparticles were chosen for this study as they give the best foam stability compared to zinc oxide and titanium oxide in combination with MFOMAX surfactant at high temperatures and the presence of oil, in reference to a published study by Razali, et al. [26]. Nanoparticles that could remain dispersed in surfactant solution for a minimum of six (6) hours are preferable (based on the estimated time required to run co-injection of a total of six pore volumes of liquid at a total injection rate of 4 cc/min).

There are two (2) types of silica nanoparticles used in this study, partially hydrophobic and hydrophilic nanoparticles. The nanoparticles-surfactant mixture is prepared according to a specific nanoparticles-surfactant concentration ratio and is fixed to a total chemical concentration of 0.3 wt.%. The test was conducted at a varied nanoparticle-surfactant concentration mixture and varied salinity conditions at ambient temperature. The proposed range of nanoparticles-surfactant ratio was based on the optimum ratio (1:3.3 nanoparticle-surfactant ratio) observed between hydrophilic silica and MFOMAX foam stability mixture at high temperature and in the presence of oil [26]. The tested samples are shown in Table 3.4. The prepared sample is stored in a

closed glass jar and monitored for the next 12 to 24 hours for any changes in solution cloudiness or nanoparticles precipitation.

Table 3.4: List of samples prepared for Nanoparticles-Surfactant Compatibility screening.

Sample	Nanoparticles	Nanoparticles: surfactant ratio	Brine Salinity (wt. % NaCl)
01	SiO ₂ – hydrophobic	1.5:1	1.5
02	SiO ₂ – hydrophobic	1:1	1.5
03	SiO ₂ – hydrophobic	1:2	1.5
04	SiO ₂ – hydrophilic	2:1	2.0
05	SiO ₂ – hydrophilic	1:1	2.0
06	SiO ₂ – hydrophilic	1:2	2.0
07	SiO ₂ – hydrophilic	1:4	2.0
08	SiO ₂ – hydrophilic	2:1	3.0
09	SiO ₂ – hydrophilic	1:1	3.0
10	SiO ₂ – hydrophilic	1:2	3.0
11	SiO ₂ – hydrophilic	1:3	3.0
12	SiO ₂ – hydrophilic	1:4	3.0
13	SiO ₂ – hydrophilic	2:1	5.0
14	SiO ₂ – hydrophilic	1:1	5.0
15	SiO ₂ – hydrophilic	1:2	5.0
16	SiO ₂ – hydrophilic	1:3	5.0
17	SiO ₂ – hydrophilic	1:4	5.0

3.3.3 Bulk Foam Stability

Based on the outcome of the nanoparticles-surfactant compatibility study, bulk foam stability was conducted to study the performance of nanoparticles and surfactant mixtures at varying salinities. The test was repeated and compared with the conventional foam performance in the absence of nanoparticles.

Bulk foam stability was measured using the Anton Paar foam tester (Figure 3.3) by measuring foamability and foam half-life. Foam half-life is the required time for the foam to reach half of its initial height or volume. A 100 mL sample was prepared accordingly and loaded into the test cylinder. A steel rod with a gas diffuser was submerged into the sample solution and secured by a sealed cap. The sample was then

left in the water bath for approximately five (5) minutes to ensure that it had reached thermal equilibrium. The N₂ gas was injected into the test cylinder through a gas diffuser at a rate of 100 mL/min using the flowmeter. The time taken for the foam to reach 1000 mL was recorded, and the foam volume was measured every hour. All experiments were conducted at a temperature of 30 °C.

The test was conducted at a varied nanoparticle-surfactant mixture ratio at which the nanoparticles were able to remain dispersed in the solution as identified during the screening of nanoparticles. The first set of experiments is designed to study nanoparticle-stabilized foam performance at 2.0 wt.% NaCl. The total chemical concentration (nanoparticles and surfactant) is fixed at 0.3 wt.%. The nanoparticles-surfactant concentration ratio was varied between 0:1 (surfactant solution only), 1:2, 1:4, and 1:6. The nanoparticle-surfactant concentration ratio of 2:1 and 1:1 was excluded as the mixture was observed to be unstable. The foamability and foam stability tests were replicated at varying salinities (1.0 wt.% to 3.0 wt.% NaCl) using the optimum nanoparticles-concentration ratio that corresponds to maximum foam stability (ratio 1:2). The test at varying salinities was not performed at 5.0 wt%. NaCl as the mixture was extremely cloudy, and the nanoparticle precipitation occurred quickly. The tested samples are shown in Table 3.5. The test was also repeated in the absence of nanoparticles to compare the effect of salinity on foam stability.

Table 3.5: List of samples prepared for bulk foam stability test.

Sample	Nanoparticles	Nanoparticles: surfactant ratio	Brine Salinity (wt. % NaCl)
01	SiO ₂ – hydrophilic	0:1	2.0
02	SiO ₂ – hydrophilic	1:2	2.0
03	SiO ₂ – hydrophilic	1:4	2.0
04	SiO ₂ – hydrophilic	1:6	2.0
05	SiO ₂ – hydrophilic	0:1	1.0
06	SiO ₂ – hydrophilic	0:1	2.0
07	SiO ₂ – hydrophilic	0:1	3.0
08	SiO ₂ – hydrophilic	1:2	1.0
09	SiO ₂ – hydrophilic	1:2	2.0
10	SiO ₂ – hydrophilic	1:2	3.0

3.3.4 Nanoparticles-Stabilized Foam Rheology Study

To investigate the nanoparticles-stabilized foam rheology behaviour, a foam rheology study was conducted using a foam rheometer at ambient temperature, as shown in **Figure 3.4**. The foam rheological behaviour in the presence and absence of nanoparticles and the changes in foam texture characteristics were studied.

Dynamic nano-foam viscosity will be measured at varied nanoparticle concentrations, shear rates, and foam qualities by testing one factor or variable at a time (OFAT). A nanoparticles-surfactant mixture with 2.0 wt.% NaCl will be prepared and loaded into a sample accumulator. Nanoparticles-stabilized foam will be generated inside the foam generator by mixing the sample mixture with N₂ gas at a specified foam quality of 50%, 70%, and 80%. The pre-generated foam will be circulated in the fixed-length flow loop tubing at a specified shear rate ranging between 50 and 750 (1/s). Differential pressure measurements will only be taken once the foam density and foam texture observed from the view-cell are uniform. A minimum of five (5) differential pressure readings at different shear rates were measured to generate the flow curve and viscosity curve for analysis. Therefore, a total of twenty-two sets of experiments were performed at varying nanoparticle concentration, foam quality, and salinity, including the measurements for surfactant foam as a reference case.

The rheology of foam in the presence and absence of nanoparticles will be determined using the power-law model as foams behave as non-Newtonian fluids [29]. In a circular tube, the shear rate (γ) and shear stress (τ) are computed using Equations (14) and (15), respectively.

$$\gamma = \frac{8v}{D} \quad (14)$$

$$\tau = \frac{D\Delta P}{4L} \quad (15)$$

where v , D , ΔP and L are the fluid velocity, the tube inside diameter, the differential pressure, and the tube's length, respectively. As shown in Equation (16), the power-law describes viscosity as a nonlinear function of the shear rate.

$$\tau = K\dot{\gamma}^n \quad (16)$$

$$\text{where, } K = K' \times \left(\frac{3n'+1}{4n'} \right)^{-n'} \quad (17)$$

$$\dot{\gamma} = \gamma \left(\frac{3n'+1}{4n'} \right) \quad (18)$$

where n' is the viscosity index determined from the curve's gradient between shear rate and shear stress in the logarithmic plot. The parameter K' is known as the consistency index and could be determined from the power law. The calculated n value from the power-law model described the rheology of the foam and could be determined by plotting either the flow curve or viscosity curve from the experimental measurements. A condition where the calculated n is smaller than 1 indicates shear-thinning behaviour, while n larger than 1 corresponds to shear thickening behaviour.

3.3.5 Foam Flooding Experiments

Multiple steady-state co-injection foam flooding runs were conducted at various nanoparticles-surfactant concentrations, injection rates, foam quality, and salinity to meet the second objective of this study. The effect of each parameter was studied using a one parameter at a time approach. This approach was chosen to understand the critical effect of each parameter on the foam mobility reduction factor in the presence of nanoparticles. In addition to that, this approach will identify the range of each parameter in which the nanoparticle stabilization effect will be effective.

The conditions for the sand pack experiments are given in Table 3.6. When studying the effect of a parameter, the remaining parameter was fixed to a value (in bold as shown in Table 3.6). For all dynamical experiments performed, the surfactant concentration was fixed at 0.3 wt.%. Although different concentrations of nanoparticles were considered, the corresponding nanoparticle-surfactant concentration ratio was kept similar to previous tests at 0:1, 1:4, 1:2, 1:1, and 2:1, accordingly.

Table 3.6: Range of parameters tested during foam flooding analysis.

Nanoparticle concentration, wt.%	Foam quality	Injection rates, cc/min	Superficial velocity, ft/day	Salinity, wt.% NaCl
0	30%	2	8	1.0
0.075	50%	3	12	2.0
0.15	70%	4	16	3.0
0.3	80%	5	20	
0.6	90%	7	28	
	95%	9	36	

The procedures for conducting the sand-pack flooding experiment are as follows.

1. A confining pressure of 100 psi and a backpressure of 20 psi were applied to the system.
2. The system was vacuumed for at least 30 minutes, or until all fluids had been removed.
3. Then, the sand-pack was saturated with four (4) pore volumes of brine at a rate of 10 cc/min, followed by 500 cc of surfactant solution at 5 cc/min to achieve maximum surfactant adsorption by the sand-pack.
4. Subsequently, co-injection of the nanoparticles-surfactant mixture with gas injection was conducted at a specified foam quality and total injection rate. A total of six (6) pore volumes of nitrogen and nanoparticle-surfactant mixture were injected into the system.
5. The pressure drops of injected gas and liquid volume and produced gas and liquid volume were recorded.
6. The response obtained from the series of experiments was analysed and compared, and the most critical parameters affecting nanoparticles-stabilized foam were identified.

3.3.5.1 Mobility reduction at varying foam quality (foam quality scan)

To investigate the effect of gas mobility reduction at different foam qualities, the foam flooding experiments were conducted at 30%, 50%, 70%, 80%, 90%, and 95% foam quality. These experiments were conducted for surfactant foam and nano-foam at a nanoparticle concentration of 0.0075wt.% (based on flow loop rheometer experiments results). These tests have been performed using a sand-pack flooding system at a fixed surfactant concentration, total injection rate, and salinity, and the procedures are described in Section 3.3.5. Pressure drops across the core were recorded for analysis, and the corresponding mobility reduction factor and apparent foam viscosity will be calculated according to Equation (4) and Equation (6), respectively.

3.3.5.2 Mobility reduction at varying nanoparticles concentration

To investigate the nanoparticle concentration effect on gas mobility reduction in foam flooding, a nanoparticle-surfactant mixture was prepared in different nanoparticle concentrations: 0.075 wt.% (1:4), 0.15wt.% (1:2), 0.3wt.% (1:1), and 0.6wt.% (2:1). A test was also conducted without nanoparticles (0.0wt.%) as the base case for comparison to surfactant foam performance. These tests have been performed using a sand-pack flooding system at 70% foam quality (transition foam quality of nano-foam as per experimental run) and at 95% foam quality (extremely dry foam condition) to evaluate the nano-foam mobility reduction performance. The procedures for the foam flooding experiments are as described in Section 3.3.5.. All pressure drops were recorded for analysis, and the corresponding mobility reduction factor and apparent foam viscosity will be calculated according to Equation (4) and Equation (6), respectively.

3.3.5.3 Mobility reduction at varying total injection rates (foam velocity scan)

To investigate the total injection rate effect on gas mobility reduction in foam flooding, the foam flooding experiments were conducted at 2cc/min, 3cc/min, 4cc/min, 5cc/min, 7cc/min, and 9cc/min. These tests have been performed using a sand-pack

flooding system at fixed surfactant concentration, in the absence and presence of nanoparticles (0.075wt.%), foam quality (70%), and salinity (2 wt.% NaCl). The procedures for the foam flooding experiments are as described in Section 3.3.5. All pressure drops were recorded for analysis, and the corresponding mobility reduction factor and apparent foam viscosity will be calculated according to Equation (4) and Equation (6), respectively.

3.3.5.4 Mobility reduction at varying salinity

To investigate the salinity effect on gas mobility reduction in foam flooding, a nanoparticle-surfactant mixture was prepared at different salinities: 1.0wt.%, 2.0wt.%, and 3.0wt.% NaCl. A test was also conducted without nanoparticles (0.0wt.%) as the base case for comparison to surfactant foam performance. These tests have been performed using a sand-pack flooding system at a fixed surfactant concentration, in the absence and presence of nanoparticles (0.075wt.%), foam quality (70%), and total injection rate (4cc/min). The procedures for the foam flooding experiments are as described in Section 3.3.5. All pressure drops were recorded for analysis, and the corresponding mobility reduction factor and apparent foam viscosity will be calculated according to Equation (4) and Equation (6), respectively.

3.4 Foam Simulation Model Analysis

This study aims to evaluate the applicability of model nano-foam only on the foam stability improvement in the presence of nanoparticles, without any factors which are detrimental toward foam (effect of high temperature and oil). At this initial stage of the study, the limitations were imposed to increase the magnitude of nano-foam performance improvement for analysis and evaluation with respect to the nanoparticle stabilization mechanism. These limitations shall be incorporated in future research to further improves and mature the nano-foam modelling techniques.

There are a few steps required to simulate foam behaviour successfully. First, foam model parameters must be identified. The simplest and most common method involves

identifying parameters related to the reference mobility, shear-thinning, and foam dry-out functions. Then, the identified foam model parameters can be incorporated into the simulator to predict foam behaviour. Since nanoparticles' foam stabilization mechanisms are slightly different from conventional surfactant foam, the current foam model's ability to compute foam model parameters and simulate the stabilized foam behaviour in nanoparticles' presence was validated. The following sub-sections describe the method used and the modelling input required to model foam behaviour in porous media.

3.4.1 Foam Model Parameters Estimation Method

A MATLAB algorithm was created to fit the foam model parameter by a method adapted from Kapetas et al., 2016. The adapted method used a constrained non-linear least-squares minimization approach. This method was chosen as all five (5) foam parameters, $fmmob$, $fmdry$, $epdry$, $fmcap$, and $epcap$, were computed simultaneously. The approach can give a good match with foam quality scan data without assuming a large $epdry$ value [75]. An initial guess and a valid range of foam parameters were assigned. Equal weights were assigned to all the experimental data except for the maximum apparent viscosity, also known as the transition foam quality. Additional requirements must be applied and reviewed for every fitted foam parameter obtained; the $fmdry$ must not exceed the value of transition water saturation calculated [23], and the F_3 must not exceed the value of 1.0.

Three sets of data inputs are crucial for foam model parameter fit; relative permeability of gas and water, foam quality scan, and foam velocity scan are established during the steady-state co-injection foam flooding. To evaluate and analyse the nano-foam behaviour in comparison to surfactant foam, foam quality scan and foam velocity scan were established in the presence and absence of nanoparticles as described in Section 3.3.5.1 and Section 3.3.5.3. The foam quality scan and foam velocity scan were generated at the standard condition and in oil-free conditions to reduce the detrimental effect of high temperature and oil, thus focusing on the foam generation (low-quality regime) and collapse mechanism (high-quality regime) in the presence of nanoparticles. The connate water saturation, $S_{wc}=0.46$, and residual gas saturation, $S_{gr}=0.0$, were

adopted from the Hadian Nasr, et al. [90] study as the experimental analysis was conducted using the same sand-pack system. Sand-pack history matching of gas and water flooding was conducted to identify the Corey exponent of gas and water.

The calculated apparent foam viscosity as a function of foam mobility reduction ratio in the algorithm is based on Equation (19):

$$\mu_{app}(s_w) = \frac{1}{\frac{k_{rw}(s_w)}{\mu_w} + \frac{k_{rg}(s_w)}{MRF \times \mu_g}} \quad (19)$$

Utilizing the STARS foam model in the presence of surfactant and absence of oil, the MRF was calculated based on the critical foam model parameters identified based on the previous study. MRF is given by Equation (20).

$$MRF = 1 + fmmob \times F_3 \times F_{dry-out} \quad (20)$$

where $fmmob$ is the reference mobility factor, F_3 is a shear-thinning function, and $F_{dry-out}$ is the critical water saturation function or the foam dry-out function. The F_3 and $F_{dry-out}$ are discussed in Equations (9), (10), and (11).

3.4.2 Evaluation of Critical Foam Model Parameters: $fmmob$, $fmdry$, and $epdry$

Foam generation and foam collapse are the main mechanisms involved in foam flow behaviour. Limiting capillary pressure and corresponding water saturation play an essential role in foam collapse, and it is one of the crucial foam model parameters needed in foam modelling. Based on previous research, nanoparticles mainly improve foam coalescence's critical capillary pressure by their attachment to the gas-liquid surface or rearrangement mechanism as the lamellae continuously thin [30]. Therefore, a sensitivity analysis was conducted to investigate the corresponding mobility reduction ratio at varying $fmmob$, $fmdry$, and $epdry$.

The mathematical model of the existing foam dry-out parameter was investigated to better understand the assumptions used and their interrelated nature. The parameters incorporated in the foam dry-out function should be able to predict the foam coalesce behaviour. A sensitivity analysis was conducted at varying $fmmob$, $fmdry$, and $epdry$.

First, the data obtained from the surfactant foam flooding experiments is used to estimate foam model parameters using the established MATLAB function as a reference case. An initial guess and a valid range of foam parameters were assigned. Equal weights were assigned to all the experimental data except for the maximum apparent viscosity. Then, each foam model parameter was varied, one parameter at a time, while fixing the remaining model parameters. Finally, the corresponding foam model parameters fit were compared with the foam quality scan experimental data and the effect of foam model parameters was analyzed.

3.4.3 Nano-Foam Model Parameters Estimation

A foam quality scan established for surfactant foam and nanoparticle-surfactant foam was analysed and compared to distinguish different dry-out mechanisms to confirm nanoparticles' effect on foam stability. Based on the experimental data available, the current foam model's ability to simulate nanoparticles-stabilized foam was investigated, and the potential gap was identified.

Nano-foam model parameters must first be established to investigate the applicability of the existing foam model for the Dry-Out function used in the implicit texture modelling technique. Both foam quality scan and foam velocity scan in the presence of nanoparticles were used to determine the nano-foam model parameters using the established MATLAB function. An initial guess and a valid range of foam parameters were assigned. Equal weights were assigned to all the experimental data except for the maximum apparent viscosity. Then, the corresponding nano-foam model parameters fit were compared with experimental data and analyzed. Finally, the estimated nano-foam model parameters were validated using a commercial simulator.

The nano-foam model parameters, specifically the *epdry*, were tuned to improve the nano-foam model parameters' fit during the foam dry-out. The *epdry* value was forced to a low (<100) and high value (>1000) in the established MATLAB function. The proposed low and high *epdry* values were chosen based on sensitivity analysis as discussed in Section 3.4.2. The initial guess of low and high *epdry* values was assigned accordingly to the MATLAB function. Equal weights were assigned to all the

experimental data except for the maximum apparent viscosity. Then, the corresponding nano-foam model parameters fit were compared with experimental data and analyzed. Finally, the estimated nano-foam model parameters were validated using a commercial simulator and compared with the un-tuned nano-foam model parameters.

Based on the study conducted on nano-foam model parameters estimation, potential gaps in the current foam model were identified and discussed. A workflow to estimate nano-foam model parameters and simulate nano-foam has been proposed, and its limitations are discussed. In addition to that, a modified foam model parameter function ($F_{dry-out}$ function) for nano-foam was introduced to improve the implicit texture modelling technique and better capture the nanoparticle stabilization mechanism observed based on the gaps identified.

3.5 Chapter Summary

This chapter described the methodology used to achieve the research objectives. It presented different materials and apparatus utilized in this study. The suitable nanoparticles to be used with the pre-identified surfactant formulation were screened based on nano-fluid mixture stability and foam half-life measurements using foam scan equipment at different salinity conditions. The sodium chloride was employed to make synthetic brine at different salinities. Nitrogen gas was selected as the injection gas throughout the experimental activities based on mentioned criteria in Section 3.1.

The procedures for foam rheology measurements using a flow loop rheometer are discussed in this chapter. Additionally, the associated procedures to evaluate and analyse experimental results were deliberated.

The steady-state foam flooding experiments were conducted using a sand-pack system, and the activities to conduct the experiments were discussed in detail. Other than identifying the critical parameters which affect the nano-foam flow performance in porous media, the foam quality scan and foam velocity scan were established as foam modelling input. The steps taken to analyse and compare the flow performance in the presence and absence of nanoparticles were discussed before the modelling analysis.

In the last section of this chapter, the methods to estimate foam model parameters and the validation process in the absence and presence of nanoparticles were discussed.

CHAPTER 4

RESULTS AND DISCUSSION

This chapter provides the results and discussion of all experimental investigations and modelling studies conducted using the approach described in the methodology chapter. The current chapter comprises four main sections as follows: the nanoparticles screening and compatibility test, the nano-foam rheology study, steady-state core flood results, and modelling of nano-foam transport behaviour through porous media.

4.1 Nanoparticles Screening and Compatibility Test

The nanoparticles were screened based on a nanofluid mixture compatibility test with MFOMAX surfactant at room temperature and standard conditions. Silica nanoparticles were chosen for this study due to their low cost and good compatibility with the formation. Two types of nanoparticles were tested: hydrophilic and slightly hydrophobic silica nanoparticles. The compatibility test was conducted at varying nanoparticles-to-surfactant concentration ratios (between 0.25 and 2.0) and salinity (between 1 wt.% and 5 wt.% NaCl).

Based on the obtained results, slightly hydrophobic silica nanoparticles were incompatible with MFOMAX at 1.5 wt.% NaCl as shown in Figure 4.1. The nanoparticles are immediately segregated upon mixing into the surfactant solutions and remain precipitated after the sonication process for up to 30 minutes at an amplitude of 15% at a 1.5:1 nanoparticle-surfactant concentration ratio. Increasing surfactant concentration in the nanofluid mixture helps the nanoparticles remain dispersed in the solution after the sonication process. However, the mixture appears cloudy and nanoparticle precipitation occurs after three (3) to five (5) hours.

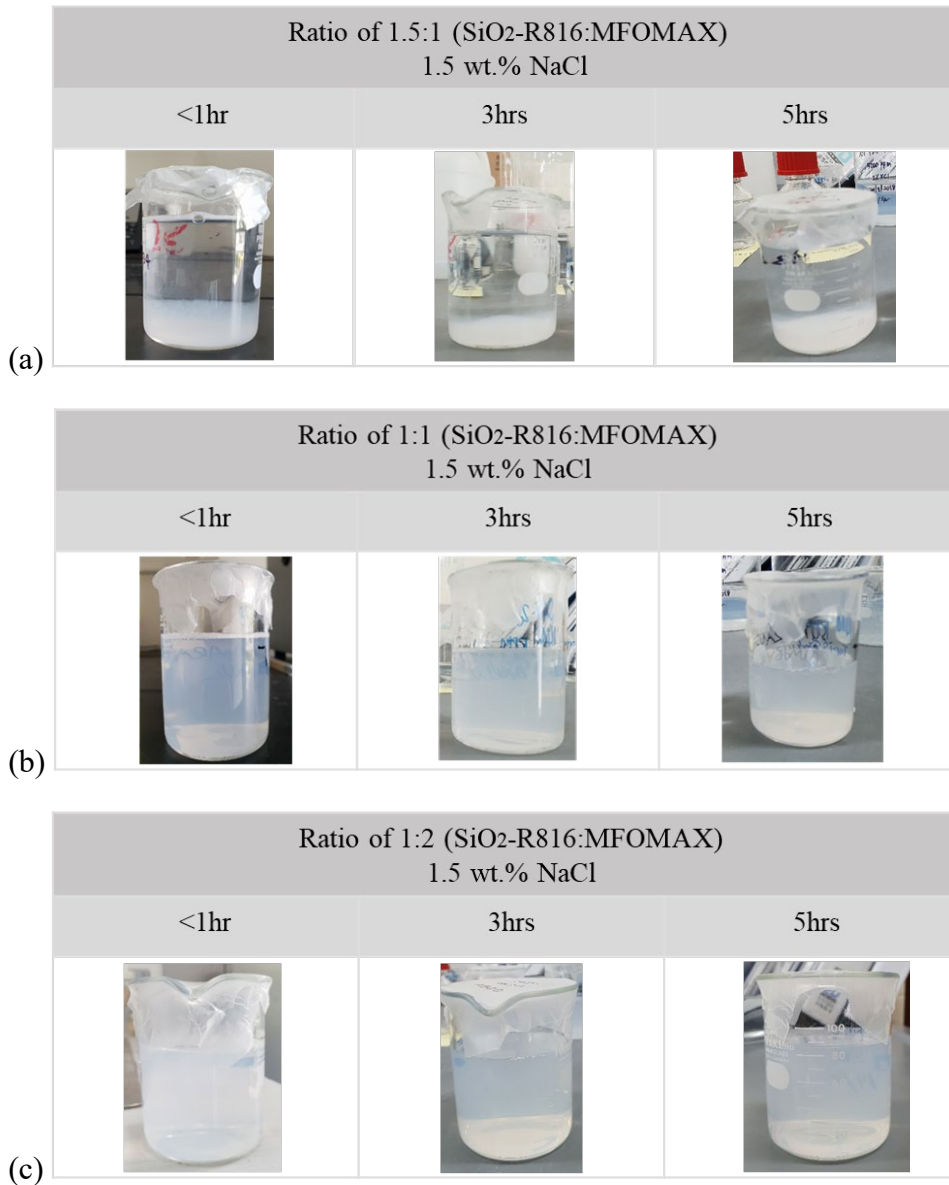


Figure 4.1: Partial hydrophobic silica nanoparticle and MFOMAX mixture at (a) 1.5:1, (b) 1:1, and (c) 1:2 concentration ratio and 1.5 wt.% NaCl shows particles precipitated at the bottom of the beaker.

During this study, the tested hydrophilic silica was able to remain dispersed in the nanoparticle-surfactant mixture for up to 12 hours, as shown in **Figure 4.2**. However, a decrease in nanofluid mixture stability was observed at 3.0 wt.% NaCl with increasing nanoparticle concentration ratio as shown in **Figure 4.3**. The nanoparticles could remain dispersed in the solution for 6 hours at a nanoparticle surfactant ratio of 1:4 and 1:1.

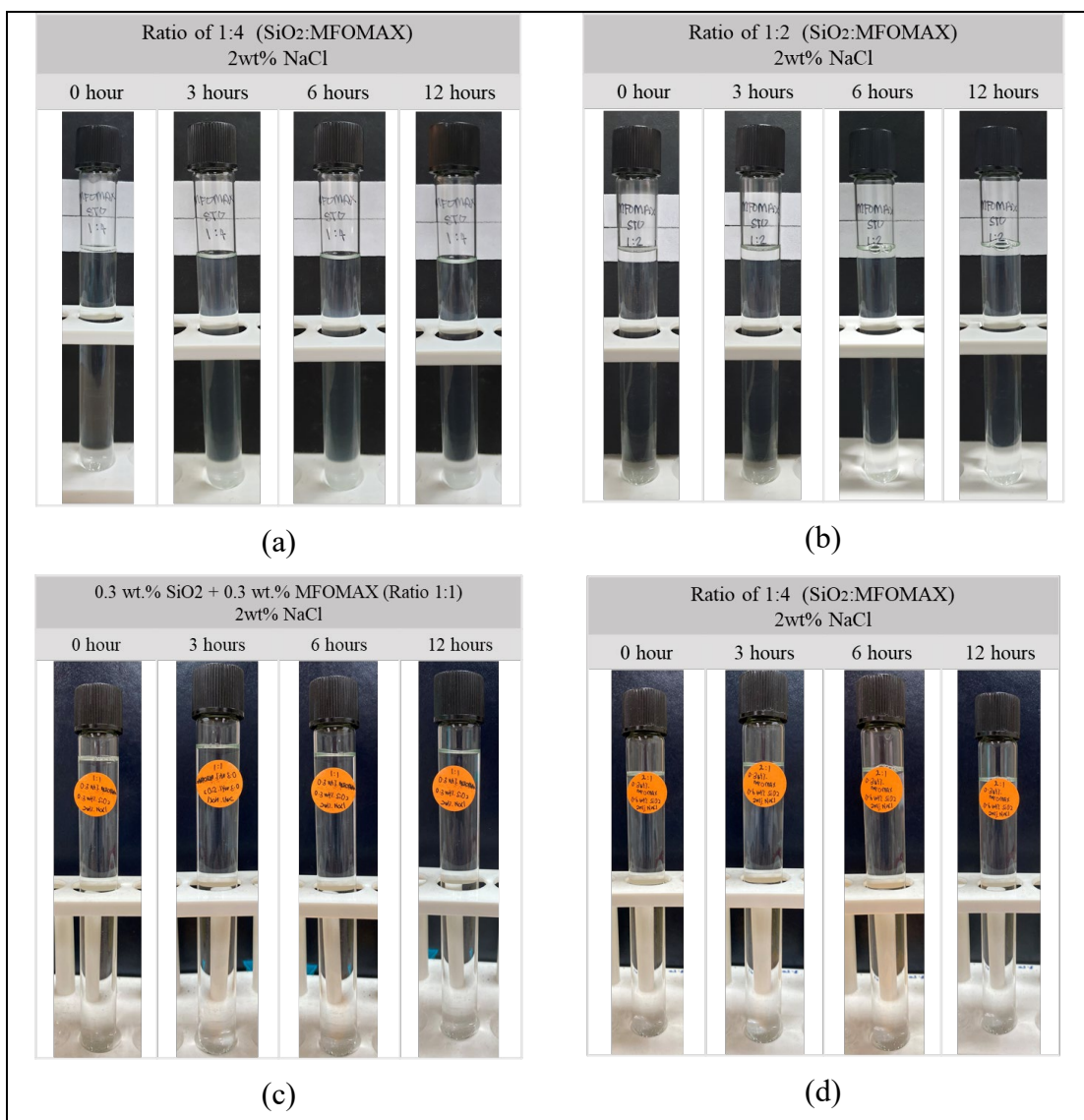


Figure 4.2: Hydrophilic silica nanoparticles and MFOMAX mixture at (a) 1:4, (b) 1:2, (c) 1:1, and (d) 2:1 concentration ratio and 2.0 wt.% NaCl show clear solution indicating well-dispersed nanoparticles up to 12 hours.

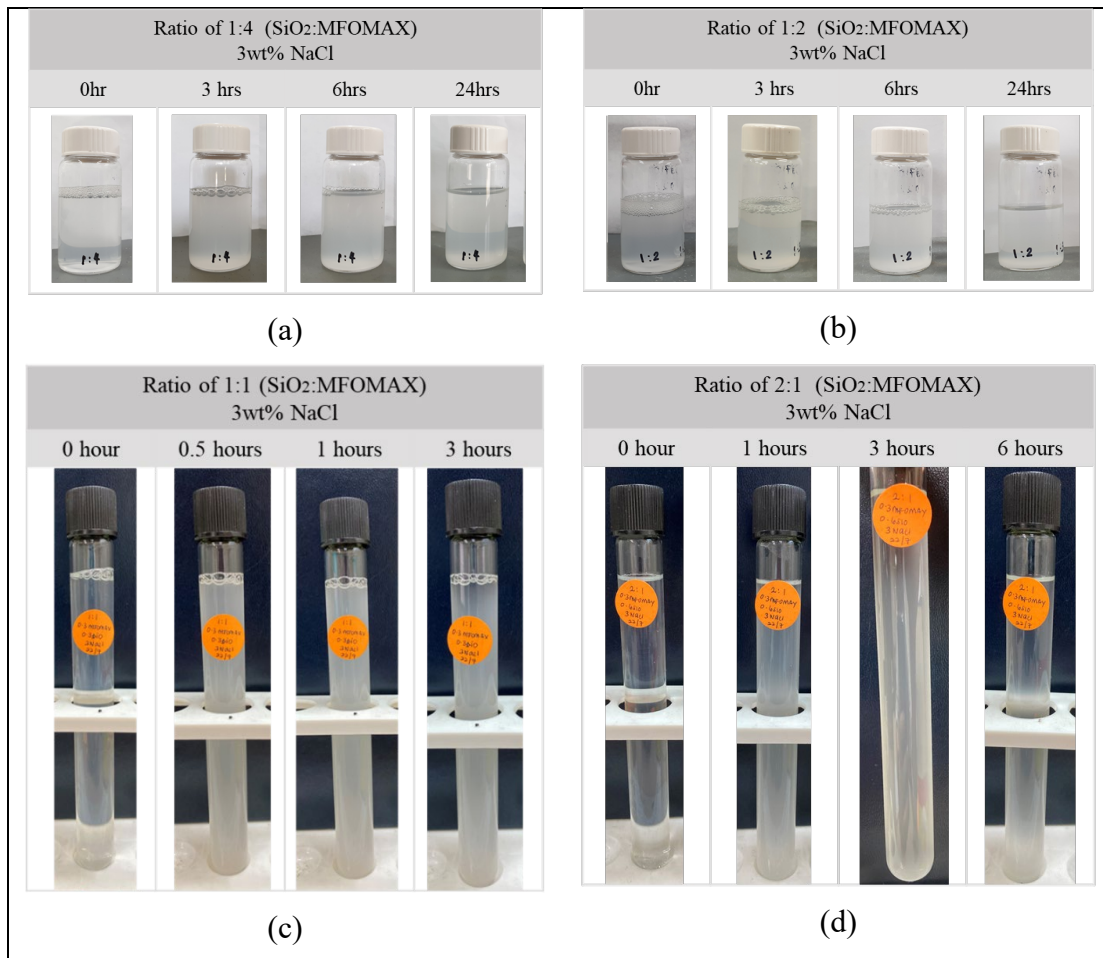


Figure 4.3: Hydrophilic silica nanoparticles and MFOMAX mixture at 1:4 (a), 1:2 (b), 1:1 (c), and 2:1 (d) concentration ratios and 3.0 wt.% NaCl. (c) shows a cloudy solution for 1:1 nanoparticle-surfactant ratio after 30 minutes, indicating the start of nanoparticle segregation.

In addition to that, the nanofluid appears cloudy and precipitated within the first 3 hours at 5.0 wt.% NaCl, as shown in **Figure 4.4**. The separation of the clear mixture at the top and the cloudy mixture at the bottom of the tube was observed in the mixture over time. Such behaviour may be due to the interaction between nanoparticles' surface charges, surfactant molecules, and salt ions in the solution, causing the particles to aggregate with increasing monovalent salt ions [61, 91]. Therefore, hydrophilic silica was chosen to be used for this study, and the salinity was limited to 3.0 wt.% NaCl due to the unstable nanofluid mixture observed at 5.0 wt.% NaCl.

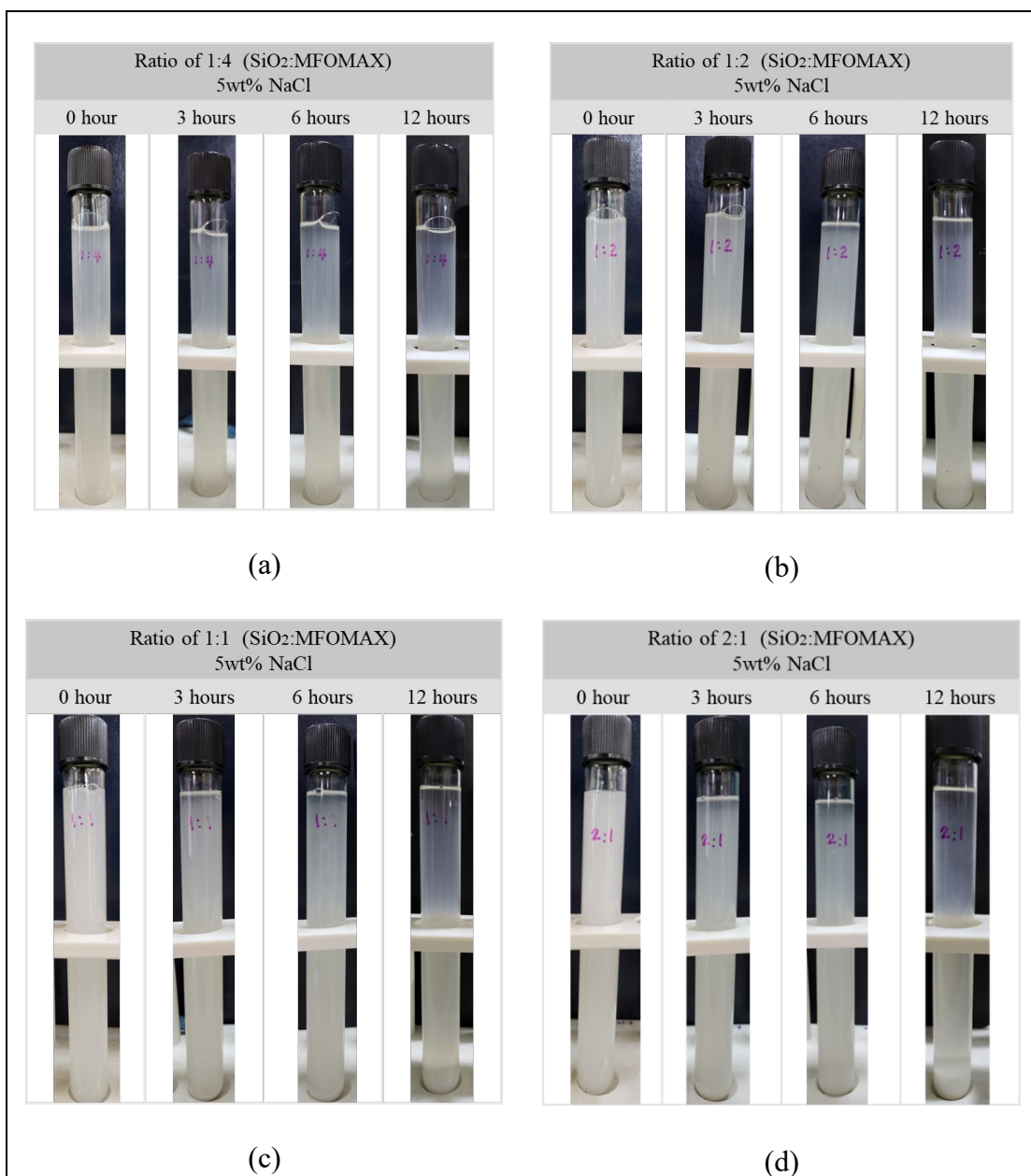


Figure 4.4: Hydrophilic silica nanoparticles and MFOMAX mixture at 1:4, 1:2, 1:1, and 2:1 concentration ratios and 5.0 wt.% NaCl show a cloudy solution. All nanoparticle-surfactant mixtures are cloudy and precipitate within the first 3 hours.

A preliminary foam stability study was conducted using foam half-life measurements to compare the foam stability in the absence and presence of nanoparticles. The foam half-life measurement was conducted at varying nanoparticle concentrations (varying nanoparticles-to-surfactant ratio) and salinity. The results show that foam half-life was improved at a one-to-two nanoparticles-surfactant ratio (at 53 hours) compared to surfactant foam (at 32.5 hours), as shown in Figure 4.5. In addition

to that, nano-foam exhibits a longer half-life at 2.0 wt.% NaCl (1.6 times longer) and 3.0 wt.% NaCl (1.4 times longer) salinity as shown in Figure 4.6. These experiments were repeated at least twice to validate the results. Therefore, based on the preliminary results obtained, the nano-foam was observed to improve bulk foam stability at a specific concentration and salinity condition [10, 26, 31, 92, 93]. However, the actual nano-foam stability and flow performance will be evaluated through foam flooding experiments.

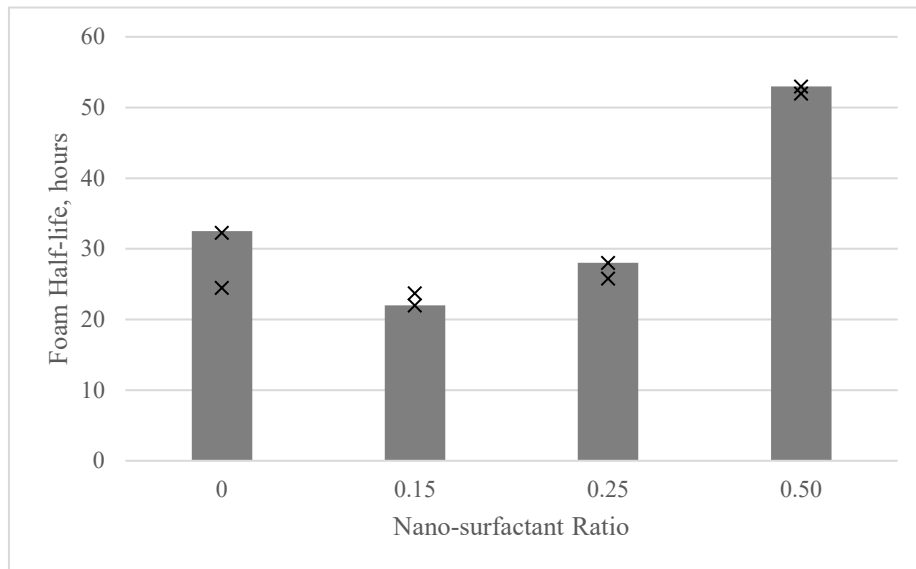


Figure 4.5: Foam half-life measurements at varying nanoparticles-surfactant concentration ratio at 2.0 wt.% NaCl. (x-mark represents repeated tests values)

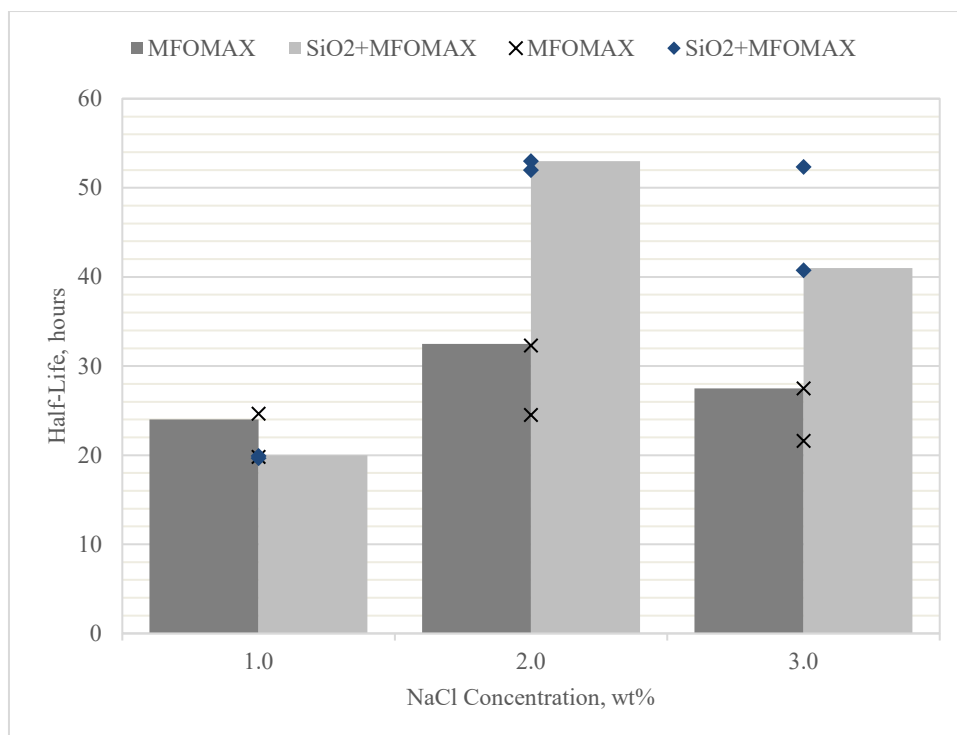


Figure 4.6: Foam half-life measurement of MFOMAX foam and nano-foam at a fixed concentration ratio (0.5) and varying salinity.

4.2 Dynamic Nanoparticles-Stabilized Foam Rheology

An extensive test was conducted using a flow loop foam rheometer to study the rheology of nanoparticle-stabilized foam at varied nanoparticle concentration, shear rate, and foam quality. In addition to that, surfactant foam testing was conducted to compare the different behaviours exhibited by the nanoparticles-stabilized foam. The summary of flow loop rheometer experiments conducted is listed in Table 4.1.

An experiment using surfactant foam was performed to understand the rheology behaviour of the nanoparticle-stabilized foam. The experiment was conducted at room temperature, and the flow loop pressure was set to a minimum value of 500 psi. The test was conducted by inserting the samples into the desired foam quality flow before being sheared at the desired shear rate. The apparent viscosity was recorded over time, and the final value was achieved as the apparent viscosity reached a stable condition, as shown in Figure 4.7.

Table 4.1: Summary of flow loop rheometer experiment runs.

Nano-surfactant Ratio	Salinity, wt.% NaCl	Foam Quality	Shear Rate, s ⁻¹
0	2	50	50- 750
		70	50- 750
		80	50- 750
	3	50	50- 750
		70	50- 750
		80	50- 750
0.25	2	50	50- 750
		70	50- 750
		80	50- 750
	3	50	50- 750
		70	50- 750
		80	50- 750
0.50	2	50	50- 750
		70	50- 750
		80	50- 750
	3	50	50- 750
		70	50- 750
		80	50- 750
1.0	2	50	50- 750
		70	50- 750
2.0	2	50	50- 750
		70	50- 750

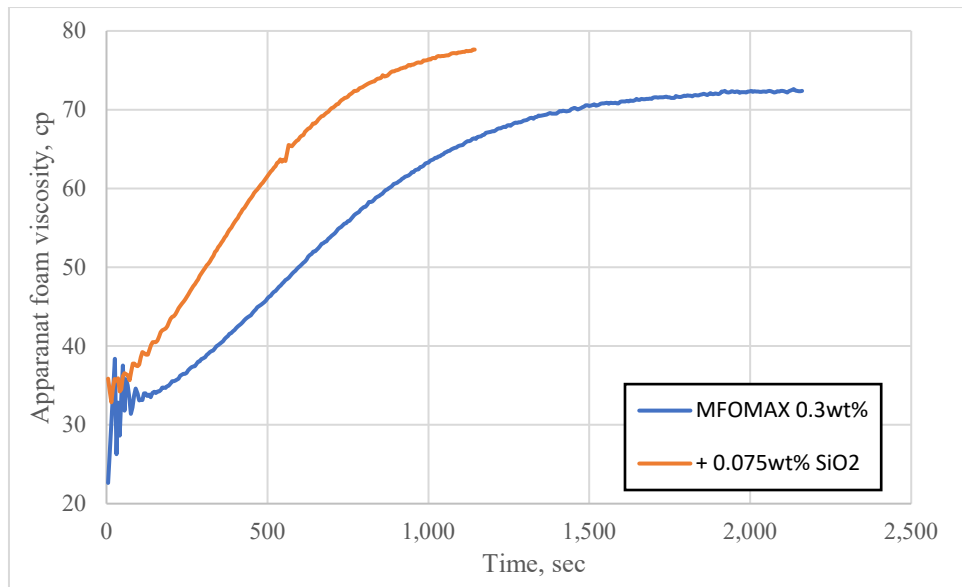


Figure 4.7: Apparent foam viscosity trend over time in the absence and presence of nanoparticles during rheology experiments at 70% foam quality and a shear rate of 250 s^{-1} .

4.2.1 Nanoparticles-Stabilized Foam Rheology Behaviour Compared to Conventional Surfactant Foam

To establish the rheological behaviour of foam in the absence and presence of nanoparticles, the test was conducted at a varied shear rate ranging between 50 s^{-1} to 750 s^{-1} . The corresponding shear stress versus shear rate curves and viscosity curves are plotted in **Figure 4.8** and **Figure 4.9**.

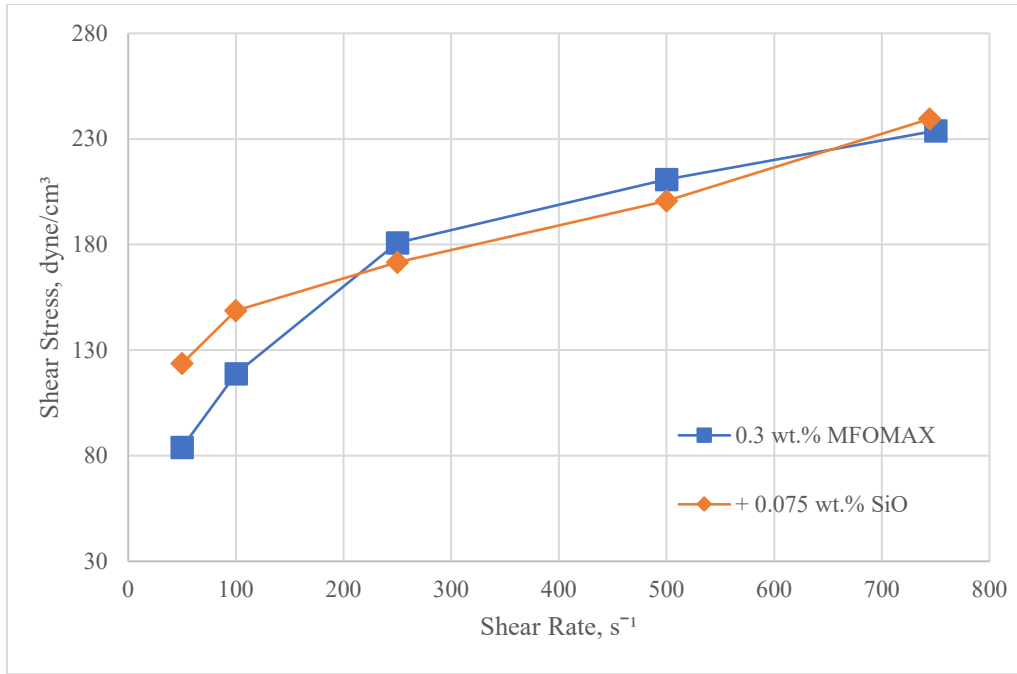


Figure 4.8: Shear rate versus shear stress in the absence and presence of nanoparticles during rheology experiment at 70% foam quality.

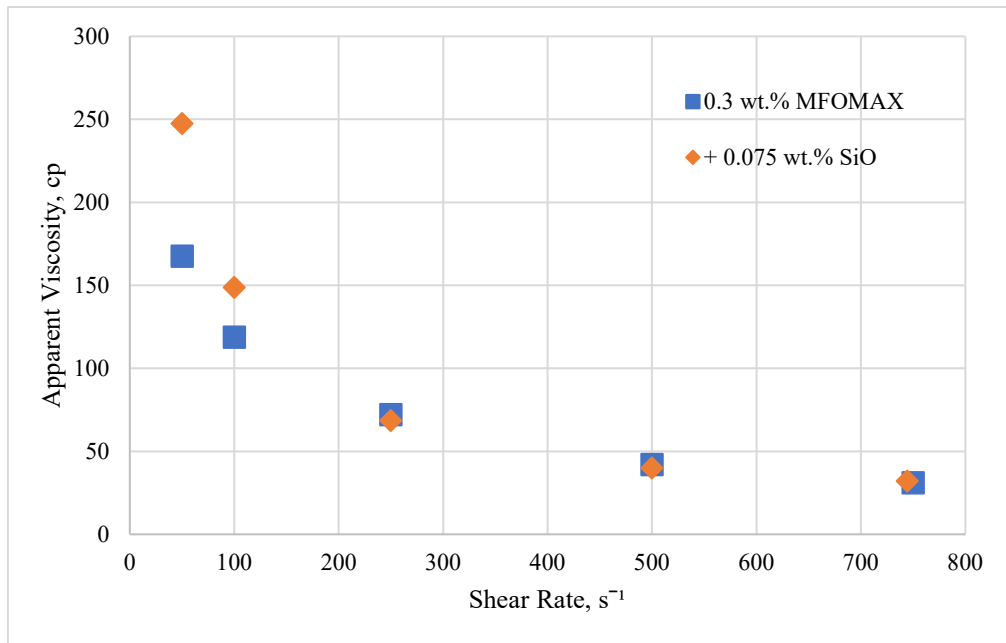


Figure 4.9: Foam viscosity curve in the absence and presence of nanoparticles during rheology experiments at 70% foam quality.

Figure 4.8 shows the flow curve of foam in the presence and absence of nanoparticles. The corresponding flow curves in the absence and presence of

nanoparticles are similar and very close to each other. Similar behaviour is also observed in the viscosity curve, as shown in **Figure 4.9**; foam in the absence and presence of nanoparticles exhibits shear-thinning behaviour, as observed by Xiao, et al. [29] and Yekeen, et al. [61]. However, nano-foam exhibits higher apparent foam viscosity than surfactant foam at a shear rate of less than 100 s^{-1} [29].

4.2.2 Nanoparticles-Stabilized Foam Rheology as a Function of Nanoparticles Concentration, Shear Rates, and Foam Quality

This section discussed the rheology of nanoparticle-stabilized foam as a function of nanoparticle concentration, shear rates, and foam quality. The surfactant concentration was fixed at 0.3 wt.%, and the nanoparticle concentration increased from 0 wt.% to 0.6 wt.% at fixed salinity and foam quality. The corresponding viscosity curve is shown in **Figure 4.10**.

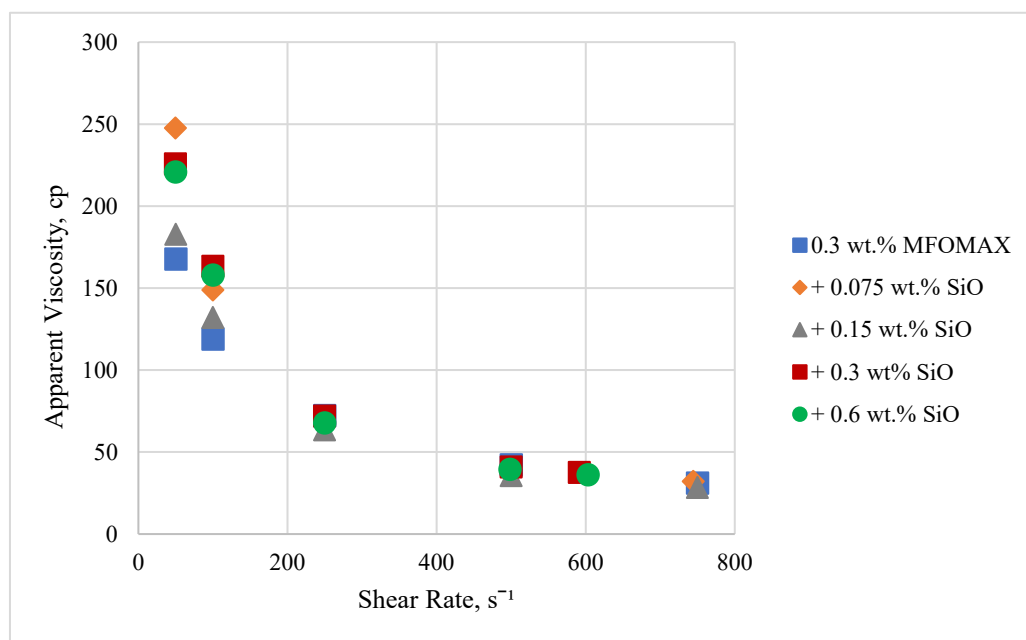


Figure 4.10: Foam viscosity curve with increasing nanoparticle concentration at a fixed 0.3 wt.% surfactant concentration at 70% foam quality.

The effect of nanoparticle concentration on apparent foam viscosity is significant at a shear rate of less than 250 s^{-1} . Based on the results presented in **Figure 4.10**, it can be observed that apparent viscosity first increases with nanoparticle concentration and

then decreases as nanoparticle concentration further increases. Previous research observed similar results, whereby excessive nanoparticles present in the solution may decrease the apparent foam viscosity due to the formation of large and dense aggregates [31, 51]. An optimum foam apparent viscosity is achieved at 0.075 wt.% nanoparticle concentration, equivalent to a 1:4 nanoparticle-surfactant ratio.

The apparent foam viscosity in the absence and presence of nanoparticles is similar at a shear rate higher than 250 s^{-1} . The nanoparticle's presence in foam lamellae could not maintain the foam structures or foam stability when being sheared at a high rate. In addition to that, the continuous foam could not be generated using 0.3 wt.% and 0.6 wt.% nanoparticles concentration at 750 s^{-1} . Therefore, the apparent foam viscosity was only achievable at a slightly lower shear rate of 565 s^{-1} and 600 s^{-1} . As high shear rate conditions exist in the near-wellbore region in actual application, having no foam presence in the near-wellbore region may avoid potential injectivity issues.

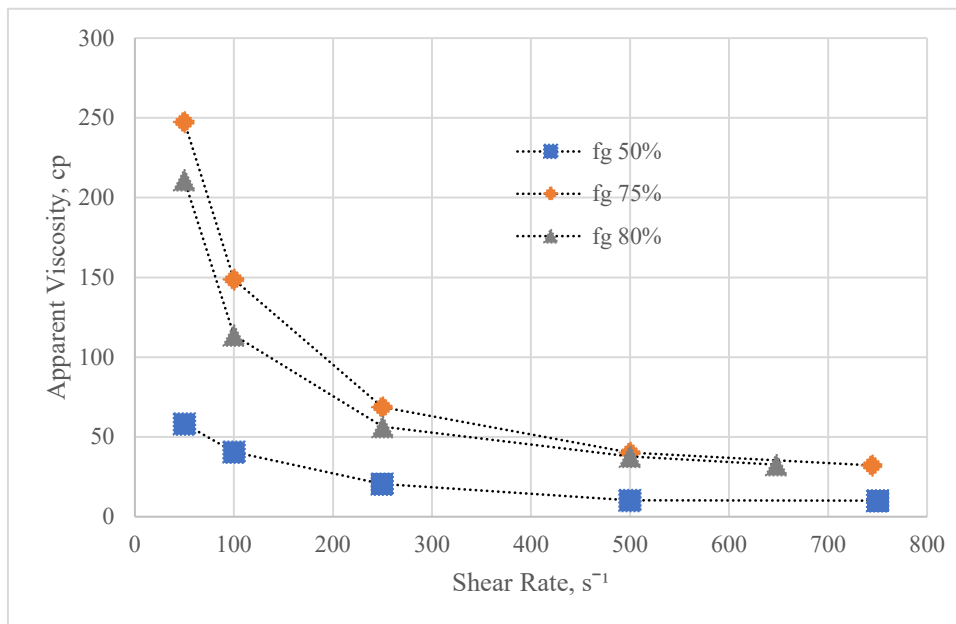


Figure 4.11: Foam viscosity curve at optimum nanoparticles-surfactant ratio and varying foam quality.

The nano-foam apparent viscosity decreases with increasing shear rate at 50%, 75%, and 80% foam quality, as shown in **Figure 4.11**. Similar behaviour was observed at higher nanoparticle concentrations and foam quality of 50%, 70%, and 80%. However, the nano-foam rheology behaviour at foam quality higher than 80% was

undetermined as it is too dry to generate a continuous foam for the measurements [87]. The same measurement limitation occurs with surfactant foam.

In summary, nano-foam exhibits shear-thinning behaviour similar to surfactant foam, with an increasing shear rate at varying nanoparticle concentrations and foam quality up to 80%. Both surfactant foam and nano-foam have rheology measurements limitations at foam quality higher than 80% as the foam easily breaks down when it is subjected to shear. Although surfactant foam and nano-foam exhibit similar rheological behaviour, the corresponding nano-foam apparent viscosity is higher at a lower shear rate. Therefore, a more stable foam exists in the presence of nanoparticles deep in the reservoir, at which the shear rate is low.

4.3 The Parameters Affecting the Mobility Reduction Factor of the Nano-Foam

Sand pack flooding experiments were conducted as a function of nanoparticle concentration, foam quality, injection rate, and salinity to understand their relative influence on the effectiveness of nanoparticles toward foam mobility reduction factor. The surfactant foam flooding was established to be compared with the nano-foam behaviour. The results obtained from sand pack flooding identify the optimum conditions and parameters at which the apparent foam viscosity of nanoparticle-stabilized foam can be achieved. It also enhances the understanding of the nanoparticle stabilization mechanism involved during flow through porous media.

4.3.1 The Effect of Foam Quality in the Absence and Presence of Nanoparticles

The experiment was conducted at a fixed surfactant concentration, total injection rate, and salinity. Two sets of experimental data were established in the absence and presence of nanoparticles, and the mobility reduction was measured at a varied foam quality of 30%, 50%, 70%, 80%, 90%, and 95%. The corresponding experimental result, known as the foam quality scan, is plotted in **Figure 4.12**.

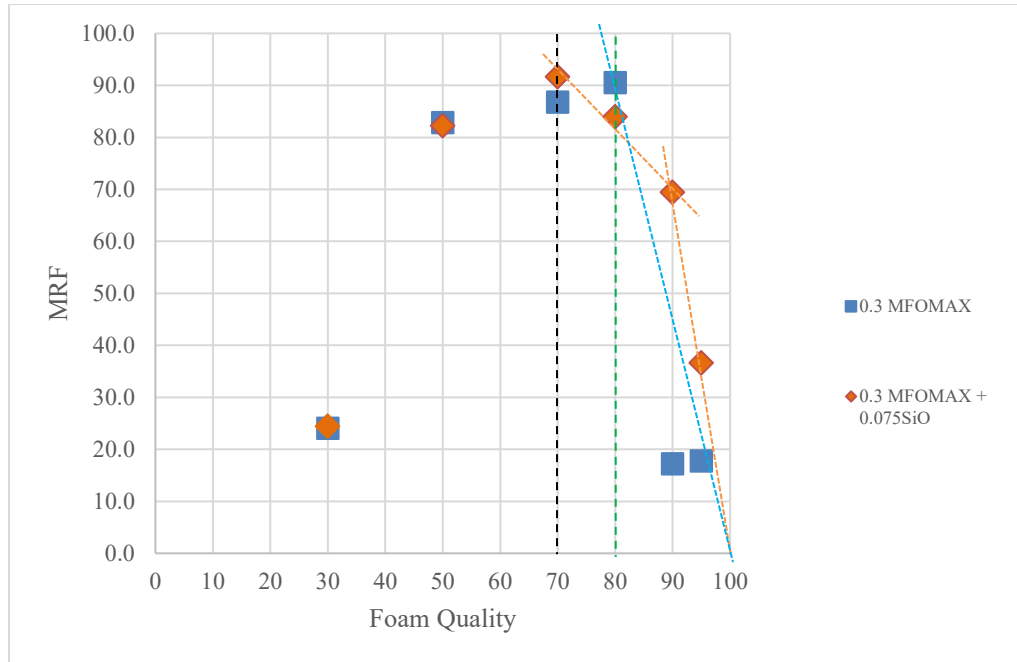


Figure 4.12: Mobility reduction ratio (MRF) with increasing foam quality in the absence and presence of nanoparticles. Foam collapse occurs beyond transition foam quality for surfactant-foam (in green dashed line) and nano-foam (in black dashed line). Unlike surfactant foam (in blue dashed line), nano-foam (in orange dashed line) does not immediately collapse after the transition foam quality.

Based on **Figure 4.12**, it can be observed that both foams, in the absence and presence of nanoparticles, exhibit similar behaviour. Two regions can be observed from the plot; a low-quality regime in which the MRF increases with increasing foam quality as the foam is generated and a high-quality regime in which the MRF decreases with increasing foam quality due to foam collapse [20, 83]. The transition between the low-quality and high-quality regimes occurs at the transition foam quality, f_g^t at which maximum MRF is achieved. The maximum MRF was achieved at a lower foam quality of 70% compared to surfactant foam at a foam quality of 80% in nanoparticles' presence. Although the transition foam quality in the presence of nanoparticles occurs earlier than surfactant foam, the MRF in the presence of nanoparticles is up to 3.5 and 4 times higher than surfactant foam at 90% and 95% foam quality, respectively.

Different foam collapse behaviour was observed between surfactant foam and nanoparticle-stabilized foam. As shown in **Figure 4.12**, surfactant foam immediately collapses at a foam quality higher than transition foam quality or a high-quality regime

[3, 20, 83]. Interestingly, MRF in the presence of nanoparticles does not decrease abruptly after the transition foam quality. Instead, the MRF decreases at a slower rate before the immediate collapse. Therefore, a two-stage foam collapse is based on two decay rates observed in the high-quality regime; a low decay rate between transition foam quality to 90% foam quality and a high decay rate beyond 90% foam quality, as shown by the orange dash line in **Figure 4.12**.

Two possible mechanisms may contribute to nano-foam collapse behaviour. The low decay rate in nanoparticles' stabilized foam collapse may be due to nanoparticles' presence in the foam lamellae. As the foam quality increases, the foam's liquid volume decreases, resulting in a thinner lamellae thickness. In this condition, the nanoparticles in the lamellae are forced to rearrange themselves into a close-packed arrangement and provide a barrier to inhibit the thin lamellae from collapsing [30, 94]. Another mechanism is associated with the foam collapse phenomena described by the capillary pressure exerted on the lamellae between two bubbles. As the thickness of the lamellae decreases with decreasing liquid volume, the capillary pressure exerted on the lamellae between two gas bubbles increases. The critical capillary pressure at which the lamellae can withstand before collapsing is known as the critical capillary pressure to coalesce [95]. However, in the presence of nanoparticles, a solid phase exists in the lamellae. The presence of nanoparticles in the lamellae enhances the ability to withstand the capillary pressure exerted before collapsing, thus increasing the capillary pressure to coalesce [36].

Therefore, the effect of nanoparticles stabilizing the foam can be significantly observed in a high-quality regime and extremely high foam quality. There is a two-stage foam collapse based on two decay rates observed in the high-quality regime, a low foam decay rate after the foam reaches the transition foam quality and an immediate collapse after reaching critical capillary pressure to coalesce in the presence of nanoparticles.

4.3.2 The Effect of Nanoparticles' Concentration at High Foam Quality

The effect of nanoparticle concentration was analysed at the transition foam quality and at a high foam quality of 95%, at which the effect of nanoparticle stabilization is observed. The sand pack flooding was conducted at a fixed surfactant concentration, salinity, and injection rate. The nanoparticle concentration was varied with 0 wt.% as a reference case in the absence of nanoparticles, followed by 0.075 wt.%, 0.15 wt.%, 0.3 wt.%, and 0.6 wt.%, respectively. The co-injection of nanoparticles-surfactant mixture and gas was initially injected at 70% foam quality for two-pore volumes of injection, followed by 95% foam quality. The corresponding results are shown in **Figure 4.13**.

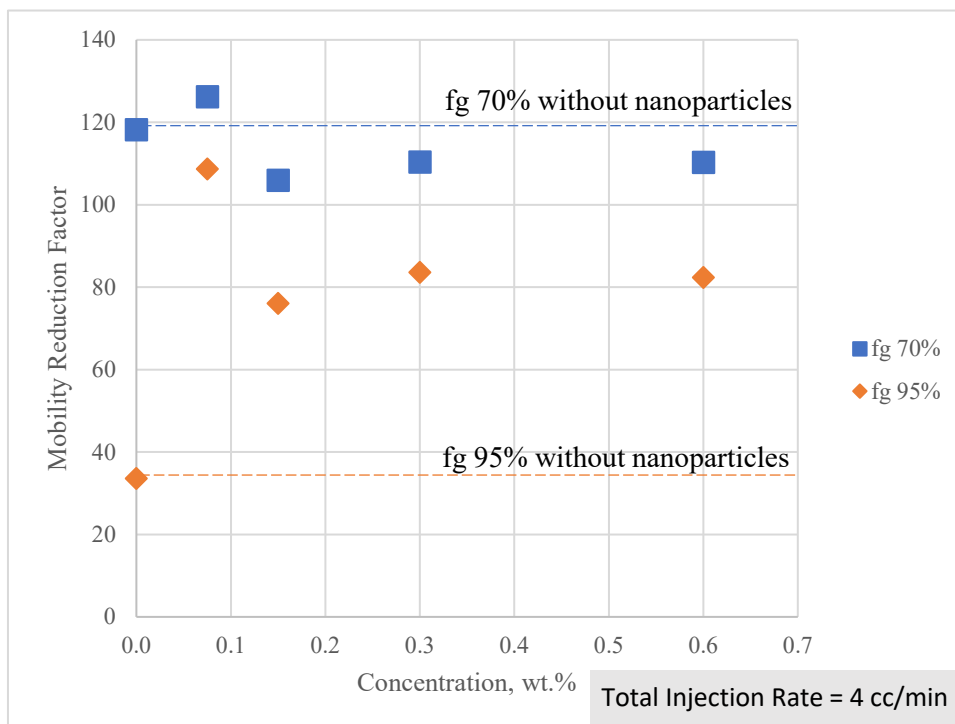


Figure 4.13: The effect of nanoparticle concentration at transition foam quality (70%) and 95% foam quality.

Based on **Figure 4.13**, it can be observed that increasing nanoparticle concentration does not necessarily enhance foam stability at 70%. Nanoparticles-stabilized foam at nanoparticles concentration of 0.15 wt.%, 0.3 wt.%, and 0.6 wt.% resulted in MRF slightly lesser compared to surfactant foam. The foam lamellae can be assumed to be considerably thick in this condition, and a sufficient amount of liquid is still available.

Therefore, the liquid in the lamellae is mainly affecting the foam collapse behaviour in this condition.

As opposed to co-injection at 95% foam quality, nanoparticles' presence does improve the foam stability compared to surfactant foam. At 95% foam quality, a dry foam exists with extremely thin lamellae between the two gas bubbles. As shown in **Figure 4.13**, the MRF of surfactant foam is very low compared to 70% foam quality. Foams are easily collapsed due to extremely high capillary pressure exerted on the thin lamellae between the two gas bubbles. However, the MRF of nanoparticle-stabilized foam is relatively higher compared to surfactant foam. This has proven that the nanoparticles in the lamellae increase the foam stability, thus generating a stronger and more stable foam lamella that can withstand higher capillary pressure.

The optimum nanoparticle concentration at the experimental conditions of this study is 0.075 wt.%, where the maximum MRF is achieved at both 70% and 95% foam quality. It can be observed that the MRF of surfactant foam significantly decreases as the foam quality changes from 70% to 95%. In the presence of nanoparticles, similar behaviour is observed. However, MRF reduction is less, indicating that strong foam still exists due to nanoparticles' foam stabilization.

It is important to note that the optimum nanoparticle concentration may vary when different types of nanoparticles or surfactants are used, as has been observed by Razali, et al. [7]. The synergy between the nanoparticle's surface charge and the surfactant molecule head charge interaction is unique to the type of nanoparticle and surfactant used. Therefore, it is recommended to identify and validate the optimum concentration when other nanoparticles and surfactants are being assessed.

4.3.3 The Effect of Total Injection Rate at Fixed Nanoparticles Concentration

The effect of the total injection rate of gas and liquid is performed through sand pack flooding. The sand pack flooding was conducted at fixed surfactant concentration, optimum nanoparticles concentration, foam quality, and salinity, whereas the total injection rates varied between 2.0 cc/min and 9.0 cc/min. The lowest possible injection rates are 2.0 cc/min due to the gas injection rate's mechanical limit. The high total

injection rate may represent how foam flows in the near-wellbore region. In contrast, the total low injection rate may represent the corresponding MRF away from the wellbore region in actual field application.

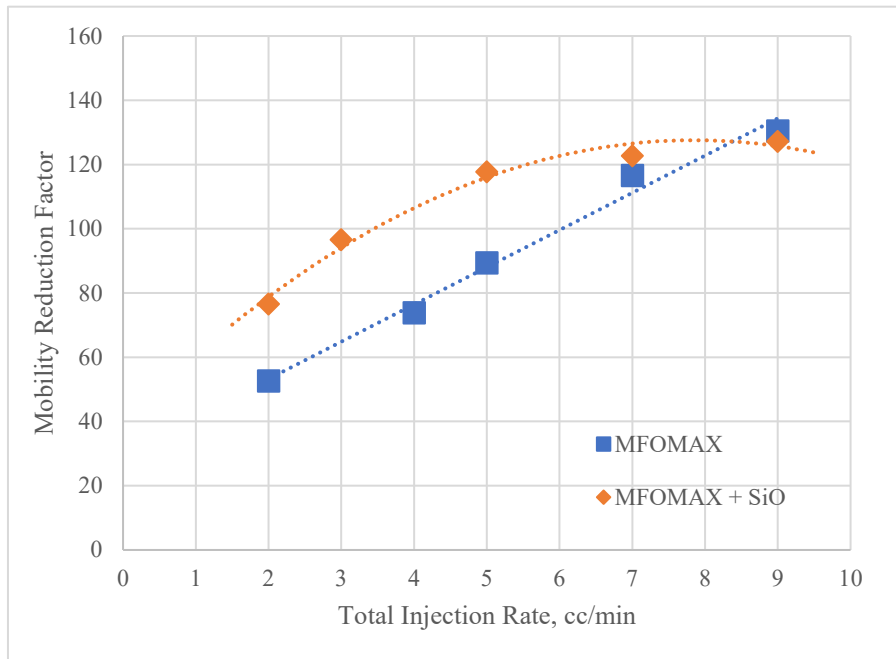


Figure 4.14: The effect of total injection rates at fixed foam quality in the absence and presence of nanoparticles.

The effect of total injection rates varies in the absence and presence of nanoparticles, as shown in **Figure 4.14**. In the absence of nanoparticles, MRF decreases linearly from 130.6 to 52.7 as the total injection rate decreases from 9.0 cc/min to 2.0 cc/min. In nanoparticles' presence, the MRF decreases slightly from 127.2 to 117.8 as the total injection rates decrease from 9.0 cc/min to 5.0 cc/min. Further reduction of total injection rates to 2.0 cc/min resulted in a significant MRF reduction to a value of 76.6. Although the MRF decreases with decreasing total injection rates, the MRF was higher in the presence of nanoparticles at low rates compared to surfactant foam. Therefore, a relatively stable foam can still exist in the presence of nanoparticles at a low total injection rate of 2 cc/min.

The foam propagation in porous media is a function of lamellae breaking and regeneration [96]. It can be assumed that as the total injection rate increases from 2.0 cc/min to 5.0 cc/min, the rate of lamellae generation is higher than lamellae breaking,

thus resulting in increasing MRF. As the MRF exhibited by the nanoparticles-stabilized foam is more significant compared to surfactant foam, it can be assumed that the rate of foam collapse is much less compared to surfactant foam. This finding further supports the mechanism by which the nanoparticles in the lamellae decrease foam collapse rate, thus improving foam stability.

As the total injection rate further increases up to 9 cc/min, the MRF achieved in nanoparticles' presence is similar to the MRF values of surfactant foam. In this condition, the rate of lamellae breaking and regenerating can be assumed to be similar in the absence or presence of nanoparticles, as the lamellae cannot withstand the applied shear force.

4.3.4 The Effect of Nanoparticles on Varying Salinity

Two sets of sand pack flooding were performed in the absence and presence of nanoparticles at the same experimental condition to understand the effect of salinity on nanoparticle-stabilized foam. The surfactant concentration, total injection rate, and foam quality were fixed at 0.3 wt.%, 4.0 cc/min, and 95%, respectively. The foam flooding experiments in the presence of nanoparticles were performed at the optimum nanoparticle concentration. The co-injection of gas and surfactant mixture is performed after the surfactant flooding. The salinity is varied between 1 wt.% and 3 wt.% NaCl. The results are shown in **Figure 4.15**.

The MRF observed in the absence and presence of nanoparticles ranged between 16 and 30 with increasing salinity. Ideally, MFOMAX is not sensitive to salinity within the tested range. However, the MRF was established at 3.0 wt.% NaCl may potentially be associated with experimental error due to potential trapped gas remaining in the sand pack based on experimental data analysed. Pre-existing trapped gas in the sand pack may result in an optimistic differential pressure reading.

The MRF of nanoparticle-stabilized foam decreases with increasing salinity, as shown in **Figure 4.15**. This behaviour's possible cause may be due to the interaction between the salt ions and the nanoparticle's surface charge. Opposite-charge salt ions can be attracted to the nanoparticles' surface charge, resulting in the neutralization of

the nanoparticles' surface charge and causing the nanoparticles to aggregate [56]. Therefore, the increasing salt ion content in the solution reduces the effectiveness of nanoparticles stabilizing the foam.

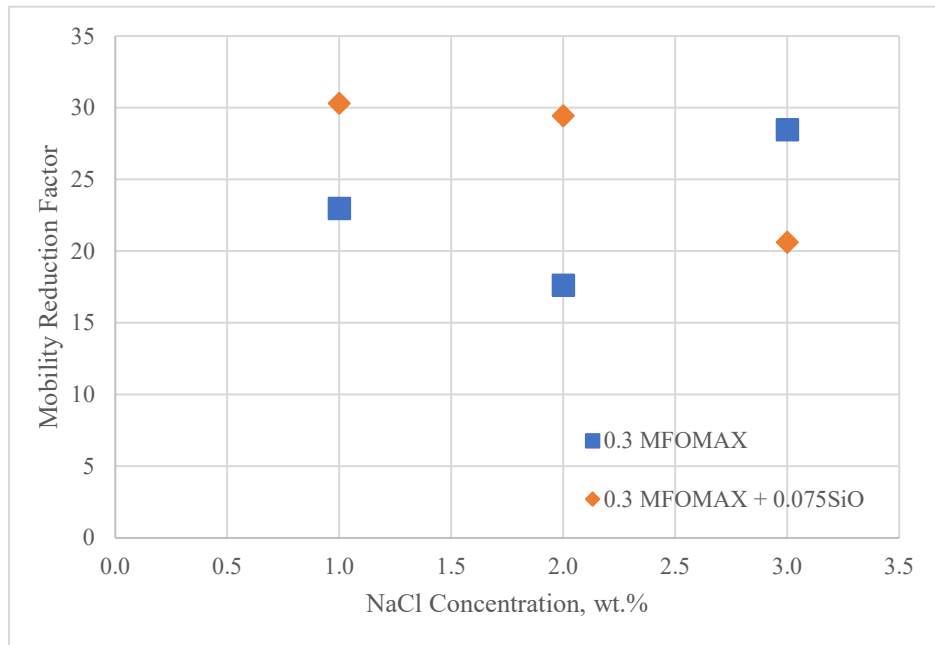


Figure 4.15: Effect of salinity in the absence and presence of nanoparticles.

4.4 Modelling of Nano-Foam Foam Transport Behaviour through Porous Media

The nanoparticles' stabilized foam transport behaviour through porous media was performed based on an empirical or implicit texture model technique. The model assumes that a foam exists whenever gas and surfactant co-exist. The effect of gas mobility reduction due to foam is modelled by modifying the relative permeability. Several parameters affect foam mobility reduction (FMR). However, before any foam modelling analysis, it is crucial to estimate the foam model parameters by fitting them to foam quality scan and foam velocity scan. First, a sensitivity analysis was conducted to understand the effects of critical foam model parameters on the foam flow behaviour. Then, the foam model parameters were estimated for nanoparticle-stabilized foam and validated using a commercial simulator (CMG STARS). The analysis and the gaps identified to model the transport behaviour of nanoparticle-stabilized foam will be discussed.

4.4.1 The Effect of Foam Model Parameters $fmmob$ and $F_{dry-out}$

A sensitivity study was conducted to understand the effect of $fmmob$ and $F_{dry-out}$ parameters on the experimental data fit. The sensitivity study was conducted using the surfactant foam experimental data. Initially, the foam model parameters were estimated based on the established MATLAB function as a reference case shown in **Figure 4.16**. Then, each foam model parameter was varied one at a time, fixing the remaining model parameters.

4.4.1.1 The Effects of $fmmob$ at Fixed F_3 and $F_{dry-out}$

The $fmmob$ value was varied between 500 and 5000 at a fixed F_{dry} , and the F_3 value and the corresponding effect of $fmmob$ is shown in **Figure 4.16**. It can be observed that increasing the $fmmob$ value increases the maximum apparent viscosity. The transition foam quality, fg^t , also shifted to a lower fg value as $fmmob$ increased. $fmmob$ is a parameter that corresponds to the maximum possible mobility reduction inflicted by the foam, which occurs at the transition foam quality. Therefore, $fmmob$ is a critical foam model parameter that determines the maximum achievable reduction in gas mobility and the transition foam quality from a low-quality to a high-quality regime.

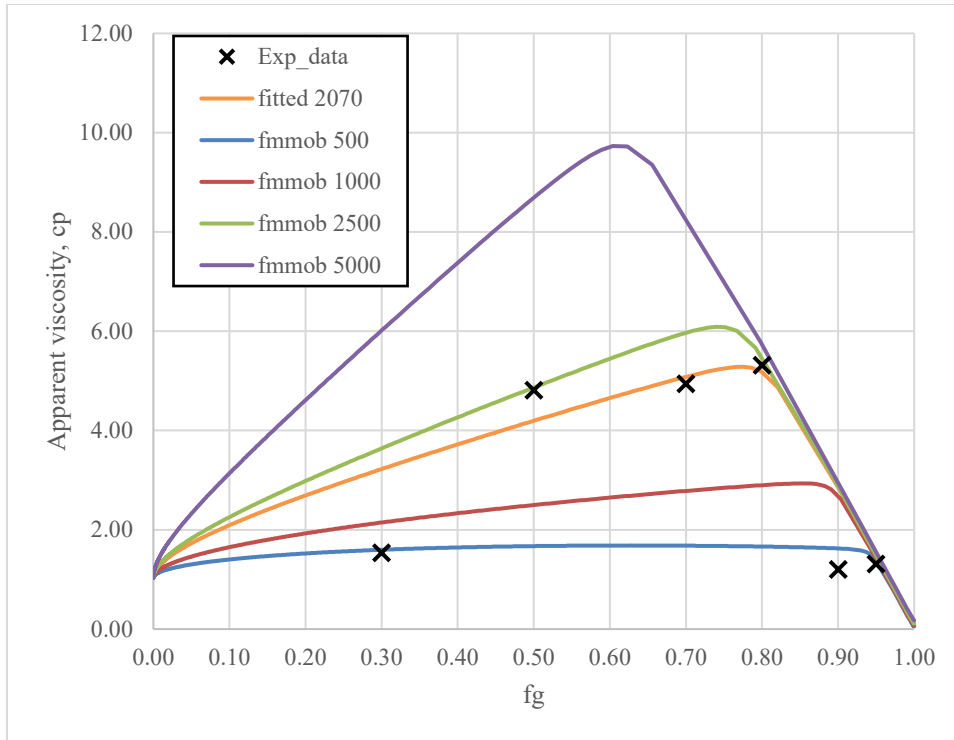


Figure 4.16: Effect of $fmmob$ toward foam strength at increasing foam quality.

4.4.1.2 The Effects of $F_{dry-out}$ at fixed $fmmob$ and F_3

The F_{dry} function captures the changes in foam strength as foam quality increases in the high-quality regime. Foam collapse behaviour is observed in a high-quality regime as foam loses its strength; apparent foam viscosity decreases with increasing foam quality. $fmdry$ is the critical water saturation at which the maximum foam strength is achieved and is described by the limiting capillary pressure phenomena [17]. As shown in Figure 4.17 and Figure 4.18, decreasing the $fmdry$ value delays foam collapse and increases the maximum achievable foam strength.

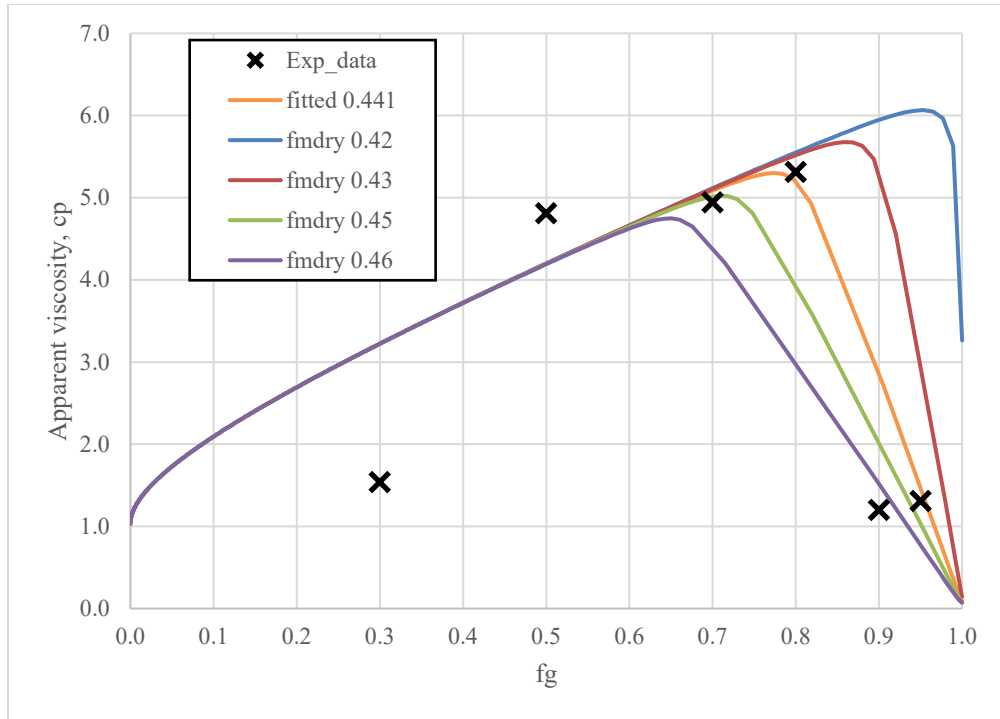


Figure 4.17: Effect of *fmdry* toward foam strength at increasing foam quality.

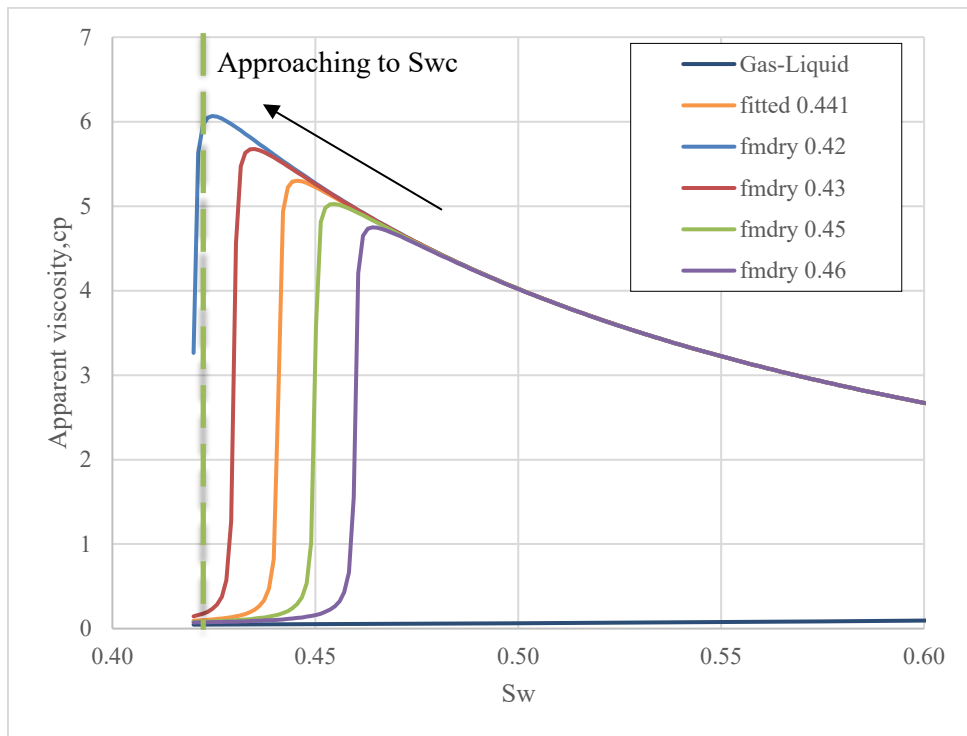


Figure 4.18: Effect of *fmdry* toward apparent foam viscosity at varying water saturation.

The $epdry$ parameter is the exponent of the $Fdry$ function. It describes the rate of foam collapse. As shown in **Figure 4.19**, increasing $epdry$ to the value of 1000 describes the behaviour at which the foam collapses almost instantaneously upon reaching the $fmdry$ value. At a lower $epdry$ value, the foam collapse rate decreases. In addition to that, it causes the maximum achievable foam strength to decrease.

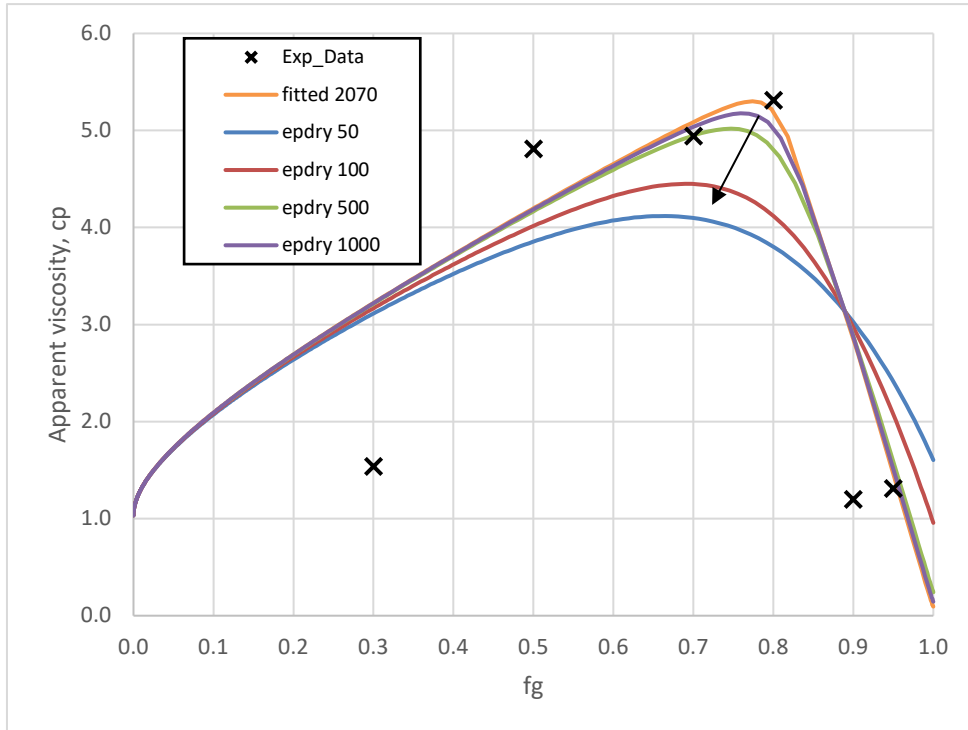


Figure 4.19: Effect of $epdry$ toward foam strength at increasing foam quality.

4.4.2 Estimation of Nano-Foam Model Parameters

Both foam quality scan and foam velocity scan in the presence of nanoparticles established through foam flooding experiments were used to estimate foam model parameters using the adapted method by Kapetas, et al. [3]. This method focuses on determining the value of the reference foam mobility factor ($fmmob$), the shear-thinning velocity effect (F_3) in the low-quality regime, and foam collapse due to critical capillary pressure ($F_{dry-out}$) in the high-quality regime. Foam parameters of $fmmob$, $fmdry$, $epdry$, $fncap$, and $epcap$ are fitted to foam quality scan data in MATLAB using a constrained non-linear least-square minimization approach. The corresponding estimated foam

model parameters based on the model algorithm and fitted foam behaviour are shown in Table 4.2 and Figure 4.20.

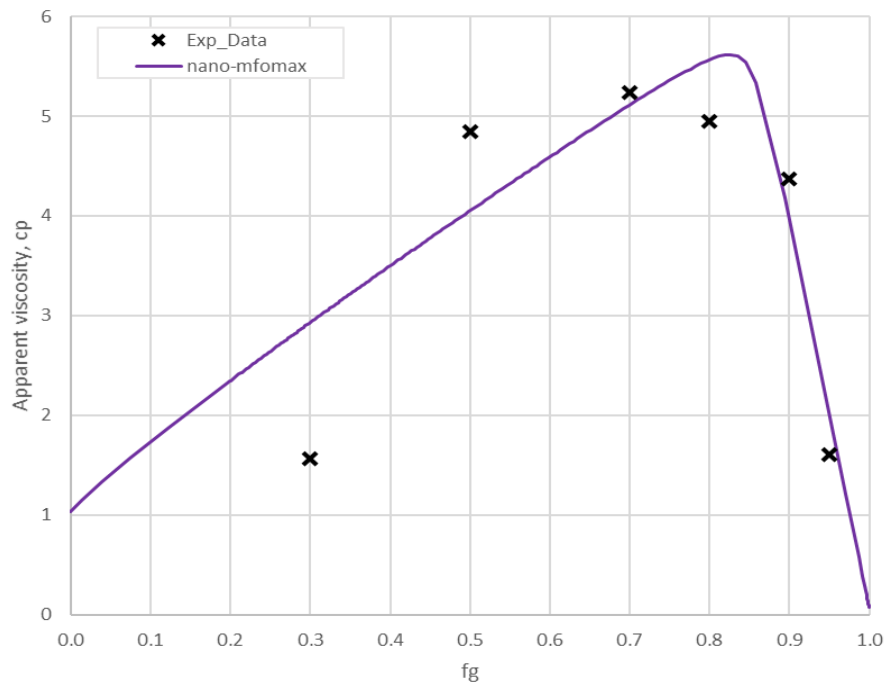


Figure 4.20: Nanoparticle-surfactant foam fitted behaviour.

Table 4.2: Estimated foam model parameters in the presence of nanoparticles.

Parameter	$fmmob$	$fmdry$	$epdry$	$fncap$	$epcap$
Nano-mfomax	3035.7	0.214	1347.9	8.07e-5	1.908

As shown in Figure 4.20, the nanoparticle-stabilized foam behaviour corresponding to the best-fit foam model parameters cannot fit the experimental data. The current model could not capture the two-stage foam collapse decay behaviour discussed in Section 4.3.1. Instead, the fitted curve estimated a higher value of maximum foam apparent viscosity. In addition to that, the transition foam quality occurred at a higher value (approximately 83% foam quality) compared to the experimental data (at 70% foam quality). The foam model parameters estimated using the current method may result in an optimistic foam behaviour. As shown in Figure 4.20, the fitted curve (the purple line) overestimated the foam strength with a higher apparent foam viscosity. It did not match the actual transition foam quality at which the foam needs to collapse.

4.4.2.1 Tuning $epdry$ to Improve the Nano-Foam Model Parameters Estimation

The $epdry$ foam model parameters were tuned to optimize the rate of foam collapse in the high-quality regime. As discussed in Section 4.4.1.2, a low $epdry$ value represents a slow foam decay rate, while instantaneous foam collapse occurs at an $epdry$ value higher than 1000. **Figure 4.21** shows the foam model parameter curve fit using low and high $epdry$ values. The corresponding estimated foam model parameters are tabulated in **Table 4.3**, respectively.

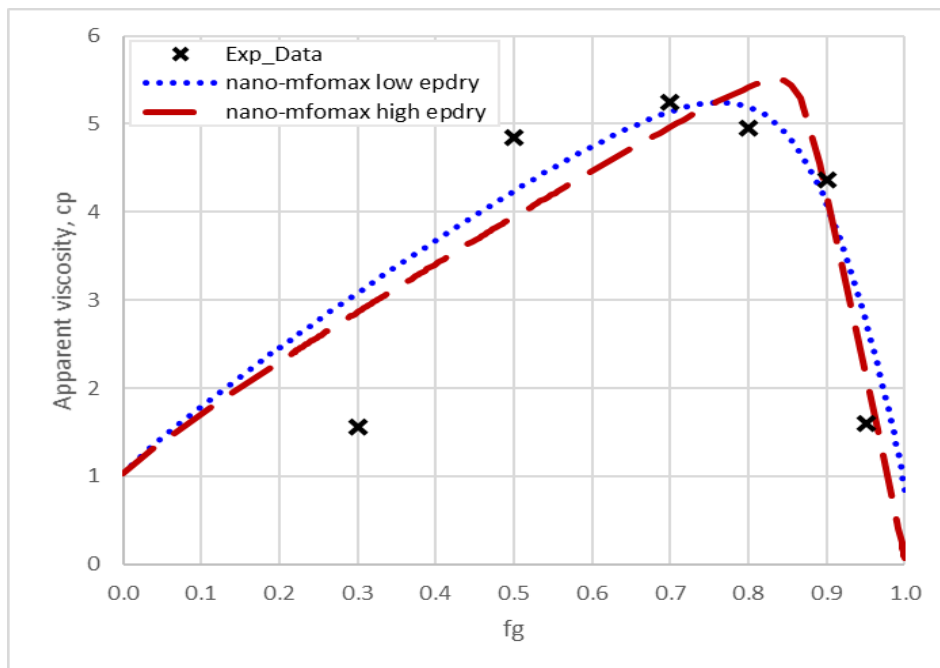


Figure 4.21: Tuned foam model parameter ($epdry$) fit for nanoparticles-surfactant foam.

Table 4.3: Tuned foam model parameters (low $epdry$ and high $epdry$ value) in the presence of nanoparticles using the current foam model function.

Parameter	$fmmob$	$fmdry$	$epdry$	$fmcap$	$epcap$
Nano-mfomax low $epdry$	1119.0	0.210	89.1	1.92e-05	0.501
Nano-mfomax high $epdry$	2341.8	0.212	1329.529	3.25e-05	1.009

The tuned foam fit curve using the high $epdry$ value exhibits similar foam behaviour to best-fit foam model parameter fitting results. It can fit the experimental results at foam quality higher than 90%. The corresponding fit curve overestimated the maximum

achievable foam apparent viscosity and the transition foam quality at which the foam starts to collapse.

The tuned foam fit curve using a low *epdry* value matched the slow decay rate observed from the experimental data between the transition foam quality (at 70% foam quality) and the 90% foam quality. Estimating transition foam quality and maximum achievable foam apparent viscosity were significantly improved compared to the un-tuned foam model parameter fit. However, the tuned foam fit curve overestimated the apparent foam viscosity at foam quality higher than 90%. At this condition, the estimated model parameters show that partial foam still exists based on the apparent foam viscosity value, although the foam should be collapsing.

4.4.2.2 Validation of Best-fit and Tuned-fit Nano-Foam Model Parameters Flow Behaviour using a Commercial Simulator

The calculated foam model parameters using the current method are incorporated into an existing commercial simulator (CMG STARS) to validate the foam flow behaviour, especially at high foam quality. The corresponding differential pressure from the simulator for best-fit and tuned foam model parameters (low and high *epdry* value) and actual data are plotted at 70% and 95% foam quality in **Figure 4.22** and **Figure 4.23**, respectively. The best-fit and tuned foam model parameters used are referred to in **Table 4.2** and **Table 4.3**.

Based on **Figure 4.22** and **Figure 4.23**, best-fit nano-MFOMAX foam model parameters (as per **Table 4.2** and **Table 4.3**) could not simulate the stable differential pressure behaviour as per the observed data. The simulated differential pressure trend was lower at 70% foam quality and higher at 95% foam quality than in experimental data. Based on **Figure 4.20**, the fitted model curve is slightly lower than the experimental data at 70% foam quality. This result is in agreement with the simulated differential pressure trend compared to experimental data. Similar behaviour was observed at 95% foam quality. Therefore, best-fit nano-MFOMAX foam model parameters are unable to simulate the foam flow behaviour in porous media.

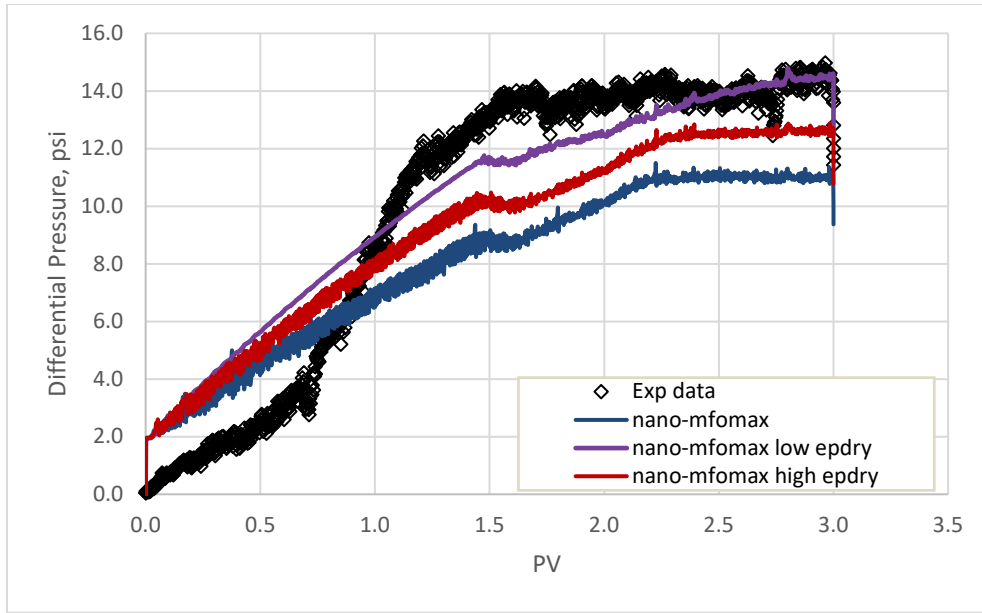


Figure 4.22: Differential pressure trend of nanoparticles-stabilized foam modelling in CMG STARS utilizing estimated foam parameters for steady-state co-injection at 70% foam quality; best-fit nano-MFOMAX, tuned with low *epdry* as well as tuned with high *epdry*.

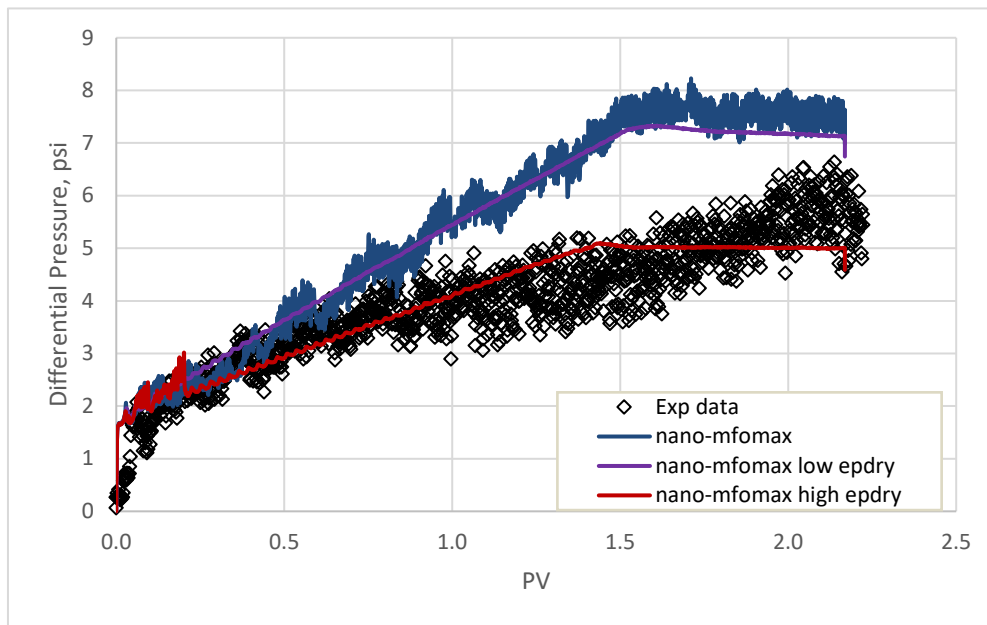


Figure 4.23: Differential pressure trend of nanoparticles-stabilized foam modelling in CMG STARS utilizing estimated foam parameters for steady-state co-injection at 95% foam quality; best-fit nano-MFOMAX, tuned with low *epdry* as well as tuned with high *epdry*.

Similar to the foam model parameter fit curve shown in **Figure 4.21**, the tuned foam model parameter using a low *epdry* value could simulate the differential pressure trend at low foam quality conditions. The tuned foam model parameters using a low *epdry* value simulated the stable differential pressure observed at the transition foam quality (70%), as shown in **Figure 4.22**. However, the model could not simulate the differential pressure observed at 95% foam quality as per **Figure 4.23**. The low *epdry* value forces the foam to collapse at a lower decay rate, simulating good foam flow behaviour in the presence of nanoparticles at low foam quality but being unable to simulate the collapse of foam at very high foam quality.

The tuned foam model parameters using high *epdry* values, in contrast, were able to simulate the differential pressure behaviour at 95% foam quality compared to the transition foam quality of 70%. As shown in **Figure 4.21**, the model fit curve using the high *epdry* value underestimated the apparent foam viscosity at 70% foam quality, thus simulating a lower differential pressure value than experimental data. Although the foam model fit curve for high *epdry* value is similar to the best-fit foam model fit curve shown in **Figure 4.20** and **Figure 4.21**, the differential pressure trend was better matched at 95% foam quality experimental data as compared to the best-fit foam model parameters. This behaviour may be contributed by the higher *fmmob* value of the best-fit foam model parameter compared to the tuned foam model parameter.

In summary, the current foam model can adequately predict the differential pressure of the nano-foam using the fitted foam model parameters. However, the current foam model is unable to represent the two-stage foam collapse behaviour observed in the presence of nanoparticles. Therefore, the current foam model parameter can only simulate the nano-foam flow behaviour at a specific foam quality using a tuned-foam model parameter established as per **Table 4.3**.

4.4.2.3 Gaps Identified in the Current Foam Model Parameters Estimation Method in the Presence of Nanoparticles

Several gaps exist in the current empirical foam modelling technique for nanoparticle-stabilized foam based on the modelling study conducted. Although the

current foam model can adequately simulate the flow behaviour of nanoparticle-stabilized foam, an improvement in the current model may increase the accuracy of simulating the nano-foam flow.

The effect of the nanoparticle stabilization mechanism may not be captured effectively in the current foam model. As discussed in Section 4.3.1, a two-stage foam collapse was observed in the nanoparticles-stabilized foam that inhibits the foam from collapsing upon reaching the transition foam quality. The foam collapse was delayed with decreasing lamellae thickness. As the foam quality increases, the nanoparticles act as a barrier to flow in the lamellae, thus increasing the critical water saturation to coalesce. The current model assumed that the foam immediately collapsed upon reaching its critical water saturation to coalesce (f_{mdry}), which usually occurs after reaching the transition foam quality. The existing foam model can capture the critical water saturation to coalesce in the presence of nanoparticles. However, the current model overestimated the maximum achievable foam apparent viscosity (f_{mmob}) and the transition foam quality. Therefore, the foam collapse or dry-out function in the current model can be optimized by incorporating the two-stage foam collapse in the presence of nanoparticles.

The current foam model can only simulate the foam flow behaviour at a fixed foam quality. The foam collapse rate ($epdry$) will be tuned to simulate the foam flow behaviour at a specific foam quality because the current model can only accommodate one foam decay rate. As shown in **Figure 4.21** through **Figure 4.23**, low $epdry$ is ideal for modelling the low foam decay rate behaviour between the transition foam quality to the foam quality at which the critical water saturation to coalesce is reached (also referred to as the critical fg), whereas a high $epdry$ value is preferred for higher foam quality. **Figure 4.24** summarizes the conditions for tuning $epdry$ parameters. Consequently, the current foam model parameters could not capture the foam flow behaviour under a condition where the foam quality was continuously changing from low foam quality to high foam quality and vice versa. Hence, the current foam modelling technique is associated with high uncertainties, especially for nano-surfactant-alternating-gas injection, in which the gas and surfactant volumes are continuously changing as per the ratio of injected fluids.

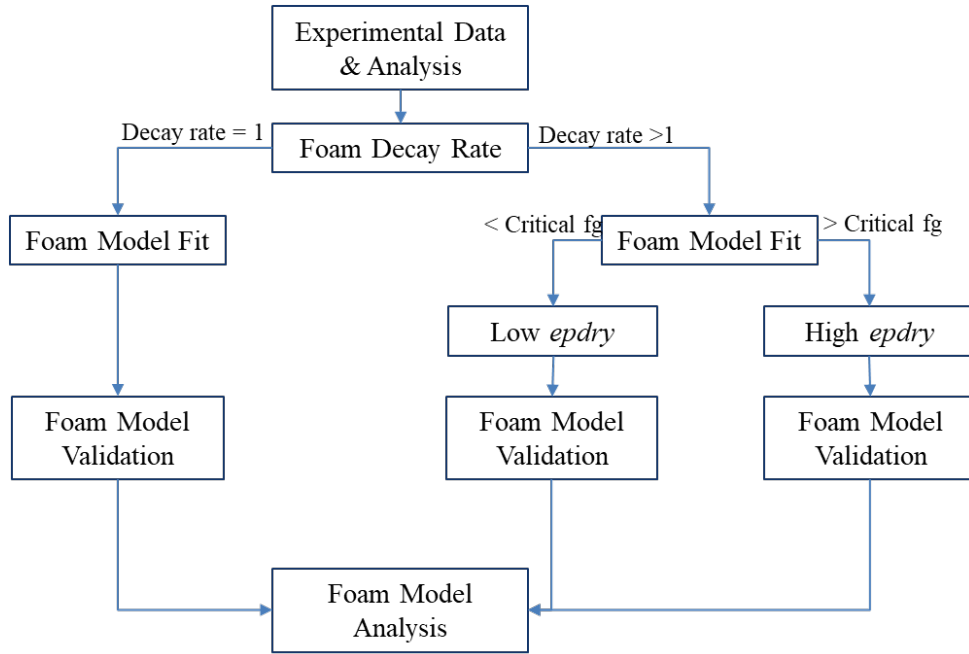


Figure 4.24: Summary workflow or the conditions for tuning $epdry$ parameters.

4.4.3 Modified Foam Model Parameter Function for Nano-Foam

A modification to the current $F_{dry-out}$ function is proposed to improve the implicit texture modelling technique for nano-foam based on the gaps discussed in Section 4.4.2.3. The proposed modified $F_{dry-out}$ function aims to:

- capture the two-stage foam collapse in the presence of nanoparticles observed from the foam quality scan, and
- increase the accuracy of nano-foam flow behaviour during simulation studies

The existing $F_{dry-out}$ function is derived from a mathematical sigmoid function. Therefore, the function only consists of one slope to describe the foam collapse decay rate. The critical water saturation at which the collapse or the $fmdry$ parameter occurs is described by the inflexion point of the “sigmoid” curve.

The $F_{dry-out}$ function is modified to have two slopes to capture two foam decay rates. The mathematical sigmoid function is preserved to retain the existing foam model parameters (water saturation, $fmdry$, and $epdry$), describing the foam collapse

behaviour. The new fitting parameter, $epcon$, is introduced in the modified $F_{dry-out}$ function shown in Equation 21.

$$F_{dry-out} = \frac{1}{1+0.5\left(\frac{S_w}{fmdry}\right)^{-epdry} + 0.5\left(\frac{S_w}{fmdry}\right)^{-epdry*epcon}} \quad (21)$$

Like in the existing foam model, S_w is the water saturation, $fmdry$ is the critical water saturation at which the foam will collapse, and $epdry$ controls the foam collapse rate.

The new parameter, $epcon$, is a constant fitting parameter that controls the rate of foam collapse at the condition in which $S_w > fmdry$, as shown in Figure 4.25. The $epcon$ parameter value shall range between zero (0) to one (1). At the condition in which $epcon$ is equal to one (1), only one (1) foam decay rate will exist; thus, the foam behaviour will be similar to surfactant foam, as shown in Figure 4.25. In the presence of nanoparticles, the $epcon$ value should be less than one (1) to capture the low foam decay rate observed between transition foam quality and the foam quality at which the nano-foam rapidly collapses.

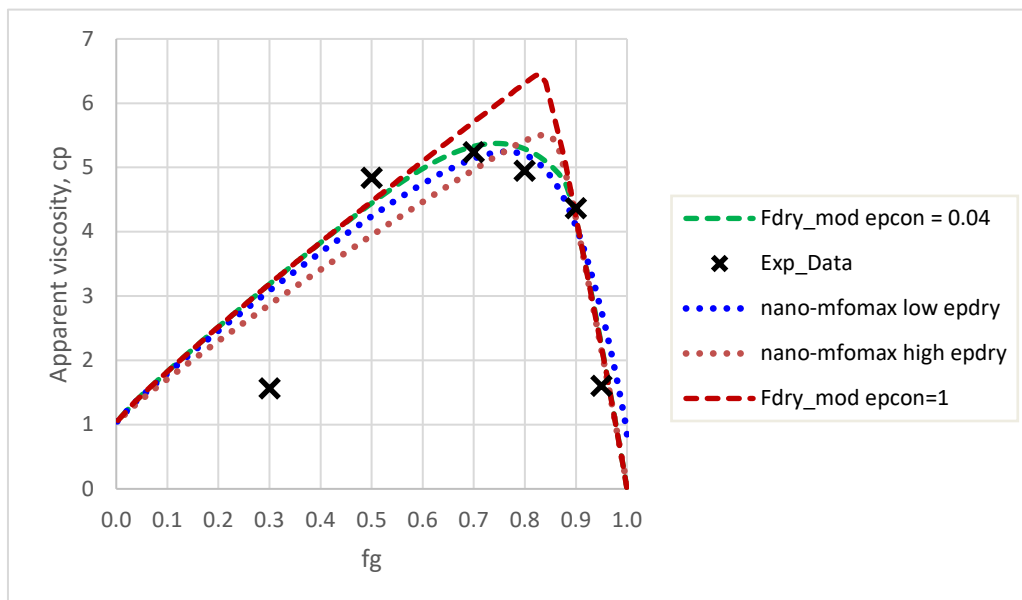


Figure 4.25: A comparison of the foam model parameter fit curve for tuned-foam model fit in dotted-line (low-epdry and high-epdry) and the modified $F_{dry-out}$ function in dashed-line (at $epcon = 1.0$ and best-fit $epcon = 0.04$).

The modified $F_{dry-out}$ function was incorporated into the MATLAB algorithm, and the corresponding foam model parameter fit was validated, as shown in Figure 4.25. The fitted curve results show that the modified $F_{dry-out}$ function with an $epcon$ value of 0.04 can capture the two-stage nano-foam collapse behaviour represented by a dashed green line in Figure 4.25. The modified function can fit the experimental data between transition nano-foam quality (70% foam quality) and the foam quality (90% foam quality) at which the nano-foam starts to collapse rapidly, as well as the nano-foam collapse behaviour beyond 90% foam quality. Therefore, the modified $F_{dry-out}$ function can describe nano-foam collapse behaviour, thus improving the accuracy of simulation of the nano-foam flow behaviour in porous media.

The proposed modified $F_{dry-out}$ function has been validated to describe the nano-foam behaviour better, as observed by the foam quality scan plot established through co-injection foam flooding experiments. However, the proposed modified function needs to be incorporated into the simulator algorithm to simulate and validate the nano-foam behaviour. This study may be potential future research to validate and optimize the implicit texture model for nanoparticle-stabilized foam.

4.5 Chapter Summary

This chapter reveals and discusses all the experimental results and nano-foam modelling findings in this research. There are several limitations associated with these findings that may be considered in future research to enhance our understanding of nano-foam stability performance further. Firstly, the optimum nanoparticle-surfactant ratios identified in this study are only applicable in this system because it is highly dependent on their synergistic effect. Secondly, this research focuses on the first level of foam stability evaluation under standard conditions and in the absence of oil, as this study attempts to evaluate the applicability to model nano-foam only on the foam stability improvement in the presence of nanoparticles without any other detrimental foam factor (effect of high temperature and oil). Thirdly, the current study only considers the effect of salinity in the presence of monovalent salt ions (NaCl) as it is the major salt present in seawater or formation water composition. Based on the

limitations considered within this research, the main discoveries are summarized in the following paragraphs.

Hydrophilic silica nanoparticle was observed able to remain dispersed in the solution better compared to slightly hydrophobic silica. However, the hydrophilic silica was unstable at 5 wt.% NaCl at all nanoparticles-surfactant concentration ratio. Therefore, the salinity were limited to 3 wt.% NaCl.

The nano-foam rheology behaviour was studied and compared with surfactant foam using a flow loop rheometer at varying nanoparticle concentration, foam quality, shear rate, and salinity. The results show that nano-foam exhibits shear-thinning behaviour at all conditions, similar to surfactant foam. However, nano-foam exhibits higher apparent foam viscosity at low shear rate conditions (50 s^{-1} to 250 s^{-1}). This result implies that stronger foam is formed at a lower shear rate in the presence of nanoparticles.

The co-injection sand pack experiments were conducted to understand the nano-foam flow behaviour in porous media and how its behaviour differs from the surfactant foam. The experiments were conducted at varying nanoparticle concentrations, foam quality, salinity, and injection rates at fixed surfactant concentrations and standard conditions. The results from the flow experiments are summarized below:

- Nano-foam exhibits a significantly high MRF value compared to surfactant foam at high foam quality, at which the foam starts to collapse (foam quality above 80%). Based on the foam quality scan, a two-stage foam collapse exists for nano-foam compared to a one-stage collapse in surfactant foam.
- Optimum nanoparticles concentration is identified at 0.075wt% which is equivalent to nanoparticle-surfactant ratio of 0.25. An optimum MRF was achieved both at the transition foam quality (70%) and at a very dry foam condition (95% foam quality).
- In general, MRF decreases with decreasing total injection rates of surfactant foam and nano-foam. However, nano-foam exhibited a higher MRF value than surfactant foam at a low total injection rate (2cc/min to 5cc/min). This behaviour indirectly indicates that better foam stability can be achieved in

the nano-foam at low flow velocity away from the injection points into the formation.

- There was an insignificant effect on MRF observed at varying salinity (10,000 ppm to 30,000 ppm) in the presence and absence of nanoparticles. The results observed may be contributed by the surfactant used, which is stable at high salinity conditions.

The modelling analysis conducted in this research focused on the method to estimate foam model parameters and the effect of foam flow behaviour, specifically on foam collapse behaviour in the presence of nanoparticles. This study focused on three (3) critical foam model parameters ($fmmob$, F_3 , and $F_{dry-out}$) needed to simulate foam flow behaviour successfully. The findings from the modelling analysis are summarized below:

- Based on the results obtained from rheology experiments, the current foam model assumption used whereby the foam is shear-thinning in behaviour is still valid for nano-foam.
- The existing foam model is unable to properly fit the nano-foam collapse behaviour as two-stage foam collapse exists.
- Better nano-foam model parameter fit can be achieved by forced-tuning the $epdry$ parameter to precisely fit one of the two-stage nano-foam collapses separately and validated in a commercial simulator with good differential pressure matching. However, the model is only able to simulate the foam's behaviour at specific foam quality conditions.

A modified $F_{dry-out}$ function was proposed to capture the nano-foam two-stage foam collapse behaviour by introducing a new fitting parameter, $epcon$. The proposed function has been validated to describe the nano-foam behaviour observed in the nano-foam quality scan.

CHAPTER 5

CONCLUSION AND RECOMMENDATION

5.1 Conclusions

The research's general objective was to establish an effective approach to estimate the model's parameters for implicit texture modelling for foam flooding with nanoparticle effect as a stabilizer. To achieve the project goal, four main stages were planned. Firstly, the silica nanofluid mixture compatibility were re-established at standard condition and the absence of oil. Secondly, the rheological behaviour of nano-foam regarding nanoparticle concentration, shear rate, and foam quality using a flow loop rheometer was assessed. Thirdly, the mobility reduction factors in surfactant foam and nano-foam flooding under the influence of nanoparticle concentration, salinity, foam quality, and total injection rate have been experimentally obtained and compared. Lastly, the existing foam model for the Dry-Out function used in the implicit texture modelling foam technique has been modified to incorporate the nanoparticles' effect. Specific conclusions are listed below:

- Hydrophilic silica was observed able to remain dispersed in the nanofluid mixture up to 3.0 wt.% NaCl. The nanofluid mixture was unstable at 5.0 wt.% NaCl.
- In laboratory studies, both surfactant foam and nano-foam exhibited shear-thinning behaviour using a flow loop rheometer. Therefore, the current implicit texture foam model's assumption is still valid for nano-foam rheological behaviour prediction.
- The mobility reduction factor (MRF) investigation in surfactant foam and nano-foam flooding under the influence of nanoparticle concentration,

salinity, foam quality, and total injection rate showed that the optimum nanoparticle-surfactant ratio is 1:4 in terms of MRF enhancement. Moreover, nano-foam MRF at high foam quality (above 90%) is 3.5 times higher than surfactant foam MRF. Besides, higher mobility reduction can be achieved at a lower total injection rate in nanoparticles' presence.

- The implicit texture model successfully predicted foam collapse behaviour in nanoparticles' presence after applying the newly revised Dry-Out function.

5.2 Recommendations

This research elaborated on the influence of different parameters affecting nano-foam behaviour and its collapse behaviour at dry foam quality conditions compared to conventional surfactant foam. A modified $F_{dry-out}$ function was proposed to capture the nano-foam two-stage foam collapse behaviour by introducing a new fitting parameter, *epcon*. However, there is potentially additional research and scientific study to improve the understanding of the foam flow in porous media. The following recommendations and future studies are suggested as described below:

- The current foam models have some problems in terms of Dry-Out function when used to simulate a foam flooding process with nanoparticle effect, especially at the high-quality condition. This study introduced a modified model to overcome the existing problems with the nano-foam process. This modified function can be used in future versions of commercial reservoir simulator software.
- Although the effect of several parameters on nano-foam behaviour was investigated in the current research, the presence of oil was not within the scope of this study. Hence, it has been left for future studies.
- The effect of salinity in this study only considers the effect of monovalent salt ions in the nanofluid mixtures prepared in sodium chloride (NaCl).

Although the brine or seawater composition mostly consists of sodium chloride, previous research has highlighted the effect of nanofluid mixture stability and nano-foam performance in the presence of divalent salt ions. Therefore, there is still potential improvement to incorporate the effect of divalent salt ions to evaluate the nano-foam performance in actual field application.

- Since current (nano) foam models do not incorporate the temperature factor in MRF calculation, the temperature effect on MRF should be studied. Eventually, the new MRF models should be developed to incorporate temperature.
- The proposed revised model function was generated based on the optimum nanoparticle-surfactant foam performance within the system evaluated. The nano-foam performance may vary with nanoparticle and surfactant type and concentration due to the synergic effect between nanoparticle surface charge and surfactant head-group charges. In addition to that, the nano-foam performance may differ at high temperatures and in the presence of oil due to its detrimental effect on foam. Therefore, there is still potential improvement to incorporate the effect of nanoparticle concentration in the current foam model by incorporating its synergistic effect under reservoir conditions.

BIBLIOGRAPHY (OR REFERENCES)

- [1] A. Andrianov, R. Farajzadeh, M. Mahmoodi Nick, M. Talanana, and P. L. J. Zitha, "Immiscible Foam for Enhancing Oil Recovery: Bulk and Porous Media Experiments," *Industrial & Engineering Chemistry Research*, vol. 51, no. 5, pp. 2214-2226, 2012/02/08 2012.
- [2] R. Farajzadeh, A. Andrianov, and P. L. J. Zitha, "Investigation of Immiscible and Miscible Foam for Enhancing Oil Recovery," *Industrial & Engineering Chemistry Research*, vol. 49, pp. 1910 - 1919, 2010.
- [3] L. Kapetas *et al.*, "Effect of temperature on foam flow in porous media," *Journal of Industrial and Engineering Chemistry*, vol. 36, pp. 229-237, 2016.
- [4] A. A. Eftekhari, R. Krastev, and R. Farajzadeh, "Foam Stabilized by Fly Ash Nanoparticles for Enhancing Oil Recovery," *Industrial & Engineering Chemistry Research*, vol. 54, no. 50, pp. 12482-12491, 2015.
- [5] A. R. Risal, M. A. Manan, N. Yekeen, N. B. Azli, A. M. Samin, and X. K. Tan, "Experimental investigation of enhancement of carbon dioxide foam stability, pore plugging, and oil recovery in the presence of silica nanoparticles," *Petroleum Science*, vol. 16, no. 2, pp. 344-356, 2018.
- [6] M. Veyskarami and M. H. Ghazanfari, "Synergistic effect of like and opposite charged nanoparticle and surfactant on foam stability and mobility in the absence and presence of hydrocarbon: A comparative study," *Journal of Petroleum Science and Engineering*, vol. 166, pp. 433-444, 2018.
- [7] N. Razali, I. C. H. Chai, S. Zainal, and A. A. A Manap, "Nano-sized particles as foam stabiliser designed for application at high temperature and light crude oil condition for EOR - a fluid-fluid case study," presented at the Offshore Technology Conference Asia, Kuala Lumpur, 20-23 March 2018, 2018.
- [8] M. Z. B. M. Noor, W. Y. Teng, and S. Irawan, "Stabilization of Silicone Dioxide Nanoparticle Foam in Tertiary Petroleum Production," *Indonesian Journal of Chemistry*, vol. 19, no. 4, 2019.
- [9] A. Bashir, A. Sharifi Haddad, and R. Rafati, "Nanoparticle/polymer-enhanced alpha olefin sulfonate solution for foam generation in the presence of oil phase at high temperature conditions," *Colloids and Surfaces A: Physicochemical and Engineering Aspects*, vol. 582, 2019.
- [10] S. Sun *et al.*, "Tunable stability of oil-containing foam systems with different concentrations of SDS and hydrophobic silica nanoparticles," *Journal of Industrial and Engineering Chemistry*, vol. 82, pp. 333-340, 2020.
- [11] V. Prigiobbe, A. J. Worthen, K. P. Johnston, C. Huh, and S. L. Bryant, "Transport of Nanoparticle-Stabilized CO₂ -Foam in Porous Media," *Transport in Porous Media*, vol. 111, no. 1, pp. 265-285, 2015.
- [12] R. Singh and K. K. Mohanty, "Nanoparticle-Stabilized Foams for High-Temperature, High-Salinity Oil Reservoirs," presented at the SPE Annual Technical Conference and Exhibition, San Antonio, Texas, USA, 9-11 October 2017, 2017.
- [13] W. Li *et al.*, "A Novel Supercritical CO₂ Foam System Stabilized With a Mixture of Zwitterionic Surfactant and Silica Nanoparticles for Enhanced Oil Recovery," *Front Chem*, vol. 7, p. 718, 2019.
- [14] M. Al-Shargabi, S. Davoodi, D. A. Wood, V. S. Rukavishnikov, and K. M. Minaev, "Carbon Dioxide Applications for Enhanced Oil Recovery Assisted by Nanoparticles: Recent Developments," *ACS Omega*, vol. 7, no. 12, pp. 9984-9994, Mar 29 2022.
- [15] H. Hematpur, S. M. Mahmood, N. H. Nasr, and K. A. Elraies, "Foam flow in porous media: Concepts, models and challenges," *Journal of Natural Gas Science and Engineering*, vol. 53, pp. 163-180, 2018.
- [16] Z. Zhou and W. R. Rossen, "Applying Fractional-Flow Theory to Foam Processes at the "Limiting Capillary Pressure"," *SPE Advanced Technology Series*, vol. 3, no. 01, pp. 154-162, 1995.
- [17] M. Abbaszadeh, A. K. N. Korrani, J. L. Lopez-Salinas, F. R.-d. I. Garza, and G. J. Hirasaki, "Experimentally-Based Empirical Foam Modeling," presented at the SPE Improved Oil Recovery Symposium, Tulsa, Oklahoma, 12-16 April 2014, 2014.
- [18] V. Prigiobbe, A. J. Worthen, K. P. Johnston, C. Huh, and S. L. Bryant, "Transport of Nanoparticle-Stabilized CO₂ -Foam in Porous Media," *Transport in Porous Media*, vol. 111, no. 1, pp. 265-285, 2015.

- [19] D. P. O. Maestre, "Mechanistic Modeling of Nanoparticle-stabilized Supercritical CO₂ Foams and its Implication in Field-scale EOR Applications," Master of Science, The Department of Petroleum Engineering, Louisiana State University LSU Digital Commons, 2017.
- [20] M. Lotfollahi, R. Farajzadeh, M. Delshad, A. Varavei, and W. R. Rossen, "Comparison of implicit-texture and population-balance foam models," *Journal of Natural Gas Science and Engineering*, vol. 31, pp. 184-197, 2016.
- [21] A. Saeibehrouzi, M. Khosravi, and B. Rostami, "Steps and Challenges in Empirical Foam Modeling for Enhanced Oil Recovery," *Natural Resources Research*, 2020.
- [22] A. Nour, "Simulation of Nanoparticle-Stabilized CO₂-Foam in Sandstone," Master Thesis in Reservoir Physics, Department of Physics and Technology, University of Bergen, Bergen, 2019.
- [23] K. Ma, G. Ren, K. Mateen, D. Morel, and P. Cordelier, "Modeling Techniques for Foam Flow in Porous Media," *SPE Journal*, vol. 20, no. 03, pp. 453-470, 2015.
- [24] L. Kapetas *et al.*, "Effect of Permeability on Foam-model parameters - An Integrated Approach from Coreflood Experiments through to Foam Diversion Calculations," presented at the IOR 2015 - 18th European Symposium on Improved Oil Recovery, 2015.
- [25] T. Tran, M. E. Gonzalez Perdomo, M. Haghghi, and K. Amrouch, "Study of the synergistic effects between different surfactant types and silica nanoparticles on the stability of liquid foams at elevated temperature," *Fuel*, vol. 315, 2022.
- [26] N. Razali, I. C. C. Hsia, S. Zainal, and Arif Azhan A Manap, "Nano-Sized Particle as Foam Stabiliser Designed for Application at High Temperature and Light Crude Oil Condition for Enhanced Oil Recovery - A Fluid-Fluid Case Study," in *Offshore Technology Conference Asia*, Kuala Lumpur, Malaysia, 2018: Offshore Technology Conference.
- [27] M. Lotfollahi *et al.*, "Experimental Studies and Modeling of Foam Hysteresis in Porous Media," presented at the SPE Improved Oil Recovery Conference, Tulsa, Oklahoma, USA, 11–13 April 2016, 2016.
- [28] N. K. Maurya and A. Mandal, "Investigation of synergistic effect of nanoparticle and surfactant in macro emulsion based EOR application in oil reservoirs," *Chemical Engineering Research and Design*, vol. 132, pp. 370-384, 2018.
- [29] C. Xiao, S. N. Balasubramanian, and L. W. Clapp, "Rheology of Supercritical CO₂ Foam Stabilized by Nanoparticles," presented at the SPE Improved Oil Recovery Conference, Tulsa, Oklahoma, USA, 11–13 April 2016, 2016.
- [30] T. Horozov, "Foams and foam films stabilised by solid particles," *Current Opinion in Colloid & Interface Science*, vol. 13, no. 3, pp. 134-140, 2008.
- [31] N. Yekeen, A. K. Idris, M. A. Manan, A. M. Samin, A. R. Risal, and T. X. Kun, "Bulk and bubble-scale experimental studies of influence of nanoparticles on foam stability," *Chinese Journal of Chemical Engineering*, vol. 25, no. 3, pp. 347-357, 2017.
- [32] S. Li, Z. Li, and P. Wang, "Experimental Study of the Stabilization of CO₂ Foam by Sodium Dodecyl Sulfate and Hydrophobic Nanoparticles," *Industrial & Engineering Chemistry Research*, vol. 55, no. 5, pp. 1243-1253, 2016.
- [33] R. Singh and K. K. Mohanty, "Synergy between Nanoparticles and Surfactants in Stabilizing Foams for Oil Recovery," *Energy & Fuels*, vol. 29, no. 2, pp. 467-479, 2015.
- [34] D. Ortiz, M. Izadi, and S. I. Kam, "Modeling of Nanoparticle-Stabilized CO₂ Foam Enhanced Oil Recovery," *SPE Reservoir Evaluation & Engineering*, pp. 971 - 989, August 2019 2019.
- [35] B. P. Binks and S. O. Lumsdon, "Influence of Particle Wettability on the Type and Stability of Surfactant-Free Emulsions," *Langmuir*, no. 16, pp. 8622-8631, March 31, 2000 2000.
- [36] G. Kaptay, "On the equation of the maximum capillary pressure induced by solid particles to stabilize emulsions and foams and on the emulsion stability diagrams," *Colloids and Surfaces A: Physicochemical and Engineering Aspects*, vol. 282-283, pp. 387-401, 2006.
- [37] S. H. Talebian, R. Masoudi, I. M. Tan, and P. L. J. Zitha, "Foam assisted CO₂-EOR: A review of concept, challenges, and future prospects," *Journal of Petroleum Science and Engineering*, vol. 120, pp. 202-215, 2014.
- [38] L. W. Lake, *Enhanced Oil Recovery*. Prentice Hall, 1989.
- [39] P. A. Gauglitz, F. Friedmann, S. I. Kam, and W. R. Rossen, "Foam Generation in Porous Media," presented at the SPE/DOE Improved Oil Recovery Symposium, Tulsa, Oklahoma U.S.A., 13–17 April 2002, 2002.
- [40] A. S. Emrani, A. F. Ibrahim, and H. A. Nasr-El-Din, "Evaluation of Mobility Control with Nanoparticle-Stabilized CO₂ Foam," presented at the SPE Latin America and Caribbean Petroleum Engineering Conference, 2017.

- [41] X. Sun, Y. Zhang, G. Chen, and Z. Gai, "Application of Nanoparticles in Enhanced Oil Recovery: A Critical Review of Recent Progress," *Energies*, vol. 10, no. 3, 2017.
- [42] D. P. O. Maestre, "Mechanistic Modeling of Nanoparticle-stabilized Supercritical CO₂ Foams and its Implication in Field-scale EOR Applications," Louisiana State University, 2017.
- [43] N. D. Denkov, I. B. Ivanov, P. A. Kralchevsky, and D. T. Wasan, "A possible mechanism of stabilization of emulsions by solid particles," *Journal of Colloid And Interface Science*, vol. 150, no. 2, pp. 589-593, 1992.
- [44] B. P. Binks and S. O. Lumsdon, "Influence of Particle Wettability on the Type and Stability," *Langmuir*, vol. 16, pp. 8622 - 8631, 2000.
- [45] N. Yekeen *et al.*, "A comprehensive review of experimental studies of nanoparticles-stabilized foam for enhanced oil recovery," *Journal of Petroleum Science and Engineering*, vol. 164, pp. 43-74, 2018.
- [46] M. Zargartalebi, R. Kharrat, and N. Barati, "Enhancement of surfactant flooding performance by the use of silica nanoparticles," *Fuel*, vol. 143, pp. 21-27, 2015.
- [47] S. I. Karakashev, O. Ozdemir, M. A. Hampton, and A. V. Nguyen, "Formation and stability of foams stabilized by fine particles with similar size, contact angle and different shapes," *Colloids and Surfaces A: Physicochemical and Engineering Aspects*, vol. 382, no. 1-3, pp. 132-138, 2011.
- [48] A. U. Rognmo, S. Heldal, and M. A. Fernø, "Silica nanoparticles to stabilize CO₂-foam for improved CO₂ utilization: Enhanced CO₂ storage and oil recovery from mature oil reservoirs," *Fuel*, vol. 216, pp. 621-626, 2018.
- [49] N. Hu, Y. Li, Z. Wu, K. Lu, D. Huang, and W. Liu, "Foams stabilization by silica nanoparticle with cationic and anionic surfactants in column flotation: Effects of particle size," *Journal of the Taiwan Institute of Chemical Engineers*, vol. 88, pp. 62-69, 2018.
- [50] W. Yang, T. Wang, Z. Fan, Q. Miao, Z. Deng, and Y. Zhu, "Foams Stabilized by In Situ-Modified Nanoparticles and Anionic Surfactants for Enhanced Oil Recovery," *Energy & Fuels*, vol. 31, no. 5, pp. 4721-4730, 2017.
- [51] Z. A. AlYousef, M. A. Almobarky, and D. S. Schechter, "The effect of nanoparticle aggregation on surfactant foam stability," *J Colloid Interface Sci*, vol. 511, pp. 365-373, Feb 1 2018.
- [52] M. Ahmadi, A. Habibi, P. Pourafshary, and S. Ayatollahi, "Zeta Potential Investigation and Mathematical Modeling of Nanoparticles Deposited on the Rock Surface to Reduce Fine Migration," in *SPE Middle East Oil and Gas Show and Conference*, Manama, Bahrain, 2011, no. SPE 142633: SPE.
- [53] S. A. Ab Rasid, S. M. Mahmood, N. I. Kechut, and S. Akbari, "A review on parameters affecting nanoparticles stabilized foam performance based on recent analyses," *Journal of Petroleum Science and Engineering*, vol. 208, 2022.
- [54] B. P. Binks, M. Kirkland, and J. A. Rodrigues, "Origin of stabilisation of aqueous foams in nanoparticle-surfactant mixtures," *Soft Matter*, vol. 4, no. 12, 2008.
- [55] P. M. Kruglyakov, S. I. Elaneva, and N. G. Vilkova, "About mechanism of foam stabilization by solid particles," *Adv Colloid Interface Sci*, vol. 165, no. 2, pp. 108-116, Jul 11 2011.
- [56] H. Vatanparast, F. Shahabi, A. Bahramian, A. Javadi, and R. Miller, "The Role of Electrostatic Repulsion on Increasing Surface Activity of Anionic Surfactants in the Presence of Hydrophilic Silica Nanoparticles," *Sci Rep*, vol. 8, no. 1, p. 7251, May 8 2018.
- [57] L. R. Arriaga *et al.*, "On the long-term stability of foams stabilised by mixtures of nano-particles and oppositely charged short chain surfactants," *Soft Matter*, vol. 8, no. 43, 2012.
- [58] L. Xu *et al.*, "Synergy of surface-treated nanoparticle and anionic-nonionic surfactant on stabilization of natural gas foams," *Colloids and Surfaces A: Physicochemical and Engineering Aspects*, vol. 550, pp. 176-185, 2018.
- [59] C. Qian, A. Telmadarreie, M. Dong, and S. L. Bryant, "Synergistic Effect between Surfactant and Nanoparticles on the Stability of Foam in EOR Processes," presented at the SPE Western Regional Meeting, San Jose, California, USA, 23-26 April 2019, 2019.
- [60] Ø. Eide, T. Føyen, E. Skjelsvik, A. Rognmo, and M. Fernø, "Nanoparticle Stabilized Foam in Harsh Conditions for CO₂ EOR," presented at the Abu Dhabi International Petroleum Exhibition & Conference, Abu Dhabi, UAE, 12-15 November 2018, 2018.
- [61] N. Yekeen, M. A. Manan, A. K. Idris, A. M. Samin, and A. R. Risal, "Experimental investigation of minimization in surfactant adsorption and improvement in surfactant-foam stability in presence of silicon dioxide and aluminum oxide nanoparticles," *Journal of Petroleum Science and Engineering*, vol. 159, pp. 115-134, 2017.

- [62] S. Jafari Daghlilian Sofla, L. A. James, and Y. Zhang, "Insight into the stability of hydrophilic silica nanoparticles in seawater for Enhanced oil recovery implications," *Fuel*, vol. 216, pp. 559-571, 2018.
- [63] W. M. S. Mat Latif, M. S. M. Musa, A. S. M. Balakirisnan, and W. R. W. Sulaiman, "The effect of surfactant concentration on nanoparticles surface wettability during wettability alteration of oil-wet carbonate rock," *Journal of Mechanical Engineering and Sciences*, vol. 15, no. 2, pp. 7993-8002, 2021.
- [64] M. Issakhov, M. Shakeel, P. Pourafshary, S. Aidarova, and A. Sharipova, "Hybrid surfactant-nanoparticles assisted CO₂ foam flooding for improved foam stability: A review of principles and applications," *Petroleum Research*, 2021.
- [65] Nanji J. Hadia, Y. H. Ng, L. P. Stubbs, and O. Torsæter, "High Salinity and High Temperature Stable Colloidal Silica Nanoparticles with Wettability Alteration Ability for EOR Applications," *Nanomaterials*, vol. Application of Nanoparticles for Oil Recovery, p. 14, 2021.
- [66] C. Xiao, S. N. Balasubramanian, and L. W. Clapp, "Rheology of Viscous CO₂ Foams Stabilized by Nanoparticles under High Pressure," *Industrial & Engineering Chemistry Research*, vol. 56, no. 29, pp. 8340-8348, 2017.
- [67] A. U. Rognmo, H. Horjen, and M. A. Fernø, "Nanotechnology for improved CO₂ utilization in CCS: Laboratory study of CO₂-foam flow and silica nanoparticle retention in porous media," *International Journal of Greenhouse Gas Control*, vol. 64, pp. 113-118, 2017.
- [68] A. J. Worthen, P. S. Parikh, Y. Chen, S. L. Bryant, C. Huh, and K. P. Johnston, "Carbon Dioxide-in-Water Foams Stabilized with a Mixture of Nanoparticles and Surfactant for CO₂ Storage and Utilization Applications," *Energy Procedia*, vol. 63, pp. 7929-7938, 2014.
- [69] A. Skauge, J. Solbakken, P. A. Ormehaug, and M. G. Aarra, "Foam Generation, Propagation and Stability in Porous Medium," *Transport in Porous Media*, vol. 131, no. 1, pp. 5-21, 2019.
- [70] M. G. Aarra, P. A. Ormehaug, and A. Skauge, "Foams for GOR control - improved stability by polymer additives," presented at the 9th European Symposium on Improved Oil Recovery, The Hague - The Netherlands, 20 - 22 October 1997, 1997.
- [71] A. K. Vikingstad and M. G. Aarra, "Comparing the static and dynamic foam properties of a fluorinated and an alpha olefin sulfonate surfactant," *Journal of Petroleum Science and Engineering*, vol. 65, no. 1-2, pp. 105-111, 2009.
- [72] J. S. Solbakken, "Experimental Studies of N₂ - and CO₂-Foam Properties in Relation to Enhanced Oil Recovery Applications," Philosophiae Doctor (PhD), Department of Chemistry, University of Bergen, Norway, 2015.
- [73] K. Mannhardt and I. Svorstøl, "Effect of oil saturation on foam propagation in Snorre reservoir core," *Journal of Petroleum Science and Engineering*, vol. 23, p. 11, 23 June 1999 1999.
- [74] A. H. Falls, G. J. Hirasaki, T. W. Patzek, D. A. Gauglitz, D. D. Miller, and T. Ratulowski, "Development of a Mechanistic Foam Simulator: The Population Balance and Generation by Snap-Off," *SPE Reservoir Engineering*, vol. 3, no. 03, pp. 884-892, 1988.
- [75] X. Lyu, D. Voskov, J. Tang, and W. R. Rossen, "Simulation of Foam Enhanced-Oil-Recovery Processes Using Operator-Based Linearization Approach," *SPE Journal*, 2021.
- [76] C. Boeije, "Experimental and modelling studies of foam enhanced oil recovery," 2016.
- [77] Q. Chen, M. G. Gerritsen, and A. R. Kovysek, "Modeling Foam Displacement With the Local-Equilibrium Approximation: Theory and Experimental Verification," presented at the SPE Annual Technical Conference and Exhibition, Denver, 21-24 September 2008, 2010.
- [78] B. Benali *et al.*, "Pore-scale bubble population dynamics of CO₂-foam at reservoir pressure," *International Journal of Greenhouse Gas Control*, vol. 114, 2022.
- [79] Ø. Eide, M. Fernø, S. Bryant, A. Kovysek, and J. Gauteplass, "Population-balance modeling of CO₂ foam for CCUS using nanoparticles," *Journal of Natural Gas Science and Engineering*, vol. 80, 2020.
- [80] W. T. Osterloh and M. J. J. Jr., "Effects of Gas and Liquid Velocity on Steady-State Foam Flow at High Temperature," in *SPE/DOE Eighth Symposium on Enhanced Oil Recovery*, Tulsa, Oklahoma, 1992.
- [81] L. Cheng, S. I. Kam, M. Delshad, and W. R. Rossen, "Simulation of Dynamic Foam-Acid Diversion Processes," *SPE Journal*, vol. 7, pp. 316-324, 2002.
- [82] L. Cheng, A. B. Reme, D. Shan, D. A. Coombe, and W. R. Rossen, "Simulating Foam Processes at High and Low Foam Qualities," in *2000 SPE/DOE Improved Oil Recovery Symposium*, Tulsa, Oklahoma, 2000: SPE International.

- [83] K. Ma, J. L. Lopez-Salinas, M. C. Puerto, C. A. Miller, S. L. Biswal, and G. J. Hirasaki, "Estimation of Parameters for the Simulation of Foam Flow through Porous Media. Part 1: The Dry-Out Effect," *Energy & Fuels*, vol. 27, no. 5, pp. 2363-2375, 2013.
- [84] Y. Zeng *et al.*, "Role of Gas Type on Foam Transport in Porous Media," *Langmuir*, vol. 32, no. 25, pp. 6239-45, Jun 28 2016.
- [85] S. A. Farzaneh and M. Sohrabi, "A review of the status of foam application in enhanced oil recovery," in *EAGE Annual Conference & Exhibition incorporating SPE Europec*, 2013: Society of Petroleum Engineers.
- [86] R. Farajzadeh, A. Andrianov, H. Bruining, and P. L. J. Zitha, "Comparative Study of CO₂ and N₂ Foams in Porous Media at Low and High Pressure-Temperatures," *Industrial & Engineering Chemistry Research*, vol. 48, no. 9, pp. 4542-4552, 2009/05/06 2009.
- [87] S. Ahmed *et al.*, "Experimental investigation of immiscible supercritical carbon dioxide foam rheology for improved oil recovery," *Journal of Earth Science*, vol. 28, no. 5, pp. 835-841, 2017.
- [88] N. H. Nasr, "EXPERIMENTAL STUDY TO SCREEN AND OPTIMIZE VARIOUS FOAM FLOODING TECHNIQUES USING SPECIALLY DESIGNED AUTOMATED SYSTEM," MASTER OF SCIENCE, PETROLEUM ENGINEERING, UNIVERSITI TEKNOLOGI PETRONAS, 2018.
- [89] N. Hadian Nasr, S. M. Mahmood, S. Akbari, and H. Hematpur, "A comparison of foam stability at varying salinities and surfactant concentrations using bulk foam tests and sandpack flooding," *Journal of Petroleum Exploration and Production Technology*, vol. 10, no. 2, pp. 271-282, 2019.
- [90] N. Hadian Nasr, S. M. Mahmood, and H. Hematpur, "A rigorous approach to analyze bulk and coreflood foam screening tests," *Journal of Petroleum Exploration and Production Technology*, vol. 9, no. 2, pp. 809-822, 2018.
- [91] T. Majeed, M. S. Kamal, X. Zhou, and T. Solling, "A Review on Foam Stabilizers for Enhanced Oil Recovery," *Energy & Fuels*, vol. 35, no. 7, pp. 5594-5612, 2021.
- [92] R. Singh and K. K. Mohanty, "Study of Nanoparticle-Stabilized Foams in Harsh Reservoir Conditions," *Transport in Porous Media*, vol. 131, no. 1, pp. 135-155, 2018.
- [93] Q. Sun *et al.*, "Aqueous foam stabilized by partially hydrophobic nanoparticles in the presence of surfactant," *Colloids and Surfaces A: Physicochemical and Engineering Aspects*, vol. 471, pp. 54-64, 2015.
- [94] D. Panahpoori, H. Rezvani, R. Parsaei, and M. Riazi, "A pore-scale study on improving CTAB foam stability in heavy crude oil-water system using TiO₂ nanoparticles," *Journal of Petroleum Science and Engineering*, vol. 183, 2019.
- [95] W. R. Rossen, "Foams in enhanced oil recovery," *Foams: theory, measurements and applications*, vol. 57, pp. 413-464, 1996.
- [96] C. Fu, J. Yu, and N. Liu, "The effect of foam quality, particle concentration and flow rate on nanoparticle-stabilized CO₂ mobility control foams," *RSC Advances*, vol. 9, no. 16, pp. 9313-9322, 2019.